

**Addressing the role of the cytoskeletal
molecules Diaphanous and Profilin in
dendritic morphogenesis in
*Drosophila melanogaster***

**Dissertation
der Fakultät für Biologie
der Ludwig-Maximilians-Universität
München**

**Vorgelegt von
Madhuri Shivalkar
München 2007**

**Dissertation eingereicht am 11.07.2007
Tag der mündlichen Prüfung: 12.09.2007**

**Erstgutachter: PD Dr. Rüdiger Klein
Zweitgutachter: PD Dr. Angelika Böttger**

Erklärung

Ich versichere, daß ich meine Dissertation selbstständig, ohne unerlaubte Hilfe angefertigt, und mich dabei keiner anderen als der von mir ausdrücklich bezeichneten Hilfen und Quellen bedient habe.

Die Dissertation wurde in der jetzigen oder ähnlichen Form bei keiner anderen Hochschule eingereicht und hat noch keinen sonstigen Prüfungszwecken gedient.

(Ort, Datum)

(Madhuri Shivalkar)

- 1. Gutachter: Dr Rüdiger Klein**
- 2. Gutachter: Dr Angelika Böttger**

To my family

The work presented in this thesis was performed from July 2003 to June 2007 in the laboratory of Dr. Gaia Tavosanis at Max-Planck Institute of Neurobiology Munich, Germany.

Index

INDEX.....	i
Figures and tables.....	vi
Abbreviations.....	ix
SUMMARY.....	xii
Chapter I: INTRODUCTION.....	1
1.1 Dendrites and Dendritic morphology.....	1
1.2 Molecular players of dendritic morphology.....	1
1.3 Cytoskeletal molecules and dendritic morphogenesis.....	5
1.4 Model system: Peripheral Nervous System of <i>Drosophila melanogaster</i> ...7	
1.5 Assay System: RNA interference.....	11
1.6 RNAi assay: positive products- Diaphanous and Profilin.....	14
1.6.1 Diaphanous.....	14
1.6.2 Profilin.....	17
1.6.3 The role of Profilin in Formin function.....	19
1.6.4 Neuronal role of Diaphanous and Profilin.....	20
1.7 Analysis of dendritic branching <i>in vivo</i> and distribution of actin and microtubule in dendrites.....	22

Chapter II: MATERIALS AND METHODS.....	25
2.1 RNA interference assay.....	25
2.1.1 Genomic DNA extraction.....	25
2.1.2 dsRNA preparation.....	25
2.1.3 Injecting dsRNA in embryos.....	28
2.2 Fly genetics.....	29
2.2.1 <i>Drosophila</i> Stocks.....	31
2.2.2 Generation of recombinants.....	32
2.2.3 Transgenic flies.....	32
2.3 MARCM (mosaic analysis with repressible cell marker).....	33
2.4 Time Lapse Imaging.....	33
2.5 Image acquisition and processing.....	34
2.6 Quantitative analysis.....	34
2.7 Immunohistochemistry.....	35
2.8 Western blot analysis.....	36
Chapter III: RESULTS.....	37
RNA INTERFERENCE SCREEN.....	37
3.1 Standardizing RNAi assay system.....	37
3.1.2 Selection of molecules.....	42

3.1.3 RNAi assay.....	47
3.1.4 Interesting candidates with no significant dendritic phenotype.....	49
3.1.5 Interesting candidates with interesting phenotype.....	50
GENETIC ANALYSIS.....	53
4.1 Diaphanous.....	53
4.1.1 Gain of function analysis.....	54
4.1.1.1 Overexpression of <i>dia</i> in class I neurons.....	55
4.1.1.2 Overexpression of <i>diaphanous</i> in class IV neurons.....	58
4.1.2 Loss of function.....	60
4.1.2.1 Dendritic phenotype of null mutant <i>dia</i> ^{K07135}	60
4.1.2.1.1 <i>dia</i> ^{K07135} – dendritic over branching phenotype in class I neurons...60	
4.1.2.1.2 <i>dia</i> ^{K07135} – no dendritic phenotype in class IV neurons.....64	
4.1.2.2 Dendritic phenotype of null mutant <i>dia</i> ⁵	65
4.1.2.2.1 <i>dia</i> ⁵ – dendritic over branching phenotype in class I neurons.....65	
4.1.2.3 Dendritic phenotype in trans-allelic combination of null mutants- <i>dia</i> ⁵ and <i>dia</i> ^{K07135}	67
4.1.4 Western blot analysis: no Diaphanous protein in null mutants.....	68
4.1.5 Expression pattern using antibody staining.....	69
4.1.6 MARCM- generating homozygous mutant clones in heterozygous animals.....	70
4.1.7 Analysis with deficiency.....	70

4.1.8 Dystrophin: insertion of <i>Gal4</i> ²⁻²¹ causes a dendritic phenotype!.....	72
4.1.9 Dendritic over branching phenotype of <i>dia</i> null mutants is lost in heterozygous marker condition.....	76
4.2 Profilin (<i>chickadee</i>).....	78
4.2.1 Gain of function analysis.....	79
4.2.1.1 Overexpression of <i>chic</i> in class I and class IV neurons.....	79
4.2.2 Loss of function analysis.....	81
4.2.2.1 Dendritic phenotype of null <i>chic</i> ²²¹ and hypomorphic <i>chic</i> ¹¹ and <i>chic</i> ³⁷ alleles.....	81
4.2.3 Expression pattern using antibody staining.....	83
4.2.4 MARCM- generating homozygous mutant clones in heterozygous <i>chic</i> ²²¹ animals.....	83
4.3 <i>chickadee</i> and <i>diaphanous</i> : analyzing the interaction.....	85
4.4 Time lapse analysis.....	88
4.4.1 Standardizing time lapse assay.....	88
4.4.2 Imaging dendrites <i>in vivo</i> over time.....	89
4.5 How do actin and microtubule contribute to dendrite formation?.....	91
Chapter IV: DISCUSSION.....	93
5.1 RNA interference screen.....	93
5.2 Diaphanous: Role in dendritic morphogenesis.....	96

5.3 Dystrophin.....	101
5.4 Diaphanous: Ambiguous results from loss of function analysis.....	102
5.5 Profilin.....	103
5.4 Higher order branches of vpda neuron are dynamic at late larval stages.....	105
5.5 Localization of actin and tubulin varies in class I vpda neuron.....	106
CONCLUDING REMARKS.....	108
REFERENCES.....	109
ACKNOWLEDGEMENTS	119
<i>CURRICULUM VITAE</i>	120

FIGURES AND TABLES

Figures:

Chapter I: Introduction

Figure 1 Morphological diversity of dendrites	2
Figure 2 Cytoskeletal players.....	6
Figure 3 Life cycle of <i>Drosophila melanogaster</i>	8
Figure 4 PNS organization.....	9
Figure 5 Different morphological classes of da sensory neurons in <i>Drosophila</i> PNS.....	10
Figure 6 RNAi mechanism.....	13
Figure 7 Domain Organization and Molecular Regulation of Diaphanous- Related Formins	16
Figure 8 Profilin in actin dynamics.....	18
Figure 9 Formin- Profilin interaction.....	19
Figure10 Localization of actin-GFP in dendritic filopodia.....	23

Chapter II: Materials and Methods

Figure11 A cartoon showing a couple of useful ways to pin the larvae while dissecting.....	35
--	----

Chapter III: Results

Figure 12 Microinjection set up for RNAi assay.....	38
Figure 13 Knock down of <i>GFP</i> expression in <i>GFP</i> -siRNA injected embryos.	40
Figure 14 Neurogenic phenotype in <i>tramtrack</i> -dsRNA injected embryo.....	41

Figure 15 GFP labeled PNS in 80G2 strain.....	48
Figure 16 Lack of Detectable Phenotype.....	50
Figure 17 Dendritic phenotype of Diaphanous and Profilin upon RNAi.....	51
Figure 18 Domain structure of Diaphanous protein.. ..	53
Figure 19 Overexpression of <i>dia</i> results in dendritic over branching phenotype of class I –vpda neuron.....	56
Figure 20 Overexpression of (<i>UAS-dia-CA</i>) in class IV neurons.....	59
Figure 21 Dendritic phenotype of class I vpda neuron of <i>dia</i> ^{K07135} embryos.	61
Figure 22 Dendritic phenotype of class I vpda neuron of <i>dia</i> ^{K07135} at late 3 rd instar larval stage.....	62
Figure 23 Absence of dendritic phenotype of class IV ddaC neuron of <i>dia</i> ^{K07135} at late 3 rd instar larval stage.....	64
Figure 24 Dendritic phenotype of class I vpda neuron of <i>dia</i> ⁵ at late 3 rd instar larval stage.....	66
Figure 25 Dendritic phenotype of class I vpda neuron in transallelic combination.....	68
Figure 26 Detecting Diaphanous protein on Western blot.....	69
Figure 27 Deficiency analysis of <i>diaphanous</i> null mutants.....	72
Figure 28 Dystrophin gene and transcripts in <i>Drosophila</i>	73
Figure 29 Dendritic over branching phenotype of Dystrophin.....	74
Figure 30 Dendritic phenotype of <i>dia</i> null mutants is lost in heterozygous marker line condition.....	77
Figure 31 Dendritic phenotype of class IV ddaC neuron upon Profilin overexpression.....	80

Figure 32 Dendritic phenotype of class I vpda neuron of <i>chic</i> ²²¹ at embryonic stage.....	82
Figure 33 MARCM Analysis.....	84
Figure 34 <i>chic</i> ²²¹ genetically interacts with <i>dia</i> ^{K07135}	87
Figure 35 Live imaging slide outlay.....	89
Figure 36 Time lapse analysis of 3 rd instar larvae- visualizing dendritic morphogenesis in live.....	90
Figure 37 Localization of tubulin and actin.....	91

Chapter IV: Discussion

Figure 38 Rho family proteins, actin filaments and membrane dynamics.....	98
--	----

Tables:

Chapter II: Materials and Methods

Table 2.1 Primers used for amplification of DNA stretches.....	27
---	----

Chapter III: Results

Table 3.1 Standardization using tramtrack RNAi.....	41
Table 3.2 Summary of RNAi assay.....	49

ABBREVIATIONS

3T3 cells 3-day transfer, inoculum 3×10^5 cells
Abi Abelson kinase
ADF Actin depolymerizing factor
ADP Adenosine diphosphate
AEL After egg laying
Aip1 Actin interacting protein 1
APF After puparium formation
Arp2/3 Actin related protein 2/3
ATP Adenosine triphosphate
BDNF Brain derived nerve growth factor
BMPs Bone Morphogenic Factors
Bni1 Bud neck involved 1
Bnr1 Bni1 Related 1
bp Base pairs
BSA Bovine Serum Albumin
C terminal Carboxy terminal
CA Constitutively Active
CaMK Calcium/ calmodulin-dependent protein kinase
cAMP Cyclic adenosine monophosphate
capt *Capulet*
capu *Cappuccino*
CC Coiled coil
Cdc42 Cell division cycle 42
ch chordotonal
chic *chickadee*
CHO1 Choline independent 1
CNS Central Nervous System
ctn Catenin
da dendritic arborization
da Dendrite arborization
DAAM dishevelled-associated activator of morphogenesis
DAD Diaphanous autoinhibitory domain
DAB 3, 3' Diaminobenzidine
DD Dimerization domain
Df Deficiency
dia *diaphanous*
DID Diaphanous inhibitor domain
DNA Deoxyribonucleic acid
DRFs Diaphanous-related formins
DRG Dorsal root ganglion
DScam Down's syndrome Cell Adhesion Molecule
ds Double stranded
dsRNA Double stranded ribonucleic acid
eGFP Enhanced *GFP*
Ena Enabled
ENC-1 Ectoderm-Neural Cortex-1

Eph Ephrin
ERK Extracellular signal-regulated kinase
es External sensory
F-actin Filamentous actin
FH Formin homology
FMR Fragile X Mental Retardation Syndrome
for3p Formin 3p
FRL formin-related gene in leukocytes
g Gram
G-actin Globular actin
GBD GTPase binding domain
GEF Guanine Nucleotide Exchange Factor
GFP Green Fluorescent Protein
GOF Gain of function
GDP Guanosine diphosphate
GTP Guanosine triphosphate
HAM Hamlet
HRP Horse Radish Peroxidase
hrs Hours
hSSHs human SSH homologues
KCL Potassium chloride
kb kilobases
kD kilodalton
LIMK Lin-11, Isl-1, and Mec-3 kinase
Lis1 Lissencephaly 1
LOF Loss of function
LPTC Lobula Plate Tangential Cell
MAP2 Microtubule associated protein 2
MARCM Mosaic Analysis with a Repressible Cell Marker
MAPK Mitogen-activated protein kinase
MB Mushroom Body
md Multiple dendrite
mDia Mouse Diaphanous
MEK MAPK and ERK kinase
mins Minutes
MKLP1 Mitotic kinesin-like protein-1
µg microgram
µl Microliter
µm Micrometer
mm Millimeter
mM millimolar
ml Mililiter
mRNA Messenger ribonucleic acid
MT Microtubules
n number
N terminal Amino acid terminal
NaPO₄ Sodium phosphate
NDR Nuclear Dbf2-Related
NGF Nerve Growth Factor
nm Nanometer

NMDA N-methyl-D-aspartic acid
NMJ Neuromuscular Junction
NT-3 Neurotrophin 3
OE Overexpression
P Profilin
PBS Phosphate Buffer Solution
PCR Polymerase Chain Reaction
PFA Paraformaldehyde
pH Potential of Hydrogen
PNS Peripheral Nervous System
ppk *pickpocket*
Rac Ras-related C3 botulinum toxin substrate
RFP red fluorescent protein
Rho Ras homologous member
RISC RNA-induced silencing complex
RNA Ribonucleic acid
RNAi RNA interference
RT Room Temperature
S2 Schneider 2
SCAR Suppressor of cAMP receptor
SDF Stromal cell-derived factor
siRNA small interfering RNA
Sra-1 specifically Rac1-associated protein 1
SSH Slingshot
Trc Tricornered
ttk *tramtrack*
UAS Upstream Activation Sequence
VASP Vasodilator-stimulated phosphoprotein
WASP Wiscott- Aldrich Syndrome Protein
WAVE WASP-family verprolin-homologous protein
wt Wild type

Summary

Precise dendritic morphogenesis contributes to functional neuronal signaling. Extrinsic and intrinsic factors affecting dendritic morphology are proposed to converge upon cytoskeletal molecules and regulators to bring about changes in dendritic structures. We used a candidate based RNAi approach to isolate cytoskeletal molecules involved in dendritic morphogenesis and differentiation using the well studied embryonic peripheral nervous system of *Drosophila*. The RNAi assay system was standardized and used successfully to carry out a pilot screen for 14 cytoskeletal molecules. Many of the candidates showed no dendritic phenotype. However, we isolated five positive candidates- Cappuccino, Diaphanous, Kelch, Profilin and Quail. Out of these, Diaphanous (*dia*) and profilin (*chic*) exhibited the most penetrant dendritic overbranching phenotype of dendritic arborization multidendritic (da-md) neurons upon RNAi. Both these molecules are important actin binding molecules regulating actin dynamics depending on their binding partners, tissues in which they are expressed and the model system. Moreover, *dia* and *chic* bind to each other as shown by *in vitro* and *in vivo* studies in yeast. However, their role in dendritic morphogenesis is not explored yet. So we chose these two molecules for further genetic analysis.

Further genetic experiments with gain of function and loss of function analysis were done to understand the role of these two molecules in dendritic morphogenesis. Overexpression of different full length, fluorescently tagged and constitutively active (CA-*dia*) constructs of *dia* in simple branching pattern Class I da-md neurons show a significant increase in the total number of dendritic branches. However, only the CA-*dia* construct showed a significant dendritic phenotype in the complex branching pattern Class IV da-md neurons. This result indicates a neuronal class specific role for *dia* in dendritic morphogenesis. Furtheron, the supernumerary dendritic branches formed upon CA-*dia* overexpression resembled filopodia. Thus, these results may suggest that *dia* functions in the formation of filopodia-like branches which later on get stabilized to become dendritic branches. However, we could not obtain a dendritic phenotype in class I neurons upon loss of function analysis. The loss of function analysis was complicated by genomic interactions between the marker line used for analysis and background on *dia* chromosome. The marker line per se in addition, turned out to have an overbranching phenotype in class I neurons.

As a marker line for the analysis of class I neurons, I used a Gal4 insertion on the 3rd chromosome. Analysis in the lab demonstrated that this Gal4 driver insertion is within the *dystrophin* (*dys*) gene. By genetic analysis I showed that, though this Gal4 insertion in the *dys* gene is contributing to the dendritic overbranching of the marker line, it is not solely responsible for it. The dendritic phenotype seen in the marker line as well as in both *dia* null mutants appear to be a product of complicated interactions which are difficult to decipher in a short period.

The gain of function analysis of profilin (*chic*) by using a full length construct exhibited a class specific dendritic phenotype with no effect on class I neurons and decreased dendritic branching in class IV neurons. However, our attempts to probe into the role of *chic* by loss of function analysis using null and hypomorphic mutants and mosaic clonal analysis (mosaic analysis with repressible cell marker- MARCM) with null mutants did not answer our the questions explicitly. Null mutants showed increased dendritic branching during late embryogenesis, for this corresponded to their lethal phase. The MARCM analysis did not show any change in dendritic branching of class I neurons of null mutants and also other classes of neurons did not seem much affected. This could exclude a role of Profilin in dendritogenesis in these neurons. Alternatively it could be due to the persistence of the protein upon induction of clones.

Altogether, we have not been able to confer a definitive role for these two actin binding molecules, namely *dia* and *chic*, in dendritic morphogenesis at this point. We need more flexible and controlled genetic tools to decipher their role.

In this thesis, we have also tried to study dendritic morphogenesis *in vivo* using time-lapse imaging. Preliminary data on the development of class I vpda neuron in late third instar larvae suggests a dynamic turnover of higher order dendritic branches whereas the primary and secondary branches are quite stable.

We also have examined the distribution of actin and microtubules in class I neurons to understand the process of dendrite branch formation. Our primary data using GFP tagged constructs demonstrates that tubulin is localized in primary and some of secondary branches whereas actin is distributed not only in primary and secondary branches but some of the higher order branches also. This is a first step of analysis which can be extended using time lapse study to understand formation, retraction and growth of dendritic branches in regards to the contribution of these cytoskeletal components in these processes.

CHAPTER 1- INTRODUCTION

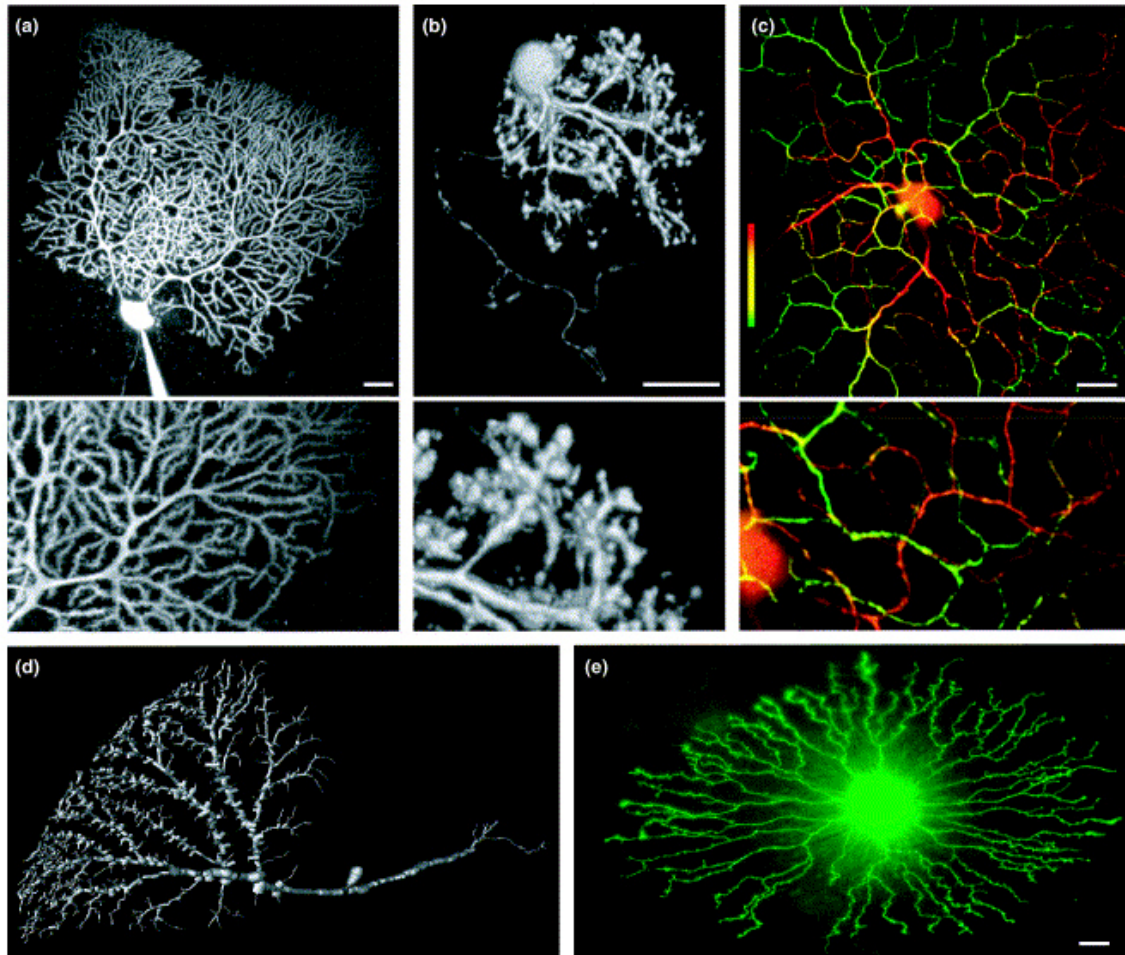
1.1: Dendrites and Dendritic morphology

Dendrites are receptive processes of neurons and contribute equally to efficient neuronal functioning along with axons. Dendrites receive information either from the external environment in the form of sensory stimuli or from axons in the form of synaptic inputs. Dendrites do not simply receive signals but also actively participate in computation and storage of information. The complex morphology of dendrites is an important determinant of how a neuron responds to multiple stimuli and how those stimuli get integrated (Borst and Egelhaaf, 1994; Brenman et al., 2001; Hausser et al., 2000). Dendritic morphology in terms of branching pattern varies widely among different types of neurons and sometimes dendrites can be highly branched accounting for ~90% of the postsynaptic surface of the neuron (Sholl, 1956). Many neuronal types show remarkably complex dendritic arborizations specific for each neuronal type. Each neuron can be identified based on its morphological aspects like branching pattern, number of branches, length of branches, the relative distance of different dendritic branches from the cell body, number and distribution of dendritic spines and synaptic composition (Figure 1) (Euler and Denk, 2001). Thus, dendrites represent a sophisticated structure designed for efficient collection of signals and the dendritic morphology is a key to the functional identity of a neuron and is a hallmark of neuronal type (Gao et al., 1999; Jan and Jan, 2001). Therefore, an essential question in neurobiology is how dendrites acquire their complex and neuron-specific morphologies.

1.2 Molecular players of dendritic morphology

Although significant progress has been made in unraveling molecular mechanisms that regulate axonal growth and guidance, comparatively very little

is known about the molecular cues that govern dendritic morphogenesis. While a comprehensive view is still lacking, many recent studies have identified and characterized some molecules involved in the establishment of dendritic patterns.



[Euler and Denk, *Curr Opin Neurobiol.* 11(4):415-22 (2001)]

Figure 1 Morphological diversity of dendrites: (A) Rat cerebellar Purkinje cell. (B) Mitral cell from zebrafish olfactory bulb. (C) Direction-selective ON/OFF ganglion cell from rabbit retina. Color coding indicates the depth (on the z axis) from the ganglion cell layer (red) to the outer border of the inner plexiform layer (green). (D) Visualization of a realistic model of a horizontal system north cell from fly lobular plate. (E) Retinal starburst cell labeled with enhanced GFP using a gene gun. Scale bars 20 μ m.

Altogether these data indicate that the differentiation of dendrites is determined by an interplay of external cues and internal factors. The external cues consist of signaling molecules (eg. Semaphorin, BDNF), transmembrane proteins (receptors) and neuronal activity, and internal factors include cell-intrinsic factors

such as transcription factors (eg. Cut, Hamlet) and cytoplasmic signaling molecules (eg. GTPases) and cytoskeletal molecules (Grueber and Jan, 2004; Landgraf and Evers, 2005; Parrish et al., 2007).

Among the extrinsic signaling molecules, neurotrophic factors [Neurotrophin 3, BDNF (Brain Derived Nerve Growth Factor) and NGF (Nerve Growth Factor)] affect dendritic morphology of cortical neurons in vertebrates. The neurons in different cortical layers have different branching pattern specific for that particular layer. Interestingly, neurons from layer 4 and layer 6 exhibit divergent responses to the same neurotrophic signal. Both BDNF and NGF affect dendritic morphology of these neurons differentially by either inhibiting or promoting dendritic outgrowth in different layers (McAllister, 2000; McAllister et al., 1997). The axon guidance cue Semaphorin 3A acts as an attractant, guiding dendritic growth in the cerebral cortex in mice (Sasaki et al., 2002), whereas graded expression of Semaphorin-1a cell-autonomously directs dendritic targeting of olfactory projection neurons in *Drosophila* (Komiyama et al., 2007). BMPs (Bone Morphogenic Proteins) affect dendritic arborization in cultured neurons and induce dendritic growth in sympathetic neurons (Beck et al., 2001; Scott and Luo, 2001).

Among the transmembrane proteins, Cadherin controls dendritic extension and spine morphology (Togashi et al., 2002) and EphB receptors regulate dendritic spine morphogenesis and synapse formation in hippocampal neurons in culture (Henkemeyer et al., 2003). The membrane receptor Notch has also been shown to inhibit dendritic growth through regulation of gene expression (Redmond and Ghosh, 2001). Recently, in *Drosophila*, a gene encoding the cell adhesion molecule *Dscam* was demonstrated to be involved in self avoidance mechanisms among the dendritic branches of the same neuron. *Dscam* generates alternatively spliced mRNAs that can be translated into thousands of different protein isoforms. Isoform-specific homophilic *Dscam* interactions cause dendritic branches of the same neuron to avoid each other ensuring the correct patterning

of dendrites in the peripheral nervous system (PNS) (Hughes et al., 2007; Matthews et al., 2007; Soba et al., 2007).

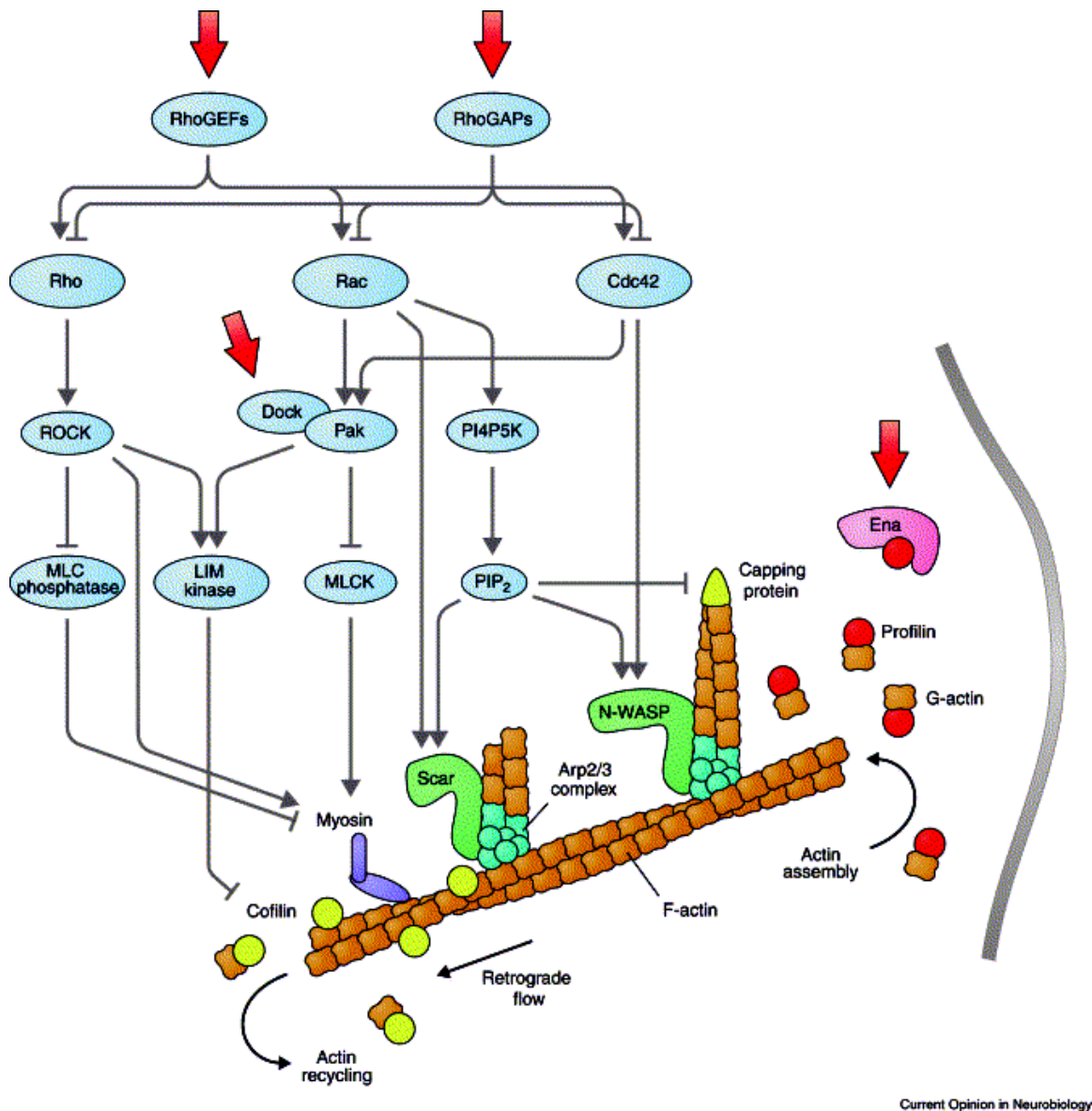
Among the intrinsic signaling molecules, the transcription factor Cut regulates distinct dendritic branching patterns of *Drosophila* multidendritic neurons based on its level of expression (Grueber et al., 2003a). The transcription factor Hamlet is a binary genetic switch between dendritic outgrowth and branching in sensory neurons of *Drosophila* PNS (Moore et al., 2002). Sequoia, a Tramtrack-related zinc finger protein, functions as a pan-neural regulator for dendrite and axon morphogenesis in *Drosophila* (Brenman et al., 2001). Tricornered (Trc), one of two NDR (Nuclear Dbf2-Related) family kinases, mediates a 'like-repels-like' behaviour of dendrites allowing for the complete but non-overlapping coverage of the dendritic fields of highly complex dendritic branching pattern neurons in *Drosophila* (Emoto et al., 2004).

Recent studies point out that some of the extrinsic factors act through signaling pathways like MEK [MAPK (mitogen-activated protein kinase) and ERK extracellular signal-regulated kinase] and CaMK pathway (Vaillant et al., 2002). These pathways act directly or through Rho family proteins to regulate cytoskeletal components and thus dendritic morphogenesis and branching (Miller and Kaplan, 2003).

However, how do the intrinsic factors as well as many of the extrinsic factors signal and regulate dendritic construction is an open question. It is conceivable that the coordinated action of intrinsic factors and external cues finally modify the structure of the dendritic cytoskeleton and determines the morphological characteristics of dendrites. Since actin and microtubule are essential structural components of dendrites, various signaling pathways regulating dendrite development must eventually end up affecting actin and/or microtubule dynamics (Jan and Jan, 2001).

1.3 Cytoskeletal molecules and dendritic morphogenesis

Two of the major components of the cytoskeleton are represented by the actin-based microfilaments and the microtubules, together with a number of molecules regulating the dynamic properties of both types of filaments. Considering the vast repertoire of cytoskeletal molecules, relatively few components of the actin and the microtubule cytoskeleton and their regulators are known to be involved in the establishment or remodeling of the dendritic arbor so far (Gao and Bogert, 2003; Landgraf and Evers, 2005; Scott and Luo, 2001) (Figure 2). For instance, the Rho family of small GTPases, including RhoA, Rac1, and Cdc-42 represent major conserved regulators of the actin cytoskeleton controlling the growth, extension and branching of dendritic arbors in a range of different systems including *Drosophila*, mouse and *Xenopus* (Cline, 2001; Grieder et al., 2000; Redmond and Ghosh, 2001; Van Aelst and Cline, 2004). Although a general consensus is not easily identifiable, each molecule seems to have relatively conserved basic functions. For instance, Rho restricts dendrite growth in *Xenopus* optical tectal cells (Adams et al., 2000) and *Drosophila* mushroom body neurons (Lee et al., 2000). In contrast, the constitutively active form of *Drosophila* Cdc-42 (Dcdc-42) dramatically alters dendritic patterning in the embryonic PNS (Gao et al., 1999). Non-receptor tyrosine kinase, Abl (Abelson kinase), is an actin-binding protein and promotes dendrogenesis by inducing actin cytoskeletal rearrangements at the actin cytoskeleton in cooperation with Rho family small GTPases in hippocampal neurons (Jones et al., 2004). Mutations in *Drosophila* enabled, an actin regulator of the Ena/VASP family, disrupt normal dendritic routing in neurons of the embryonic PNS and decrease dendritic branching (Li et al., 2005). In the same neurons, mutations in Tropomyosin, an actin filament-stabilizing molecule, produce increased dendritic fields (Ackermann and Matus, 2003).



[Dickson BJ, Curr Opin Neurobiol. 11(1):103-110 (2001)]

Figure 2 Cytoskeletal players: Representation of some of the cytoskeletal molecular players emphasizing signal transduction pathways that link Rho GTPases to the actin cytoskeleton. All the three small RhoGTPases act through several downstream effectors to affect cytoskeletal elements. Rho GTPase pathways regulate actin dynamics at several points, including filament nucleation and branching (Arp2/3 complex), filament extension (capping protein), retrograde flow (myosin) and actin recycling (cofilin). Red arrows indicate points at which these pathways are likely to be regulated in response to extracellular guidance cues.

More fragmented evidence is available for the role of microtubules in dendrite differentiation. For instance, MAP2 (microtubule associated protein 2) deficient

mice show reduction in microtubule density in dendrites leading to reduction in dendritic length (Harada et al., 2002), while inhibition of the microtubule-associated motor protein, CHO1/MKLP1, in hippocampal neurons in culture suppresses dendritic differentiation (Lee et al., 2000). Expression of the microtubule associated protein, MAP1A, is required for activity-dependent growth, branching, and stabilization of the dendritic arbor (Szebenyi et al., 2005). Another highly conserved protein and microtubule interactor, Lis1, has been implicated as a regulator of the microtubule cytoskeleton and is required in dendritic growth and branching in mushroom body neurons as well as in axonal transport (Liu et al., 2000). For the coordination of microtubules and actin cytoskeleton the molecules that cross-link them, such as Kakapo, should be of particular importance. Indeed, *kakapo* mutants display reduced branching of the dendrites in *Drosophila* embryo peripheral nervous system (PNS) neurons and motor neurons (Gao et al., 1999; Prokop et al., 1998).

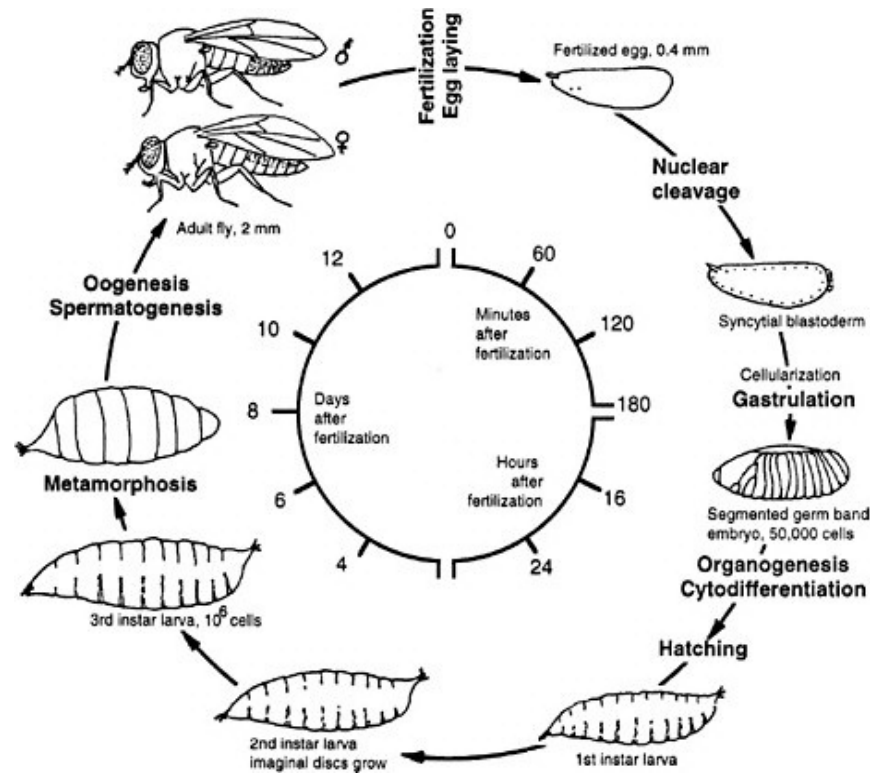
This limited number of identified cytoskeletal factors is far below the expectations and does not seem to correlate with the degree of diversity of dendrite structures. Therefore, it is essential to identify more molecular components that will allow us to elucidate the mechanisms of dendrite growth, branching and stabilization. This question can now be addressed in detail in *Drosophila*, owing to technological advances that allow *in vivo* labeling of the dendrites of identifiable neurons.

The aim of this project was to focus on cytoskeletal molecules by taking a candidate-based reverse genetics approach using RNA interference (RNAi) and to isolate cytoskeletal molecules affecting dendritic morphogenesis in the *Drosophila* embryonic PNS.

1.4 Model system: Peripheral Nervous System of *Drosophila melanogaster*:

The fruit fly *Drosophila melanogaster* has been at advantage over other model systems in many ways due to its well studied, elaborate classical and molecular

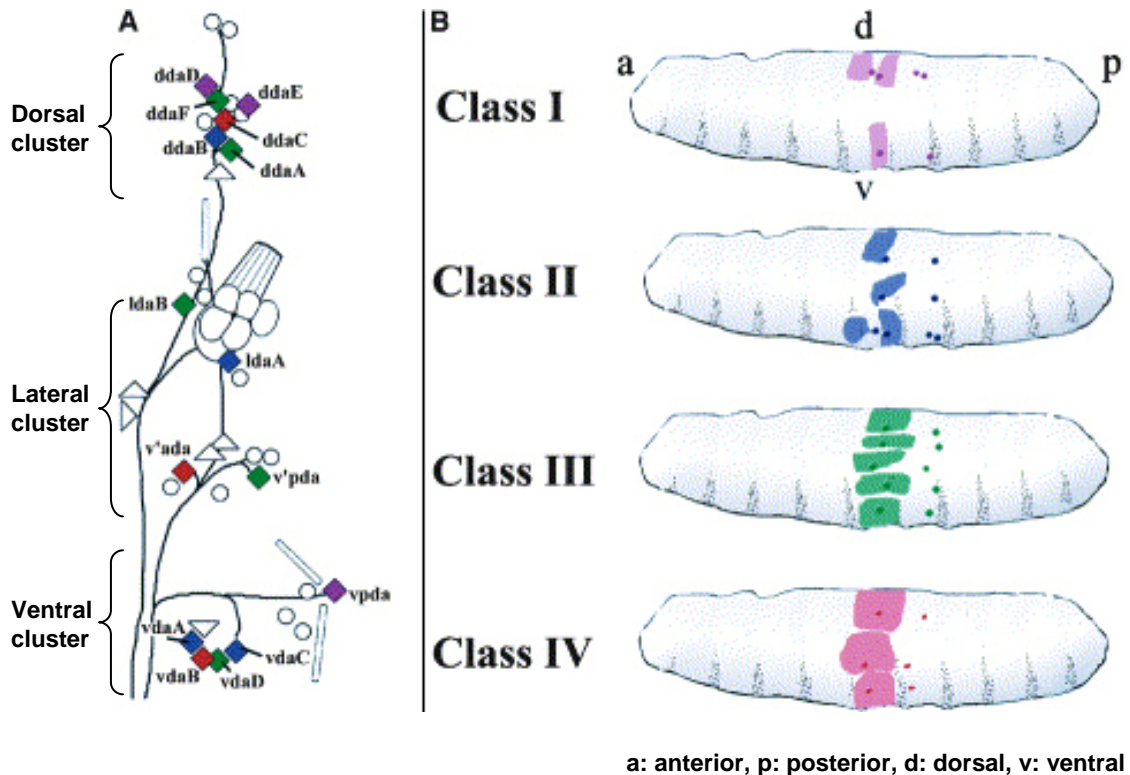
genetics. Therefore it has been widely used for uncovering important aspects of cell biology, neurobiology and development (Reaume and Sokolowski, 2006). *D. melanogaster* has a life cycle of 10 days at 25°C, during which it undergoes developmental morphogenesis from embryo to larva to pupa and finally the adult fly (Figure 3).



(Adapted from Wolpert, L., R. Beddington, J. Brockes, T. Jessell, P. Lawrence, and E. Mayerowitz. 1998. P. 484 in Principles of Development. New York: Current Biology.)

Figure 3 Life cycle of *Drosophila melanogaster*: The *Drosophila* egg is about half a millimeter long. Following fertilization, mitosis (nuclear division) begins. However, cellularization does not occur in the early *Drosophila* embryo till stage 5, resulting in a multinucleate cell called a syncytium, or syncytial blastoderm. It takes about one day after fertilisation for the embryo to develop and hatch into a worm-like larva. The larva eats and grows continuously, moulting one day, two days, and four days after hatching (first, second and third instars). After two days as a third instar larva, it forms an immobile pupa. Over the next four days, the body is completely remodelled to give the adult winged form, which then hatches from the pupal case and is fertile within about 12 hours. (timing is for 25°C; at 18°, development takes approximately twice as long.)

The larva hatches 1 day after the egg is fertilized. First, second, and third instar are larval stages, each ending with a molt. During pupation most of the larval tissues are destroyed and replaced by adult tissues derived from the imaginal discs that grow during the larval stages.

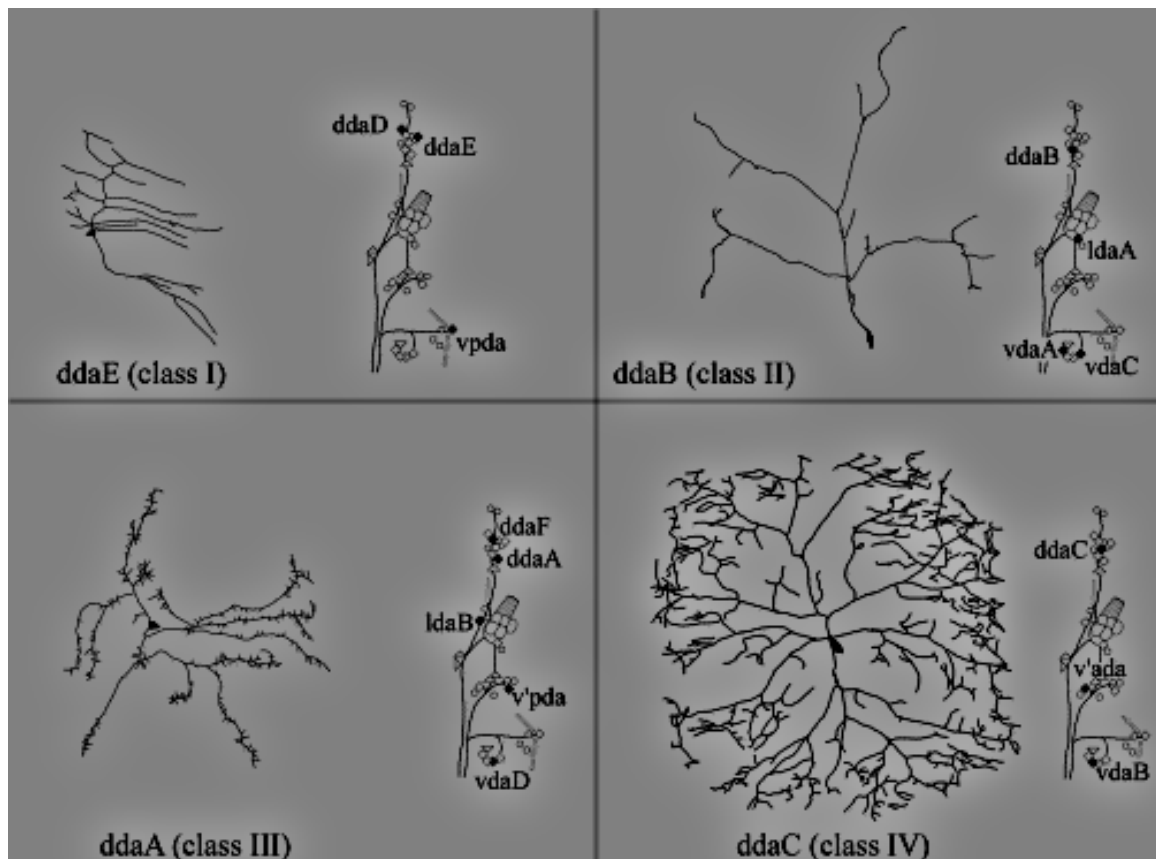


[(Grueber et al, Curr Biol. 13(8):618-26 (2003))]

Figure 4 PNS organization: Arrangement of da Sensory Neurons and their dendritic territories in the *Drosophila* Peripheral Nervous System. (A) A PNS schematic of a single abdominal hemisegment. da neurons of the same color have been placed in the same morphological class. (B) Arrangement of the territories of different da neuron classes along the larval body wall. The pattern shown is repeated in each abdominal hemisegment, although only two segments are schematized in this diagram (left segments with cell body and dendritic field indicated, and right segment with cell body only).

The peripheral nervous system (PNS) of *Drosophila* has been successfully used for studying the development of dendrites (Gao et al., 1999; Grueber et al., 2003b). PNS neurons of *Drosophila* embryos and larvae have been grouped into 3 major types – external sensory (es) neurons, chordotonal (ch) neurons and

multiple dendrite (md) neurons, including the dendritic arborization (da) neurons (Bodmer et al., 1987). These neurons have stereotyped dendritic morphologies and position in each abdominal hemi-segment of the embryo. The da neurons are further divided into four different groups depending on their dendritic complexity (Figure 4) (Grueber et al., 2002).



[Grueber et al, Cell. 21;112(6):805-18 (2003)]

Figure 5 Different morphological classes of da sensory neurons in *Drosophila* PNS: Mature morphologies of representative class I (A), class II (B), class III (C), and class IV (D) da neurons with the positions of other same-class neurons (closed diamonds) in a schematized abdominal hemisegment of the PNS. Dorsal is up and anterior is to the left.

Class I neurons comprise simple dendritic arborization neurons (Figure 5) and there are three of them in each abdominal hemi-segment, two in the dorsal cluster and one in the ventral cluster (labeled in violet in figure 4A). The four class II neurons (labeled in blue in figure 4A) have little more complex dendritic pattern and five class III neurons (labeled in green) are recognized by comb-like

small branches protruding from the main dendritic branches. The three class IV neurons (labeled in red in figure 4A) in each abdominal segment, instead, have a very complex arbor and altogether encompass the whole body wall on each hemi-segment (Figure 5) (Grueber et al., 2002).

The genetic programs that regulate the development and morphological diversification of these neurons are beginning to be elucidated. These neurons are supposed to be tension-sensitive, mechanoreceptors and proprioceptors. Their sensory input has recently been reported to be necessary for the generation of *Drosophila* larval locomotion, a form of rhythmic behavior (Song et al., 2007). As yet, however, there is no evidence of the functional relevance of their diverse dendritic morphologies. The class IV neurons are hypothesized to be mechanosensitive from genetic studies on pickpocket gene which is exclusively expressed in this specific class and mutates to show mechanosensory dysfunction (Adams et al., 1998; Ainsley et al., 2003). On the other hand the class I neurons are proposed to be proprioceptive because they have dendrites oriented in a preferential direction relative to the body axis and their axons target a more dorsal region of the neuropil, which is generally a characteristic of proprioceptive afferents in insects (Grueber et al., 2007).

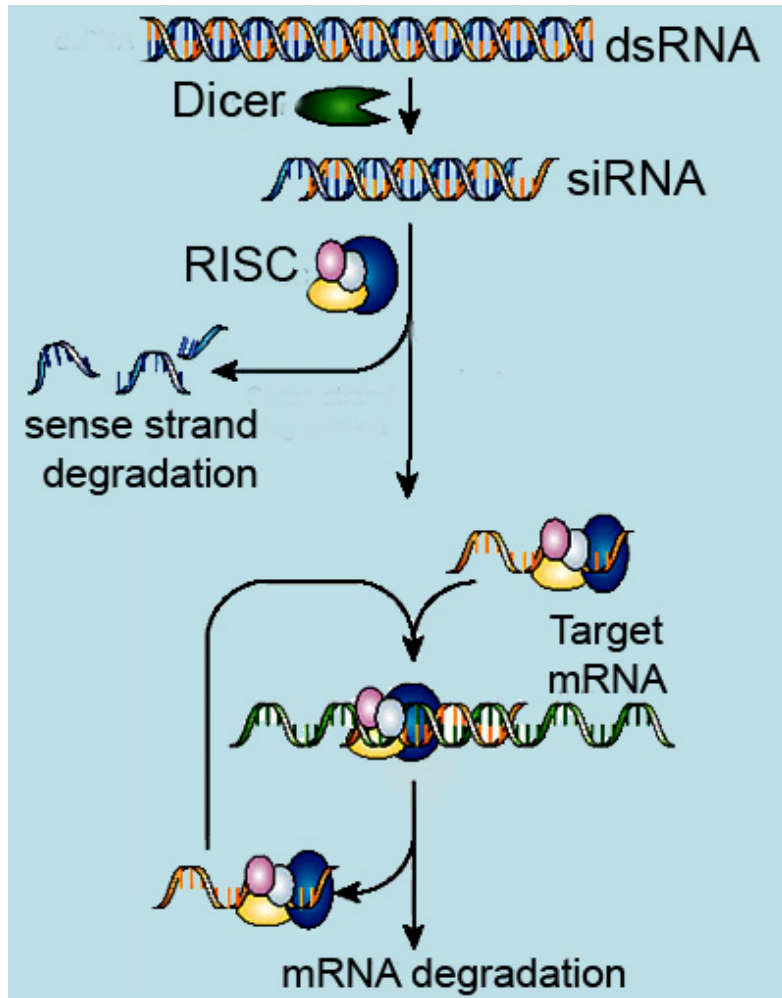
These well characterized da neurons present a very apt model system to understand developmental aspects of dendrites as well as structural differences between classes of neurons, which result in their unique dendritic patterns. Thus, we have used the PNS of *Drosophila* for insightful analysis of dendritic morphology establishment.

1.5 Assay System: RNA interference

RNA interference (RNAi) is a process of silencing of gene expression by double stranded RNA molecules in the cell. Research to date has hinted that RNAi is an ancient process which predates evolutionary divergence of plants and animals. RNAi in both plants and animals is mediated by small RNAs of approximately 21-

23 nucleotides in length for regulation of target gene expression at multiple levels through partial sequence complementarities (Ma et al., 2006). RNAi is triggered when a cell encounters a long double-stranded RNA (dsRNA), which might be produced from an introduced transgene, a viral intruder or a rogue genetic element (Figure 6). An enzyme called Dicer cleaves the long dsRNA into siRNAs. An RNA-induced Silencing Complex (RISC) then degrades the sense strand and the antisense strand is used for targeting complementary mRNA destruction. The repetitive cycles of degradation of specific mRNAs, results in no protein made and thus effectively silences the gene from which the mRNAs were produced (Novina and Sharp, 2004).

Combined with wide spread genome sequencing, experimental use of RNAi as an assay system has the potential to interrogate systematically all genes in a given organisms with respect to a particular function (Ma et al., 2006). Thus, this thesis presents a small scale analysis to identify genes encoding cytoskeletal molecules required in dendritic morphogenesis on the basis of phenotypic profiles.



[Modified from Novina and Sharp, *Nature*. 430(6996):161-4 (2004)]

Figure 6 RNAi mechanism RNAi is triggered when a cell encounters a long double-stranded RNA (dsRNA). An enzyme called Dicer cleaves the long dsRNA into siRNAs. An RNA-induced silencing complex (RISC) then distinguishes between the different strands of the siRNA. The sense strand (blue) is degraded. The antisense strand (yellow) is used to target genes for silencing, and has one of several fates depending upon the organism. In fruitflies and mammals, the antisense strand is incorporated directly into RISC to target a complementary mRNA (green) for destruction. In the absence of siRNAs, the RISC lacks sequence-specific mRNA-binding properties. But when bound to the antisense strand, the now activated RISC can participate in repeated cycles of degradation of specific mRNAs, such that no protein is made — effectively silencing the gene from which the mRNAs are produced.

RNA interference (RNAi) has been used successfully to study the role of molecules affecting dendrite morphology like CaMKII β and Hamlet (HAM). Introduction of dsRNA targeting CaMKIIB results in reduction of dendritic arborization in hippocampal neuronal cultures (Fink et al., 2003). RNAi of *ham*

transcript abolishes all HAM protein expression in *Drosophila* embryo and results in significant increase in the number of external sensory neurons as well as reduction of dendritic arbors in multidendritic neurons in the PNS of *Drosophila* (Moore et al., 2002). Thus, RNAi can be used as an effective tool to screen for molecules affecting dendritic morphogenesis.

While using RNAi as a screening assay, some important facts about complications associated with this method should be noted. Owing to a tolerance for mismatches and gaps in base-pairing with targets, small RNAs could have up to hundreds of potential target sequences in a genome and some small RNAs in mammalian systems have been shown to affect the levels of many messenger RNAs besides their intended targets (Ma et al., 2006). In *Drosophila* also off target effects mediated by short homology stretches within long dsRNAs are prevalent leading to false positive results. Another weak point of RNAi screens is that the effectiveness of dsRNA for each molecule varies depending on the organism, cell type or target sequence leading to differential phenotypic output of the knockdown of each gene (Asikainen et al., 2005).

1.6 RNAi assay: positive products- Diaphanous and Profilin

This thesis describes the knock down by RNAi of cytoskeletal molecules suspected to be involved in dendritic morphogenesis and the genetic analysis of positive candidates resulted from this assay. The 2 positive candidates which were isolated and selected for further studies were Diaphanous and Profilin.

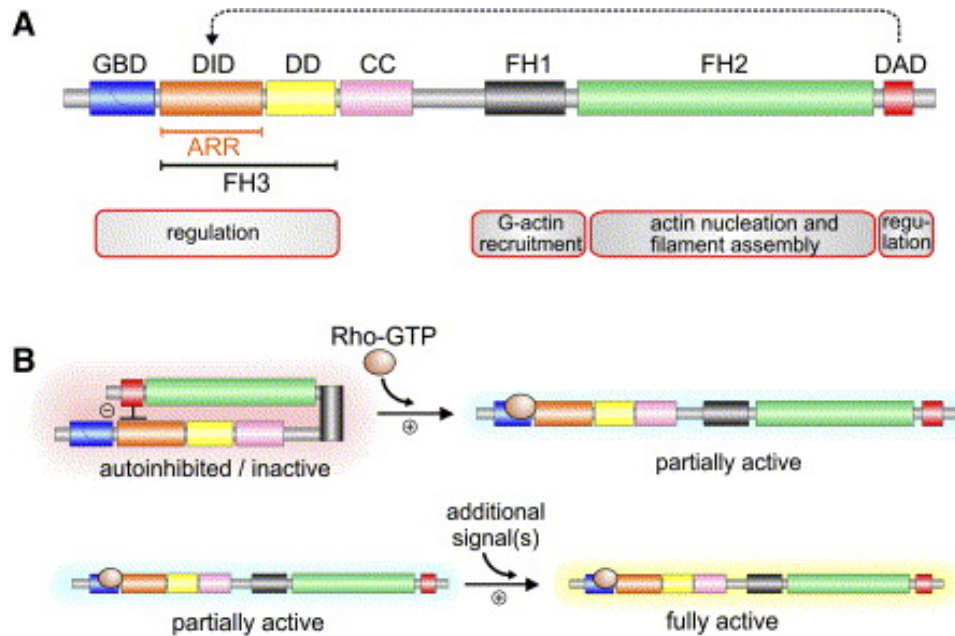
1.6.1 Diaphanous

Diaphanous is a member of the formin homology (FH) domain protein family. Formins are a widely expressed family of proteins that govern cell shape, adhesion, cytokinesis, and morphogenesis by remodeling the actin and microtubule cytoskeletons. The predominant class of formins in fungi and animals are diaphanous-related formins (DRFs), which are regulated by autoinhibitory intramolecular interactions between their N and C termini.

Diaphanous is the founding member of the DRFs. The DRFs include the Diaphanous, *DRF1* and *DRF2* in humans, *DRF2* in mouse and *Bni1*, *Bnr1*, and *for3p* in yeast (Peng et al., 2003).

Diaphanous is predicted to have 3 FH domains (Figure 7A), of which the FH1 and FH2 domains and the linker between them have been implicated in the nucleation of actin filaments (Sagot et al., 2002). In addition, FH1 is marked by its high proline content and is responsible for the binding of Profilin (Chang et al., 1997), upon which the actin elongation activity of formins can be enhanced (Kovar, 2006). Formin FH2 domains are involved in binding to actin and other actin binding molecules. The FH2 domains have been shown to alter actin polymerization dynamics by accelerating *de novo* filament nucleation, altering filament elongation/depolymerization rate, and by preventing filament barbed-end capping by capping proteins. This effect varies between formins with varying potency (Higgs, 2005). A third Formin homology domain, FH3, was reported to exist N-terminal to the FH1 of several formins but its true identity as a functional domain is doubtful.

Other than FH domains, Diaphanous has other important domains which affect its activity. The Diaphanous Autoinhibitory Domain (DAD) is a stretch of 20–30 amino acids found C-terminal to the FH2 domain (Figure 7B) that binds with sub-micromolar affinity to the Diaphanous inhibitor domain (DID), a ~250 residue region located near the N terminus. The DAD–DID interaction is sufficient for auto-inhibition and to affect actin dynamics (Kovar, 2006). RhoA competes with DAD for binding the mDia1 N terminus, relieving the auto-inhibitory interaction and enabling mDia1 to influence actin dynamics. Based on the relative approximate positions of their putative GTPase binding domains and diaphanous inhibitory domains, other Rho GTPases are likely to have similar activating roles for other Formins (Ridley, 2006). Thus, different GTPases may regulate different Formins specifically.



[Faix and Grosse, *Dev Cell.* 10(6):693-706 (2006)]

Figure 7 Domain Organization and Molecular Regulation of Diaphanous-Related Formins: (A) Schematic representation of the domain organization of a representative DRF such as mDia1. Abbreviations: GBD, GTPase binding domain; DID, Diaphanous-inhibitory domain; DD, dimerization domain; CC, coiled coil; FH1, formin homology 1 domain; FH2, formin homology 2 domain; FH3 formin homology 3 domain; ARR, armadillo-repeat region. The loosely defined FH3 region is based on sequence similarities to other DRFs and does not match true domain boundaries. (B) Autoinhibition of DRFs, caused by the interaction of DAD with DID, is partly relieved by association of an active, GTP bound Rho GTPase to GBD, allowing DID to adopt a structured conformation that, in turn, appears to induce release of DAD, leading to a partial activation of the DRF.

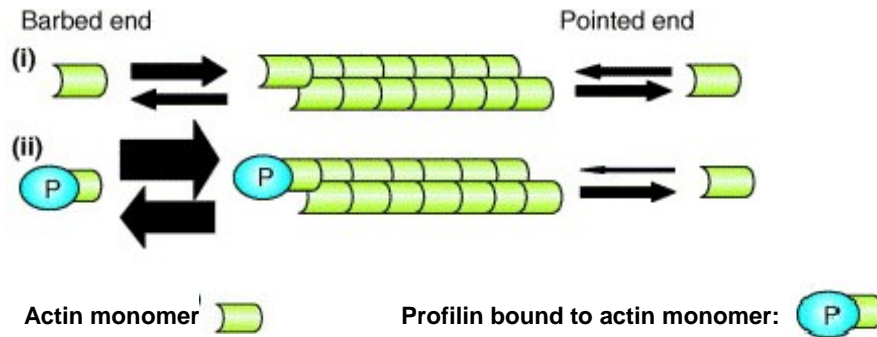
The connection between formins and microtubules (MT) is less well understood. In yeast, the MT effects appear to be dependent on the ability of formins to generate polarized actin cables whereas, in mammalian cells, formin signals that cause MT stabilization and polarization might be more direct (Wallar and Alberts, 2003). Recent studies have also shown that formins bind to microtubules through a peptide domain situated in their N-terminal region and separate from the FH domains (Zhou et al., 2006).

These versatile regulators of actin nucleation, elongation and of filament stability have been involved in a number of cellular and morphogenic processes (Faix

and Grosse, 2006). The various processes include filopodia formation, cell adhesion and motility, endocytosis, cell polarity, etc. *in vivo* studies in *Drosophila* implicate a role for Diaphanous in cell division, which is apparent by cytokinesis defects during spermatogenesis and oogenesis giving rise to germlineless phenotype (Castrillon and Wasserman, 1994). Diaphanous also controls the formation of the furrow canal by directed actin assembly during *Drosophila* cellularization (Grosshans et al., 2005).

1.6.2 Profilin

Profilin was among the first actin-binding proteins to be characterized. Profilins bind to actin monomers in 1:1 ratio. Conflicting data suggest that Profilin might function to promote either actin polymerization or depolymerization in cells. Perhaps the most accurate description of Profilin emphasizes its ability to boost actin-filament dynamics, both in polymerization and in depolymerization (Figure 8) (Yarmola and Bubb, 2006). Profilin-bound monomers cannot nucleate. Thus, Profilin inhibits spontaneous nucleation, making essential the nucleation factors that can overcome the high cellular concentration of Profilin. One essential function of Profilin seems to be the nucleotide-exchange activity that accelerates the ADP–ATP exchange on G-actin 1000-fold, thereby replenishing the pool of ATP–actin in the cell. Once filaments are nucleated, they can use the Profilin-bound monomer to elongate at their barbed ends. The filament elongates from both barbed and pointed ends but barbed-end elongation is favored ~10:1 over pointed end elongation. Besides accelerating the nucleotide exchange on actin monomers, Profilin can also promote filament elongation at free barbed ends following the dissociation of capping proteins. The free filament ends associate with Profilin–actin (profilactin) complexes, and the Profilin-bound actin is released and added to the filament. By this mechanism, Profilin can funnel actin monomers to the growing barbed end of the filament and promote actin polymerization. Thus, Profilin allows barbed end but not pointed end elongation of bound monomers (Higgs, 2005; Witke, 2004; Yarmola and Bubb, 2006).



[Yarmola EG, Bubb MR. Trends Biochem Sci. 31(4):197-205 (2006)]

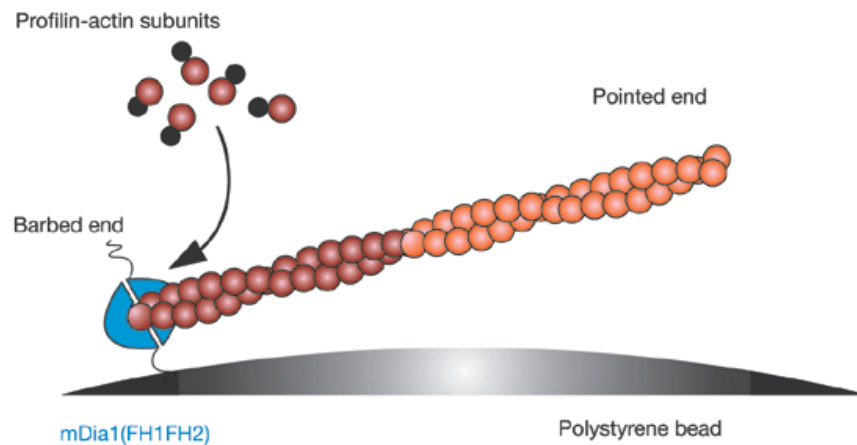
Figure 8: Profilin in actin dynamics Acceleration of actin-filament dynamics by profilin. (a) The effect of profilin (P) on the rates of elongation and dissociation at the barbed and pointed ends at steady-state is illustrated. The width of the arrows indicates the relative rates of reactions at steady state. As compared with dissociation in the absence of profilin (i), saturation by profilin accelerates the dissociation of subunits from the barbed end (ii) and accelerates the association of subunits in proportion to the formation of profilin-actin and the fraction of filaments not capped by profilin.

Profilin is an essential protein with cellular functions related to the actin cytoskeleton, including motility, development, signaling and membrane trafficking. In the absence of Profilin, actin-dependent processes such as cytokinesis and polarized growth fail in flies, Dictyostelium, yeasts and mammalian cells (Witke, 2004).

In addition to formins, several other proteins that are important to actin dynamics, including WASp (Wiskott-Aldrich syndrome protein) /Scar proteins and VASP (vasodilator-stimulated phosphoprotein), contain Profilin-binding poly-proline motifs. Profilin is estimated to have more than 50 characterized ligands from different organisms, although this is probably only a fraction of the number of actual Profilin-binding partners. The binding of Profilin to different ligands might provide a means of linking different pathways, by a mechanism that remains unclear, to cytoskeletal dynamics (perhaps in a cell-type-specific manner). Alternatively, the Profilin–ligand interaction might work in an actin-independent manner to regulate the ligands directly (Witke, 2004).

1.6.3 The role of Profilin in Formin function:

Profilin can bind to an actin monomer and a poly-proline sequence simultaneously, and both interactions are in rapid equilibrium, binding and releasing multiple times per second. Profilin binding to stretches of five or more prolines in the Formin homology 1 (FH1) domain brings an actin monomer in the vicinity of the FH2-bound barbed end. Profilin-bound monomer adds readily to the barbed end. For all Formins studied, Profilin accelerates barbed-end elongation by FH1–FH2 domain constructs (Figure 9). It is currently unclear whether this acceleration is due to increasing the local concentration of monomer, or to inducing a change in the processivity rate of the FH2 domain.



[Modified from Kovar et al, Nat Cell Biol. 6(12):1158-9. (2004)]

Figure 9 Formin- Profilin interaction Profilin–actin subunits add to a filament associated with mouse formin mDia1(FH1FH2) (in blur) attached to a polystyrene bead. Mouse formin mDia1 requires profilin–actin to remain processively associated with the elongating barbed end, which can grow at rates 10- to 15-fold faster than the rate of free barbed ends.

In contrast to its acceleration of Formin-mediated filament elongation, Profilin inhibits nucleation by formins. This effect is suggested by the strong inhibitory effect of Profilin on nucleation in the presence of mDia1 (Mouse Diaphanous 1) FH2 domain and the lower number of filaments generated by FH1–FH2 domains of mDia1, mDia2 or Bni1 in the presence of Profilin than in its absence.

Competition for monomer binding between the FH2 domain and Profilin might be the mechanism for this effect (Higgs, 2005).

1.6.4 Neuronal role of Diaphanous and Profilin:

The structural and molecular aspects of Diaphanous have been studied really well but mostly *in vitro* except some studies in Yeast, *Drosophila* and Zebrafish. A recent study in zebrafish reported the involvement of mDia in the regulation of convergence and extension movements during gastrulation and tail formation downstream of RhoA and Wnt signaling (Zhu et al., 2006). However, the neuronal role of diaphanous *in vivo* still remains ambiguous. The neuronal role in *Drosophila* has not been investigated till now.

One of the *in vitro* studies found that Swiss3T3 cells can elongate prolonged neurite-like processes best when higher mDia activity was achieved by overexpression a dominant active form of mDia1. This study uses stromal cell-derived factor (SDF)-1(Arakawa et al.), a neural chemokine, that can turn on two distinct Rho-dependent pathways with opposite consequences. A low concentration of the ligand stimulates a Rho-dependent pathway that mediates facilitation of axon elongation in culture in cerebellar granule cells. In contrast, Rho/ROCK activation achieved by a higher concentration of SDF-1 causes repression of axon formation and induced no further increase in axon length. A dominant negative mDia1 mutant interferes with SDF-1– dependent axon elongation and initiation. Further, mDia1 knockdown by RNAi annihilates both SDF-1– dependent axon elongation and axon initiation. The same study describes high expression of mDia1 in the cerebellar external granule layer where the earliest events in axonogenesis occur during early postnatal development in mice. In round cerebellar granule cells, mDia1 protein was found to be already colocalized with F-actin and tubulin at spots where an axon was likely to initiate and after axon outgrowth started, mDia1 was heavily enriched at the base of early initiating process and within its growth cones in close spatial

vicinity with actin filaments and microtubules (Arakawa et al., 2003). This study hints at the neuronal role of Diaphanous *in vivo*.

In case of Profilin, its functional aspects have been extensively studied *in vitro* as well as *in vivo*. In mice, neurons express two independent gene products – Profilin I and Profilin II. While Profilin I is ubiquitously expressed, Profilin II is found only in brain, skeletal muscle and kidney. Subcellular localization analysis of Profilin I has revealed that Profilin I is expressed in individual subtypes of brain neurons with high expression levels in hippocampal pyramidal cells in brain sections and cultured hippocampal neurons, and it localizes at individual pre- and postsynaptic specializations. Profilin I also localizes at both glutamatergic and GABAergic synapses and depolarization protocols significantly recruit Profilin I toward synaptic sites (Neuhoff et al., 2005). Another study in primary neuronal cultures showed activity-dependent targeting of Profilin II in dendritic spine heads (Ackermann and Matus, 2003). Interestingly, an *in vitro* study in neuronal cell cultures indicated, brain specific isoform of Profilin, Profilin II, as a negative regulator of neurite sprouting. Primary cultures of hippocampal neurons of Profilin II null mice display an increased number of highly branched budding neurites, with higher mean lengths (Da Silva et al., 2003). In flies, Profilin is required for motor axon outgrowth in the *Drosophila* embryo. Mutations in Profilin display a growth cone arrest phenotype for axons of inter-segmental nerve indicating its function in controlling axonal outgrowth (Wills et al., 1999). Thus from vertebrate and invertebrate studies, Profilin is shown to have a role in neuronal development as well as morphological alterations. However, its role in dendritic morphogenesis has not been investigated till now.

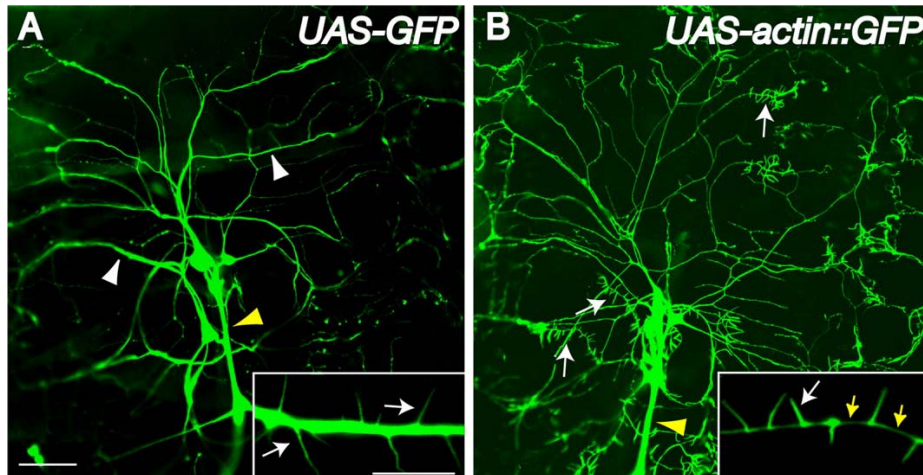
in vivo data about the role of both molecules -Diaphanous and Profilin- in dendritic morphogenesis are missing. In flies, both Profilin and Diaphanous mutate to germlineless phenotypes. However, their direct genetic interaction and binding in this system has not been demonstrated till date.

1.7 Analysis of dendritic branching *in vivo* and distribution of actin and microtubule in dendrites:

While molecular players of dendritic morphogenesis have been explored, the exact process of dendritic morphogenesis and how the cytoskeletal molecules are localized in the branches *in vivo* is not very clear. The *Drosophila* da neurons present a very ideal system to answer these questions. Different classes of md neurons have characteristic different morphologies and they are postulated to preferentially transduce different sensory modalities consistent with their distinct dendritic morphologies. It is conceivable that different classes of da neurons follow different pathways to finally attain their distinguished dendritic morphologies. However, it is not clear how the cytoskeleton *per se* contributes to formation of dendritic branches and to the final morphology. How does the interplay between microtubules and actin architect the dendrites? Some preliminary studies have been done to understand these issues.

Initial studies in *Drosophila* embryos have demonstrated distinct modes of initial dendrite formation and branching of class I –*ddaD* and *ddaE* neurons, and of class IV –*ddaC* neuron. In both class I -*ddaD* and *ddaE*, a first-order branch with a simple growing tip emerges at 13-14 hr AEL followed by one or two additional first-order branches. Within 1 hr, a number of lateral/second-order branches sprout laterally from the first-order branches undergoing repeated cycles of extension and retraction until a subset gets stabilized by ~18 hr AEL (Sugimura et al., 2003). On the other hand, cell bodies of *ddaC* are first visible at 15.5-16.5 hr AEL due to late expression of the Gal4 line used in this study. Every *ddaC* cell body is associated with two or three growing dendrite roots. In contrast to the morphologically simple tips of *ddaD* and *ddaE*, ends of *ddaC* dendrites look like growth cones with numerous filopodia. *ddaC* increases in arbor complexity by repeated bifurcation of the ends making it difficult to distinguish first-order and higher-order branches. Another interesting observation of these studies was that *ddaD* and *ddaE*, but not *ddaC*, almost fixed the shape of overall dendritic arbors at early larval stages. This study describes the development of dendrites at

earlier larval stages but not in the last larval stages. Also, it describes 2 of the class I neurons but the third one- vpda neuron- remains undescribed. It is possible that class I neurons have dynamic formation and withdrawal of their branches or branch extensions during late larval stages because the body surface of the larva grows very fast and so do the dendritic branches to cover the increased area.



[Andersen et al, J Neurosci. 25(39):8878-88(2005)]

Figure 10 Localization of Actin-GFP in dendritic filopodia *Drosophila* da neurons contain actin-rich filopodia restricted to dendrite compartments. Single-neuron dendrite images from the ddaA neuron from the dorsal cluster of sensory neurons from hemi-segment A6 with anterior toward the left and dorsal toward the top. A, A second instar larva (yw; Gal4-109(2)80, UAS-GFP) expressing GFP in da neurons demonstrates strong dendritic shaft (white arrowheads) and axon fascicle (yellow arrowhead) labeling. B, In comparison, a second instar larva (yw; Gal4-109(2)80, UAS-actin::GFP) expressing actin::GFP reveals actin-rich dendritic filopodia along dendrites (white arrows) that are absent on axonal shafts (yellow arrowhead). Actin::GFP demonstrates strong enrichment in dendritic filopodia with only limited fluorescence in dendritic shafts (inset, yellow arrows). Scale bars: (in A) A, B, 50 μm; insets, 5 μm.

Further studies using the Gal4/UAS system to express fluorescently tagged proteins to assess the dendritic compartmentalization and structure of class III da neurons resulted in visualizing actin-rich filopodia with GFP tagged actin construct. However, numerous *in vivo* microtubule reporters, including Tau::GFP, which binds microtubules *in vivo*, and Tubulin::GFP failed to label dendritic filopodia indicating that these dendritic filopodia were enriched in actin and devoid of microtubules (Figure 10) (Andersen et al., 2005; Grueber et al.,

2002). The filopodial like structures mentioned in above study are a key feature of class III neurons and it is not clear whether other classes of neurons also follow similar distribution of actin and microtubules.

in vivo live time lapse imaging could help a great deal to understand different events that occur during dendritic morphogenesis as well as to examine the cytoskeletal dynamics. It will especially help in understanding roles of different molecules in dendritic morphogenesis, for example, removing one particular molecule can affect withdrawal of branches but not the de-novo formation of branches.

This thesis describes standardization of *in vivo* live imaging set up to examine development of dendrites of PNS neurons over time. It also describes preliminary efforts to visualize class I vpda neuron with tagged Actin and Tubulin constructs to check the localization of Actin and Tubulin in dendritic branches and compartments. The latter approach will help to understand dynamic remodeling of cytoskeleton during dendritic branching and growth.

CHAPTER-2 MATERIALS AND METHODS

2.1 RNA interference assay

To generate dsRNA, we used genomic DNA from *Drosophila* embryos as initial template and amplified target DNA stretches by PCR using specific primers. The amplified product was then used to make double stranded RNA by T7 polymerase. The entire procedure is explained below in detail.

2.1.1 Genomic DNA extraction

Genomic DNA was extracted from wild type flies (80G2) with standard methods using DNA extraction protocol by Sigma DNeasy Kit. We then purified the genomic DNA using phenol-chloroform extraction and concentrated it by ethanol precipitation. The air-dried DNA pellet was suspended in water and stored at -20°C.

2.1.2 dsRNA preparation

Conserved sequences of around 500 bps for each candidate protein were chosen. The conserved sequences were blasted against the *Drosophila* genome to check their specificity for the selected molecule. Once assured of the uniqueness of the selected stretch reducing the risk of non-specific effects, we used it as template for RNAi assay for that particular protein.

The procedure can be described in short as follows:

A) Amplification of the target cDNA from genomic DNA by PCR with primers containing T7 promoter sequence tags at the 5' of the specific sequence. The primers were designed based on a published primer database (Table 1) (Rogers et al., 2003).

The following PCR protocol was used for amplification with minor alterations whenever required depending on the set of primer pairs:

Step1: 92⁰C -2mis

Step2: 92⁰C -45 sec

Step3: 60⁰C -1min

Step4: 72⁰C -1min

Repeat Step 2 to 4 - 35 times

Step5: 72⁰C -4mins

Step6: 10⁰C -infinite

Table 1: Primers used for amplification of DNA stretches:

T7: 5' TAA TAC GAC TCA CTA TAG GGA GA 3'

Gene (dsRNA length)	CG Number	FORWARD PRIMER	REVERSE PRIMER
adf/cofilin homologue	CG6873	GT136 GAAACTCTCGCTTGAGCACC	GT137 ATCTGGAATTAATTTGAGCCGC
Aip1 (665 bp)	CG10724	GT19 TTCAAGTTCAAGATGACCAAGC	GT20 TTCACCACATAGTCCGTGTAGG
Capulet (464 bp)	CG5061	GT21 ACTGCAGTACGTGACGCTGG	GT22 CACTCAGATCCAGCATGGG
Cappucino (685)	CG3399	GT138 ATATTGGACACGGATAGTGACG	GT139 CGTAAGGATGATGGAGAAGACC
Cofilin (twinstar) (208 bp)	CG4254	GT23 ATGTTGTA CTCCAGCTCCTTCG	GT24 ACAGGATACGTGTTTCCATCG
Diaphanous (695 bp)	CG1768	GT25 TCGTTCTGCATTGTCTATGAGC	GT26 ATCTTCTTCTCGTACTCCTCCG
δ-catenine (269 bp)	CG17484	GT6 ACCTTTCATTGACGCACGA	GT7 CCCAGAGATCTTGTACGTTGC
Kelch (668 bp)	CG7210	GT146 CAGATGTCAAATCCGTATGGC	GT147 TCGTT CAGATTATTGCTGTTGG
Profilin (chickaddee) (452 bp)	CG9553	GT31 CTTCCGTGGTAGAGAACTTGG	GT32 TTCTTA ACTATTGATTGGGGCG
Quail (661)	CG6433	GT150 GTACCGAGATGCCTTACAATGG	GT151 GCATTTTGGACATAACTTTGGG
Scar (562 bp)	CG4636	GT33 GTGTATCAGCAGGATGAGCTGC	GT34 TCTTCTGTTTCTTATTGCCACG
Slingshot (622 bp)	CG6238	GT35 GGAGATCGATAACTTCTTTCCG	GT36 GTTCTCCATAGACTGGCTTTGC
Sra-1 (604 bp)	CG4931	GT37 GATCACGTCAAGTACATTTCCG	GT38 ATAGCTGAGTGGAGGAAGGTCC
Twinfillin (591 bp)	CG3172	GT39 ATAGGTCCCCTACTGGAAAAGG	GT40 GTACGACTCAAAGTAGTCGCC

B) The amplified cDNA stretches were used as templates to transcribe dsRNAs using T7 RNA polymerase, and let it anneal to form dsRNA. This was done using MEGAscript RNAi kit from Ambion which is supplied with all the necessary reagents needed for reaction except for the specific primers.

C) The dsRNA was resuspended in water and after measuring its concentration was stored at -20°C . This dsRNA was diluted to get $50\text{mg}/\mu\text{l}$ final concentration in injection buffer to inject in stage 4 embryos (syncytial blastoderm stage) before the process of cellularization starts to have ubiquitous uptake of the dsRNA.

2.1.3 Injecting dsRNA in embryos

The whole process of injection can be described in short as follows. Cages were set up using 2- to 4-day-old 80G2 flies. Apple juice agar plates were alternated every hour to synchronize the egg collection for 1 day. The eggs were collected over a 30- min period for subsequent injection. The embryos of 80G2 flies were collected from the apple agar plate after incubation at 18°C for 30 mins. All these embryos were at early embryonic stage and were injected within an hour before they reached stage 5 when the cellularization begins. The collected embryos were bleached to get rid of their chorionic membrane and were aligned in a row on an agar strip with their anterior tip, recognized by a micropile, facing out. The embryos were aligned very close to each other to increase the injection rate and efficiency. These embryos were then transferred to a sticky coverslip with heptane glue to fix the embryos on to it. This transfer changed the orientation of embryos which now had their posterior tip facing out. The embryos were dried on silica gel for appropriate time (usually 13 mins) just enough to aid injections but letting the embryos humid enough to survive. The embryos were then covered with 10S halocarbon oil to avoid more dehydration and at the same time allow air exchange. These embryos were then ready for injections and were carefully kept on the microscope stage which aided fine tuning during injection procedure.

Special 1.5mm diameter capillaries (Science products GmbH) were used for injections. These capillaries were pulled to get fine tapering tip. A needle is filled

using a pipette by sucking injection buffer or RNAi solution from its fine tip which was cut wide enough just to pierce the embryos but not rupture them. It was very important to have a tremendous fine control over the pressure to manipulate the amount of liquid injected into the embryos. We used a FemtoJet microinjector (Eppendorf AG, Germany) to control the pressure, amount of solution injected and the speed of injections. The resting constant (compensation) pressure was usually 25hPa, while the injection pressure was 91hPa. The time of one injection event was 0.5 sec. After injections, slides were stored at 18⁰C in a moist chamber to prevent drying out the embryos.

2.2 Fly genetics

All the flies and crosses were grown and amplified at 25⁰C in humidity controlled incubators. Flies were fed on fly food made using following protocol for 5 lit volume:

Water 3.5 lit

Agar 82gm

Molasses 560gm

Maize Flour 420gm

Yeast 105gm

Propionic acid 44ml

Methyl Paraben 16.8gm

Agar was added in boiling water with constant stirring. Molasses, maize flour and yeast were added and mixed well once the agar was completely dissolved. This food was let cook for ~1 hr at 96⁰C and then cooled down to 60⁰C before adding and mixing propionic acid and methyl paraben to it. This fly food was then immediately used to pour into food bottles and vials. The vials and bottles with fly food were generally stored at 4⁰C and allowed to dry at room temperature for ~2hrs before using them for fly cultures. A dollop of yeast paste was added to the food for inducing egg laying.

Flies were fed on apple agar for embryo collection and the following protocol was used for making this apple agar:

500 ml 100% Apple juice

480 ml ddH₂O

40 gm Agar

10.5 ml 95% Ethanol

10 ml Glacial Acetic Acid

The apple juice and ddH₂O were boiled together and agar was added to it with constant stirring. The solution was cooled to ~60°C once the agar was dissolved completely. Ethanol and glacial acetic acid were added and mixed well. The pH was adjusted to 4.25- 4.40 with 100% NaOH. The plates were poured and stored at 4°C after solidifying.

2.2.1 *Drosophila* Stocks

Flies were obtained from different labs or the fly stock center as noted below.

Fly stock	(Reference)	Source
$y^1 w^-$; P(w^+ lacW) $dia^{K07135} cn^1$ / Cyo	(Butler et al., 2001)	Bloomington stock center, USA
$dia^5 cn$ / Cyo	(Castrillon and Wasserman, 1994)	J Grosshans, ZMBH, Heidelberg, Germany
$dia^9 cn$ / Cyo	(Castrillon and Wasserman, 1994)	Bloomington stock center
P(UAS-dia-CA)/TM6	(Somogyi and Rorth, 2004)	P. Rorth, EMBL, Heidelberg, Germany
$chic^{221} cn^1$ / Cyo; ry^{506}	(Verheyen and Cooley, 1994)	Bloomington stock center
P(ry^+) $chic^{11}$ / Cyo; ; ry^{506}	(Castrillon et al., 1993)	Bloomington stock center
$chic^{37}$ / Cyo	(Verheyen and Cooley, 1994)	Bloomington stock center
P(UAS-chic)/TM3	(Hopmann and Miller, 2003)	L. Cooley, Yale University, USA
w^{1118} ; P(w^+ EP) Dys ^{EP3397} /TM6B, Tb ¹	(van der Plas et al., 2006)	Bloomington stock center
ElavGal4 UAS- <i>mCD8GFP</i> hs-FLP; TubGal 80 FRT 40A /Cyo	(Moore et al., 2002)	Y N Jan, UCSF, USA
Gal4 109(2)80-UAS <i>mCD8GFP</i>	(Gao et al., 1999)	Y N Jan, UCSF, USA
Gal ²⁻²¹ UAS <i>mCD8GFP</i>	(Grueber et al., 2003b)	Y.N.Jan, UCSF, USA
Gal ¹²⁻²¹ / Gal ¹²⁻²¹	(Grueber et al., 2003a)	Y.N.Jan, UCSF, USA
Gal ⁴⁴⁷ UAS <i>mCD8GFP</i>	(Grueber et al., 2003b)	Y.N.Jan, UCSF, USA
<i>ppk</i> -eGFP	(Grueber et al., 2003a)	Y.N.Jan, UCSF, USA
p[w^+ ,UASp-GFP- α -tub]/ MKRS	(Grieder et al., 2000)	Nicole Grieder, HHMI, Baltimore, USA
UAS-GMA	(Dutta et al., 2002)	Bloomington stock center
w^- ; $al^1 dp^{ov1} b^1 pr^1$ P(neo FRT 40A)/Cyo		Bloomington stock center

2.2.2 Generation of recombinants

To obtain FRT- combining lines of *dia* and *chic* for MARCM analysis, stocks of *w*; *al*¹ *dp*^{ov1} *b*¹ *pr*¹ P(neo FRT 40A)/*Cyo* were crossed with *y*¹ *w*⁻; P(*w*⁺*lacW*) *dia*^{K07135} *cn*¹/ *Cyo* and *chic*²²¹ *cn*¹/ *Cyo*; *ry*⁵⁰⁶ respectively and females of the genotype *dia*^{K07135} *cn*¹/ *al*¹ *dp*^{ov1} *b*¹ *pr*¹ P(neo FRT 40A) and *chic*²²¹ *cn*¹/ *al*¹ *dp*^{ov1} *b*¹ *pr*¹ P(neo FRT 40A) were selected to induce female meiotic recombination. Prospective recombinant lines were set up and tested for the presence of FRT element by neomycin resistance and for the presence of the respective mutations by following visible phenotypic markers [eye color (*w*⁺) in case of *dia*^{K07135} and loss of *cn*¹ in case of *chic*²²¹] and by lethality non-complementation with the original mutations. Confirmed recombinant lines were started from a single male crossed to a balancer stock and amplified for further use.

2.2.3 Transgenic flies:

Full length cDNA of *diaphanous* gene was amplified from a cDNA library (Drosophila Genomics Research Center, Indiana, USA) by PCR using the following primers:

Forward primer (GT399) 5'- ATAAGAATGGTACCAAGAATGTCTCGTCACGAGAAAAC
Reverse primer (GT42) 3'- TATCAATCGCCGGCGCCGGAGCCTAGAACCTC.

This construct was cloned into a BglII/NotI-digested pP(UAS) vector (Brand and Perrimon, 1993). For mRed tagged constructs, a mRed tag was fused to the N terminus with an ATG codon using forward primer (GT41) 5'- CGGAATTCGAAGAATGTCTCGTCACGAGAAAAC and then cloned into the P (UAS) vector.

These vectors were then amplified in bacterial cultures from which the DNA was purified (Plasmid Maxi kit, Quagen), and was then dissolved in water and stored at -20⁰C before being used for injections. The injections were done as per the procedure described above (section 2.1.3) except that a stock of *w*¹¹¹⁸ flies was used for embryo collection.

The establishment of transgenic lines was done according to standard procedures (Spradling and Rubin, 1982). Two lines containing different insertion of the full length UAS-*dia* construct were used: (UAS-*dia*)^{A3-1}/FM7 (X chromosome) and (UAS-*dia*)^{G3-1}/TKG (3rd chromosome), and one for the mRed tagged construct: (mRed-UAS-*dia*)^{E3-1} (3rd chromosome).

2.3 MARCM (mosaic analysis with repressible cell marker)

To identify and characterize the peripheral dendrites of each da neuron we used the MARCM system (Lee and Luo, 1999). For producing clones, females of *ElavGal4* UAS-*mCD8GFP* *hs-FLP*; *TubGal* 80 FRT 40A /*Cyo* and males of *dia*^{K07135} P(neo FRT 40A)/ *Cyo* or males of *chic*²²¹ P(neo FRT 40A)/ *Cyo* were crossed with each other. The mated flies were provided with a freshly yeasted apple agar plate and allowed to lay eggs for 2 hours. Developing eggs were kept at 25°C for 3-5 hrs after the end of the laying period before the heat shock. The heat shock was performed at 38°C for 45 min, followed by room temperature recovery for 30 min, and an additional exposure to 38°C for 30 min. The embryos were then incubated at 25°C till they developed into larvae. We identified GFP-labeled clones by examining living third instar larvae under a fluorescence microscope fitted with a 10x lens. Selected larvae were pressed carefully between a slide and a coverslip in 90% glycerol to restrict movement but not cause bursting of the body wall and imaged using confocal microscope at 20X or 40X.

2.4 Time Lapse Imaging

As described in the results section (4.4.1) a round coverslip (12mm) was fixed on the metallic imaging slide directly over a 1 cm big and 2mm deep hole with the help of vaselin. Third instar larvae of the genotype *Gal4*²²¹UAS-*mCD8GFP* were covered in a small amount of Halocarbon oil that restricted movement on the coverslip. An air permeable ring was pressed on top of the larvae and screwed on the metallic slide (Figure 36). After imaging at confocal microscope the larva

was recovered with forceps and left to develop until the next imaging session at 18°C on an apple juice agar plate.

2.5 Image acquisition and processing

Confocal images were taken using a Leica TCS SP2 confocal microscope (Leica Microsystems Heidelberg GmbH, Germany) by exciting GFP using the 488 nm line of the argon laser. Abdominal hemi-segments A6 or A5 were imaged for all experiments. Z stacks were acquired at ~1 μm intervals at 20X or 40X magnification with 1024 x 1024 pixels format and projected into a 2D image using Leica confocal software (Leica Microsystems Heidelberg GmbH). For class I vpda neurons, 10-25 image stacks containing the entire neuron were collected at 20X. For time lapse, around 5-10 image stacks were collected for each vpda neuron. For class IV vpda neurons, ~50 stacks were generated of each quarter of the cell at 40X. Projection images were processed for brightness and contrast and assembled in Adobe Photoshop CS (Adobe Systems). Tracings of the neurons for measurement of dendritic length were made in Image J (National Institute of Health) by tracing the arbors using a mouse.

2.6 Quantitative analysis

We used Image J for quantifications of dendritic branch number and length of class I vpda neurons. Total number of branches was quantified by counting all the branch termini. The branches arising from the cell body were counted as primary branches. The branches arising from primary branches were defined as secondary branches and the branches arising from secondary branches were counted as tertiary branches and so on.

For class IV ddaC neuron, we printed projections of each quarter of the cell, aligned them manually and counted the termini to marking them with a pen to make sure not to recount the same termini.

Data in graphs are presented as means \pm SD (standard deviation). Statistical analysis was performed in Microsoft Excel.

2.7 Immunohistochemistry

3rd instar larvae were dissected in PBS flat on Sylgard with microscissors and pinned down with insect pins (Figure 11). Fixation was carried out for 30–60 min in 4% paraformaldehyde in PBS at room temperature, and the larvae were rinsed several times in PBS with 0.3% Triton X-100 (PBS-TX) for 10-30 mins each.

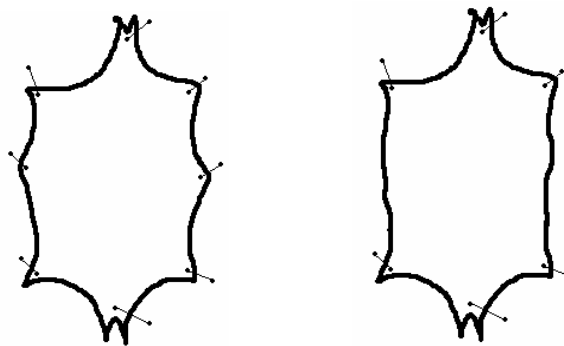


Figure 1: A cartoon showing a couple of useful ways to pin the larvae while dissecting 3rd instar larvae is pinned in PBS at their anterior and posterior tips with insect pins. They are then cut along their long body axis with dissection scissors. The body epidermis is opened with forceps and pinned to open up the entire body. The interior enteric system along with CNS and trachea is removed to get just the body wall with body muscles and PNS.

The fixed larvae were then unpinned and collected in an eppendorf tube in PBT. They were then blocked in 10% normal donkey serum or goat serum (Jackson Laboratories). Primary antibodies were used at a concentration of 1:5000 for rabbit anti-diaphanous (Grosshans et al., 2005), 1:400 for Rabbit anti- β gal (Molecular Probes) (for staining *dia*^{K07135}) and 1:200 for mouse anti-profilin (Hybridoma Bank) and incubated overnight at 4^oC. Secondary antibodies were Rhodamine goat anti-rabbit (diluted 1:200; Jackson Laboratories), Cy5-conjugated donkey anti-rabbit (Jackson Laboratories diluted 1:200) Cy3-conjugated donkey anti-mouse (Jackson Laboratories diluted 1:200) and Cy3-goat anti-mouse (Molecular Probes diluted 1:500), respectively. After overnight

incubation at 4⁰C or 2hrs at room temperature in secondary antibodies, the tissue was rinsed for three times in PBS-TX (30 mins each) and mounted in 90% glycerol to examine using confocal microscope.

2.8 Western blot analysis

Third instar larvae of the following genotypes were collected using fluorescent microscope at 10X magnification:

dia^{K07135}/*dia*^{K07135}; Gal-4²⁻²¹ *UAS-mCD8-GFP*/Gal-4²⁻²¹ *UAS-mCD8-GFP*

*dia*⁵/*dia*⁵; Gal-4²⁻²¹ *UAS-mCD8-GFP*/Gal-4²⁻²¹ *UAS-mCD8-GFP*

Gal-4²⁻²¹ *UAS-mCD8-GFP*/Gal-4²⁻²¹ *UAS-mCD8-GFP*

Samples were prepared from 5 larvae each for all the genotype. Extraction of proteins from larvae was carried out in lysis buffer. Western blots were done with standard western blot protocol. Western blots were incubated first with primary antibody (rabbit α -diaphanous, 1:5000 dilution) and then with a horseradish peroxidase-coupled goat α -rabbit secondary antibody at a 1:3000 dilution.

CHAPTER 3 – RESULTS (I)

RNA INTERFERENCE SCREEN

To identify cytoskeletal molecules involved in dendrite differentiation we took a candidate-based reverse genetics approach using RNA interference, RNAi. RNAi is a recently developed technique used widely in different model systems including *Drosophila melanogaster* (see introduction). This technique is often used to have an indication of the function of a molecule. In short, it is a post-transcriptional gene silencing process by which double stranded RNA (dsRNA) introduced into a cell, causes sequence-specific degradation of homologous mRNA sequences (Dykxhoorn et al., 2003).

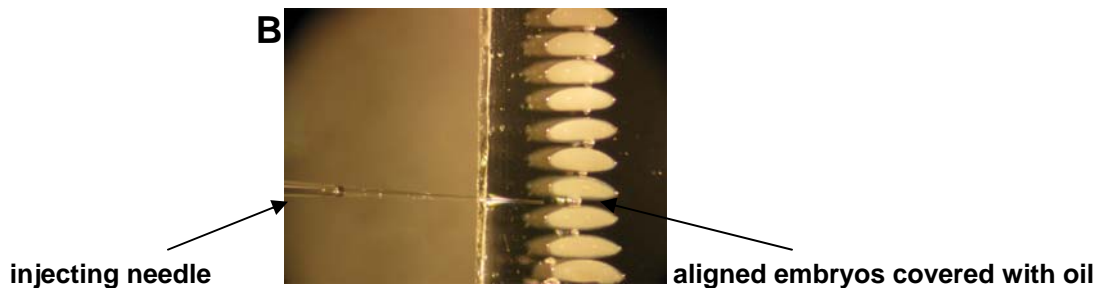
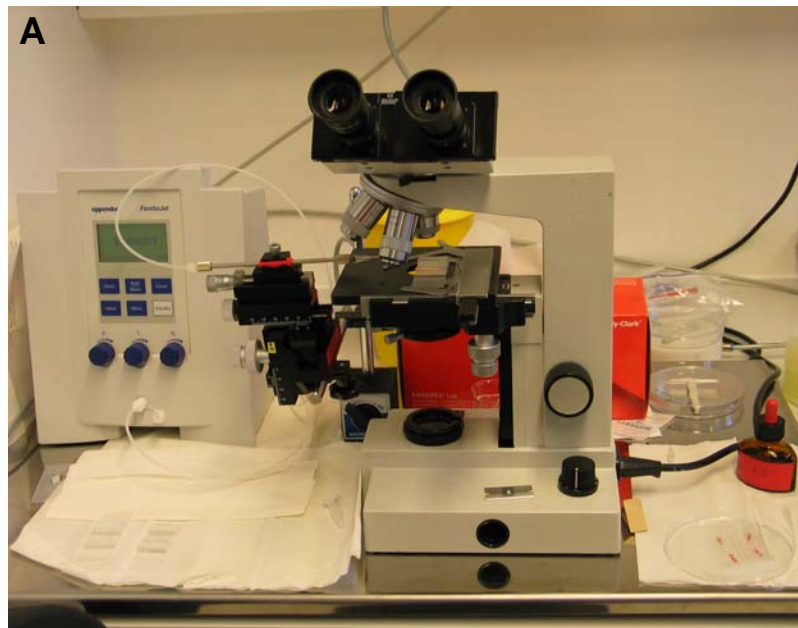
In the last few years, several *in vivo* as well as *in vitro* RNAi screens have been carried out in *Drosophila* to identify molecules involved in different processes, such as embryonic nervous system development or the establishment of cellular morphology (Koizumi et al., 2007; Rogers et al., 2003). Taking advantage of the published *Drosophila* genome and RNAi screens in *Drosophila* S2 cells I screened a few molecules based on their known functions, phenotypes, expression patterns and availability of reagents. Positive candidates from this screen were selected for further genetic analysis to study their role in dendritic morphogenesis.

3.1 Standardizing RNAi assay system

For the RNAi assay, *Drosophila* embryos were injected with dsRNAs using a micro-injector. The injection set up was built using a known protocol (see details in materials and methods). This set up included the following parts:

- A micro-injector which could regulate the pressure and the time of injection (Figure 12). Adjusting these parameters ensured to a certain extent that the amount of RNAi solution delivered in each embryo was similar.

Figure 12: Microinjection set up for RNAi assay (A) A micro-injector was used to control the pressure and approximate amount of solution at every injection shot. The injector was connected to a holder which held the injecting needle via a thin tube. Previously aged and carefully dried embryos were aligned on a coverslip and covered with 10S halocarbon oil. This coverslip was put on a slide to be visualized at the light microscope for the injection process. (B) Ready to inject embryos: Embryos were collected for 30 mins and dechorionated by bleaching. They were then aligned on an apple agar strip and then transferred to a heptane glue applied coverslip in a way that they were stuck to the coverslip. These embryos were then dried in on silica gel airtight container for ~13 mins and covered with halocarbon oil. The coverslip was then mounted on a slide and the embryos were thus ready to be injected with a pulled needle with a slanted end. The needle was always kept submerged in the halocarbon oil after it was filled with the injecting solution to avoid drying and precipitation of salts at the tip and thus blocking of the tip.



- Glass capillaries of $1.5\mu\text{m}$ diameter were pulled using a needle puller to form extremely thin tapering injecting tips. To obtain a sharp tip for easier insertion in the embryo, this tip was further broken to get a slanting edge using a blade.

- A light microscope to visualize and inject embryos.
- Apple agar plates with the right thickness and moisture to collect embryos and to align them. The apple agar plates for collecting embryos were thinner (~3-4mm) than the ones (~7-8mm) used for aligning the embryos.
- Drying chamber containing silica gel for drying the embryos prior to injection. The time of drying was carefully monitored (13 mins in most of the injection rounds).
- 10S Halocarbon oil was used to cover the embryos just enough to prevent them from drying and making sure of air exchange.
- A humidity controlled incubator at 18⁰C to incubate the injected embryos till they develop to embryonic stage 17 after around 40-42 hrs.

All these delicately managed elements were crucial to have a successful round of injections with good survival rate. After the set up was ready, the feasibility and the efficiency of the RNAi approach was first tested by injecting injection buffer (0.1 mM NaPO₄, pH 7.8/5 mM KCl) (Misquitta and Paterson, 1999) and scoring survival rates and the percentage of embryos that showed defective development simply due to the injection procedure. About 23% of the injected embryos (n=209) survived without any visible defect thus making them suitable for analysis of phenotypic changes.

The next step was to check the functionality of RNAi in the model system. Since a *GFP* expressing fly line was going to be used for the screen, it was possible to examine knock down of *GFP* expression by injecting ~50µg/ml siRNAs for *GFP* (Guido Pante- Personal communication). In this experiment, a distinguishable reduction was observed in *GFP* expression of *GFP*-siRNA injected embryos (Figure 13). This proved that we were able to knock down protein translation successfully with RNAi.

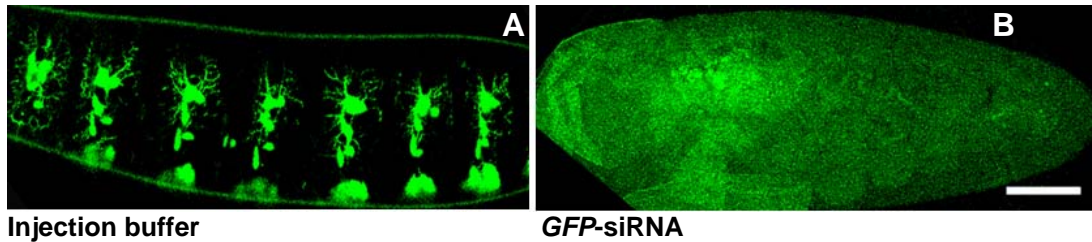


Figure 13: Knock down of *GFP* expression in *GFP*-siRNA injected embryos
 Embryos of 80G2 strain were injected with either injection buffer or *GFP* siRNA and visualized at late stage 17 for *GFP* expression. The embryos injected with injection buffer did not show any difference in the expression level of *GFP* (A) whereas the embryos injected with *GFP* siRNA showed a complete knockdown of *GFP* with almost no expression of *GFP* (B). Scale bar: 70 μ m

We subsequently needed to standardize the final injection concentration of dsRNAs for all the molecules to be screened. *tramtrack* (*ttk*) was used as a testing control molecule since it exhibits a well described phenotype with RNAi. *ttk* is a transcription factor expressed in the peripheral nervous system (PNS) and it suppresses neuronal cell fate in developing embryos, including chordotonal (ch) organs of the embryonic nervous system (Vervoort et al., 1997). *ttk* RNAi gives a typical and easily recognizable neurogenic (increased number of neurons) phenotype in embryos, which is very similar to the one exhibited by mutations in the gene. Moreover, depending on the level of injected dsRNA two similar phenotypes can be observed (Kennerdell and Carthew, 1998). Wild-type embryos injected with ds-*ttk* RNA form extra neurons in the *lch5* organs (sensory organs) of some injected embryos whereas other embryos exhibit a neurogenic phenotype with a highly condensed PNS containing many extra neurons. dsRNAs for *ttk* were generated to amplify the same stretches of DNA used in the above mentioned studies and injected to knock down specifically the transcript for the *tramtrack* gene and used as a positive control. We tested different concentrations of *ttk* dsRNA to obtain a fairly good survival rate with a well defined neurogenic phenotype.

Figure 14: Neurogenic phenotype in *tramtrack*-dsRNA injected embryo Early embryos of 80G2 strain were injected with either injection buffer or tramtrack dsRNA (50µg/ml) and analyzed at late embryonic stage 17. Embryos injected with injection buffer showed normal morphological features (A, C) but embryos injected with tramtrack dsRNA showed neurogenic phenotype (B,D). Scale bar: A, B- 110µm and C,D- 50µm

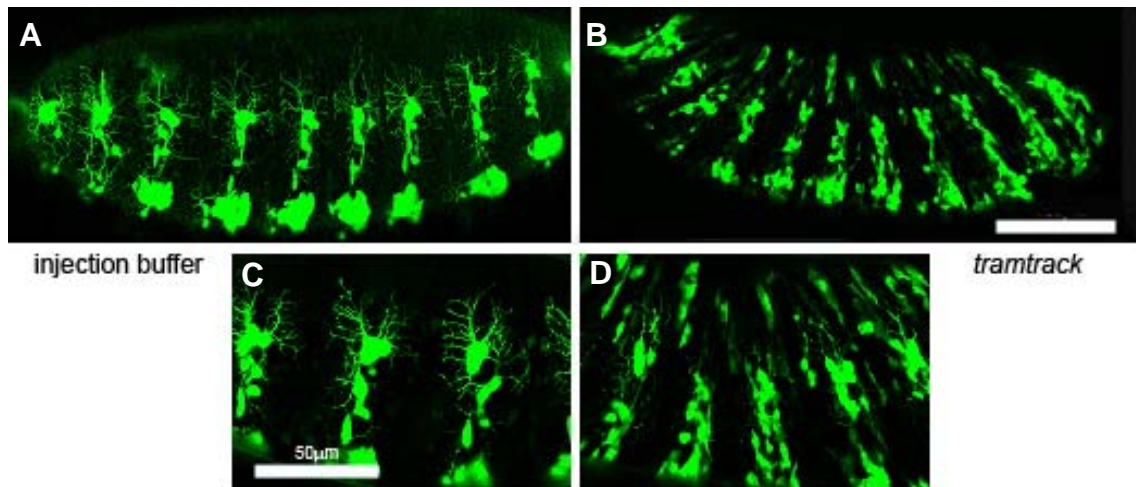


Table 3.1: Standardization using tramtrack RNAi

	Injected embryos	Embryos alive	Embryos with injection defects	Neurogenic defect	Embryos with no defect (normal)	Survival rate*
Control: Injection buffer	209	118	69	0	49 (23%)	56%
Positive control: <i>tramtrack</i>	277	36	20	14	2(<1%)	13%

*Survival rate= embryos alive/ embryos injected

Compared to the injection of buffer only, upon *tramtrack* injection of 50 µg/ ml dsRNA a reliable stronger, neurogenic phenotype was obtained in 87% of the surviving embryos, however, the survival rate decreased considerably (13%, n=277) (Figure 14, Table 3.1). Based on the above results, it was decided that around 250 embryos should be injected for each candidate molecule to obtain at least 15 embryos that could be analyzed for eventual phenotypes and to use 50 µg/ ml of dsRNA.

3.1.2. Selection of molecules

Selection of candidate molecules is a very crucial step in any candidate gene based screen. Since the *Drosophila* genome has been sequenced, a complete list of known and predicted actin binding and microtubule binding molecules was obtained from Flybase- a database of *Drosophila* genes and genome (Crosby et al., 2007). Altogether these represent more than 150 molecules. While for some of the candidates, mutants already existed, others were simply predicted coding sequences identified by the *Drosophila* genome project- annotation project, or based on sequence similarity to molecules known in other model systems. Since the number of known cytoskeletal molecules is very large and they are very varied, for convenience a short list of known molecules was prepared for testing the efficiency and reliability of the screening assay. The molecules were selected depending on their known functions and role in cytoskeletal regulation, availability of reagents and expression patterns (whenever possible). The molecules which were selected for an initial round of screening were as follows:

ADF (actin depolymerizing factor) / cofilin (twinstar): ADF/ cofilin is a member of a family of small actin severing proteins. The actin severing activity of Adf/ Cofilin is critical to axon extension and growth cone motility in central and peripheral neurons in vertebrates (Sarmiere and Bamburg, 2004). The *Drosophila* ADF/ Cofilin is called *twinstar* (*tsr*). Mutations in this ubiquitously expressed molecule show defects in centrosome migration and cytokinesis and exhibit abnormal accumulation of F-actin (Gunsalus et al., 1995). In the *Drosophila* genome there is a second predicted ADF gene called CG6873 (*ADF*) and not much information is available about it.

Aip1: It is an actin interacting protein promoting actin turnover in living cells (Okada et al., 2006; Rogers et al., 2003). It interacts with Cofilin to disassemble actin filaments and restricts Cofilin localization to cortical actin patches in yeast cells (Rodal et al., 1999). Studies in model organisms, other than *Drosophila*, have demonstrated that Aip1 interacts genetically with ADF/Cofilin and

participates in several actin dependent cellular processes like cytokinesis, phagocytosis, cell motility in yeast and contractibility of body wall muscles in *C.elegans* (Ono, 2003). Its function in *Drosophila* is not analyzed till date.

Capulet (*capt*)/ *act up*: It is a homolog of the Adenylyl Cyclase-Associated Protein (CAP) that binds and regulates actin. Consistent with a vital role in regulating actin structures, loss of CAP activity results in cytoskeletal defects in yeast, *Dictyostelium*, and *Drosophila* (Benlali et al., 2000; Gottwald et al., 1996; Vojtek et al., 1991). *capt* is expressed in neurons at embryonic stages 12 and 13 during axonal development in *Drosophila*. It is also involved in the regulation of cytoskeletal dynamics in axon guidance along with Abl Tyrosine Kinase resulting in midline crossing error mutations in CNS of *Drosophila*. Furthermore, it also genetically interacts with important axon guidance molecules like Slit and Robo (Wills et al., 2002). It suppresses the hyper assembly of actin microfilaments and thus prevents premature neuronal differentiation in eye disc (Benlali et al., 2000).

Cappuccino: Cappuccino (*capu*) is one of the 6 formin homology (FH) domain proteins in *Drosophila*. Cappuccino protein acts at a functional interface between the tubulin- and actin based cytoskeletons (Wasserman, 1998). Mouse Cappuccino is expressed exclusively in the developing and mature central nervous system (Leader and Leder, 2000). However its role in vertebrates is not yet clear. Mutations in the *capu* locus of *Drosophila* cause females to produce embryos which have disorganized microtubules and lack proper anteroposterior and dorsoventral patterning as a result of failure to properly position mRNAs (Emmons et al., 1995; Manseau and Schupbach, 1989).

Diaphanous: The *Drosophila* FH domain protein Diaphanous belongs to a family of formin-related proteins containing repetitive polyproline stretches. Diaphanous has a role in actin cytoskeleton organization and is essential for many, if not all, actin-mediated events like membrane invagination and filopodia formation. Besides regulating actin cytoskeleton reorganization, mDia (mouse

Diaphanous) is also required for microtubule stabilization at the leading edge of migrating cells (Afshar et al., 2000). Diaphanous binds to Profilin and RhoA and all these proteins are co-localized in the spreading lamellae of cultured fibroblasts. In *Drosophila*, Diaphanous has an essential role during cytokinesis (Watanabe et al., 1997).

δ-catenin: It belongs to the p120- δ -catenin [p120ctn] protein family, which is characterized by ten characteristically spaced Armadillo repeats that bind to the juxta-membrane segment of the classical cadherins. Besides their junction localization, they are also located in nucleus and cytoplasm. Cytoplasmic p120 functions in Rho signaling and regulation of cytoskeletal organization and actin dynamics. Targeted deletion of δ -catenin results in severe learning deficits and abnormal synaptic plasticity in mice (Kosik et al., 2005; Niessen and Yap, 2006). Recently it was found to modulate dendritic branching of a subset of sensory neurons in *Drosophila*. Mutations in *p120ctn* affect the formation of spine-like protrusions on class III neurons but did not significantly affect dendritic branching of class I- vpda neurons that extend comparatively smooth dendrites (Li et al., 2005).

kelch: It is a member of the Kelch protein family containing Kelch repeat domain, which in a variety of organisms bind to actin filaments and/or have important roles in assembling cellular actin structures. Kelch family proteins are diversely localized and are involved in varied cellular processes including cell growth, cell fusion and morphology, spermatocyte differentiation and cell adhesion. The mouse homologue, ENC-1, functions as an actin-binding protein important in the organization of actin cytoskeleton during neural fate specification and development of the nervous system (Hernandez et al., 1997). In *Drosophila* Kelch is located in actin-rich intercellular bridges, termed ring canals, which connect the developing oocyte to 15 supporting nurse cells (Adams et al., 2000).

Profilin/Chickadee: It is an actin monomer binding molecule, which functions as a regulator of actin assembly. Conflicting data suggest that Profilin might function

to promote either actin polymerization or depolymerization in cells (see Introduction- 1.5.2). Profilin has been reported to be widely expressed with multiple functions. Profilin is located at spines upon activity in vertebrates. Studies in *Drosophila* have established a role for Profilin in motor axon guidance and in cytoplasmic transport during oogenesis (Cooley et al., 1992; Wills et al., 1999; Witke, 2004; Yarmola and Bubb, 2006).

Quail: Quail is an actin-regulating protein with sequence homology to Villin. Its homologue, Villin, induces growth of microvilli in transfected fibroblast-like CV-1 cells and the capacity of Villin to induce growth of microvilli in cells correlates with its ability to bundle F-actin in vitro but not with its nucleating activity (Friederich et al., 1999). Quail efficiently assembles actin filaments into bundles in nurse cells and maintains their stability under fluctuating free calcium levels. The abundant network of cytoplasmic filamentous actin is absent in quail mutant egg chambers (Matova et al., 1999).

Scar (Suppressor of cAMP receptor): It is a primary Arp2/3 complex activator stimulating the ability of the Arp2/3 complex to nucleate actin filaments. In mice, expression of Scar/WAVE1 is mainly restricted to the brain whereas Scar2 is widely expressed. Accordingly, the Scar1 null mice display several CNS-related problems, such as limb weakness, neuroanatomical malformations and behavioral abnormalities, which presumably lead to postnatal lethality (Dahl et al., 2003). In contrast, Scar2 null mice die at embryonic day 10 to 12.5 suffering from haemorrhages, cardiovascular defects due to impaired angiogenesis, developmental delay and growth retardation (Yamazaki et al., 2003). Scar/WAVE2 appears to be required for leading edge extension during directed migration in general, whereas Scar/WAVE1 is essential for matrix-metalloproteinase-dependent migration through the extracellular matrix (Vartiainen and Machesky, 2004). In *Drosophila*, SCAR function is essential for cytoplasmic organization in the blastoderm, axon development in the central nervous system, egg chamber structure during oogenesis, and adult eye morphology (Ibarra et al., 2005; Zallen et al., 2002).

Slingshot: Slingshot (SSH) belongs to a family of phosphatases which dephosphorylates ADF cofilin leading to its activation and has the property of controlling actin reorganization by binding to F actin. In mammalian cells, human SSH homologues (hSSHs) suppress LIMK1-induced actin reorganization and expression of one of these homologues, SSH1, in DRG neurons in culture increases growth cone motility and extension and alters the shape of the growth cone (Endo et al., 2003). In *Drosophila*, loss of *ssh* function dramatically increases levels of both F actin and phospho-cofilin and disorganizes epidermal cell morphogenesis, including the bifurcation phenotypes of the bristles and wing hairs, after which Slingshot was named (Niwa et al., 2002).

Sra-1 (specifically Rac1-associated protein 1): Sra-1 is part of a complex modulating the activity of WASP and WAVE proteins, which are important regulators of F-actin formation. In tissue culture cells as well as *in vivo* Sra-1 function is required for F-actin organization. Genetic analysis demonstrate that Sra-1 function at the membrane depends on the presence of Wasp (Bogdan et al., 2004). In *Drosophila* embryos, it is a maternally contributed protein and later in development becomes concentrated in the developing nervous system (CNS). Sra-1 is highly expressed in growth cones and neuromuscular synapses. It is required for axonal growth and also during formation and maturation of neuromuscular junctions (NMJ). Expression of double stranded *sra-1* RNA in photoreceptor neurons leads to stalling of axonal growth (Schenck et al., 2003).

Twinfilin: Twinfilin is a ubiquitous actin-monomer-binding protein that is composed of two ADF-homology domains. It forms a 1:1 complex with ADP-actin-monomers, inhibits nucleotide exchange on actin monomers and prevents assembly of the monomer into filaments. In cells, Twinfilin shows diffused cytoplasmic localization but it is also concentrated to the cortical actin cytoskeleton which is dependent on a direct interaction with capping protein (Moseley et al., 2006). Mouse Twinfilin is important in clathrin-mediated endocytosis and distribution of endocytic organelles in mammalian cells. It has a role in the regulation of active actin dynamics (Helfer et al., 2006). Available

Drosophila mutants show different developmental defects including aberrant bristle morphology and rough eye phenotype correlating with abnormal actin structure (Palmgren et al., 2002).

3.1.3. RNAi assay

For the RNAi assay, short stretches of interfering dsRNAs specific for each molecule were made using genomic DNA from adult flies. While making the dsRNAs, primers were selected very carefully so that

-they were specific without affecting other molecules causing non-specific defects and

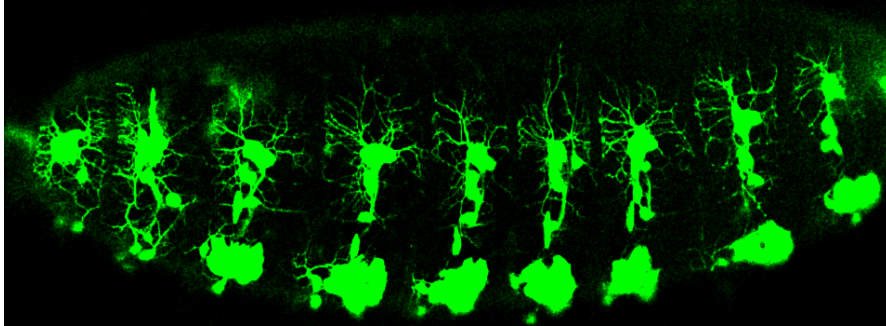
-they were efficient in knocking down the specific molecule.

To design target dsRNA sequences, primers from a published database, for which these sequences had been tested in S2 cell cultures successfully, were used (Rogers et al., 2003). The dsRNAs were made from genomic DNA and were suspended in injection buffer to get the standardized concentration (50 µg/ml) for the injection procedure (see methods).

For the injections, early *Drosophila* embryos were collected, processed and injected before the beginning of embryonic stage 5. Embryonic stage 5 marks the beginning of the cellularization process and injecting the embryos before this stage ensured ubiquitous distribution of injected dsRNA solution.

For the screen, a *GFP*-expressing strain, 80G2 was used (Figure 15). This strain highlights a subset of PNS neurons, including eight md (multi-dendritic) neurons expressing *GFP* under the control of the 109(2)80*Gal4* driver [the 80G2 line contains the 109(2)80 driver and two *UAS-eGFP* reporter insertions] (Gao et al., 1999). Six of those are da (dendritic arborization) neurons that generate a complex and stereotyped arbor (see introduction).

Figure 15 GFP labeled PNS in 80G2 strain A late stage 17 embryo of 80G2 strain showing elaborate dendritic morphology of dorsal cluster neurons of PNS.



The injected embryos were allowed to develop at 18⁰C in an incubator with controlled humidity and then observed using confocal microscopy for dendritic defects at late embryonic stage 17 when the PNS neurons have established their basic dendritic arborizations.

The results of the RNAi screen are summarized in Table 2. Knocking down of most of the selected genes by RNAi considerably reduced the viability of the injected embryos. The survival rate of injected embryos for different dsRNAs was quite varied. This could be due to several reasons including effective knock down of the specific protein below its threshold level of requirement. However, the low survival rate could also be associated with slight differences in either one or more of the parameters (eg. Needle diameter, injection pressure, and coverage slightly more or less halocarbon oil, etc).

Table 3.2: Summary of RNAi assay

Gene name	Total Injected embryos	% Survival rate*	Embryos with injection defects	Embryos which could be used for analysis	Embryos with dendritic phenotype
ADF	412	51%	26%	25%	No(0/104)
Cofilin	475	42%	39%	3%	No (0/15)
ADF+cofilin	235	23%	12%	11%	No(0/26)
Aip1	540	41%	34%	7.22%	No(0/39)
Capulet	242	49%	34%	15%	No(0/36)
Cappuccino	617	19%	7%	12%	Yes(5/81)
δ -catenin	1054	26%	20%	5%	No(0/54)
Diaphanous	675	65%	44%	11%	Yes (23/74)
Kelch	385	18%	11%	7%	Yes(18/45)
Profilin	779	66%	59%	6%	Yes(32/47)
Quail	576	21%	14%	7%	Yes(3/45)
Scar	225	27%	11%	16%	No(0/36)
Slingshot	460	32%	25%	7%	No(0/34)
Sra-1	324	37%	27%	11%	No(0/36)
Twinfilin	131	18%	12%	6%	No(0/8)

*Survival rate = $\frac{\text{Embryos with injection defects} + \text{Embryos which could be used for analysis}}{\text{Total injected embryos}}$

Though many interesting candidates showed no effect on dendritic morphogenesis, there were a few candidate molecules, which showed significantly affected dendritic morphogenesis.

3.1.4 Interesting candidates with no significant dendritic phenotype

Nine of the fourteen molecules screened did not show any obvious dendritic phenotype in stage 17 embryos upon RNAi (Figure 16A-D). These molecules were ADF, Aip1, Cofilin, Capulet, δ -catenin, SCAR, Slingshot, Sra-1, Twinfillin. In case of ADF and cofilin, both of them did not show any noticeable dendritic phenotype respectively and their combination also failed to show any defective phenotype. *Drosophila* genome contains three homologues of ADF/cofilin known

till date and the absence of phenotype may be attributed to the redundancy of molecular functions of these 2 homologues. In case of other molecules, the absence of phenotype might have happened due to various reasons which are explored in the discussion chapter.

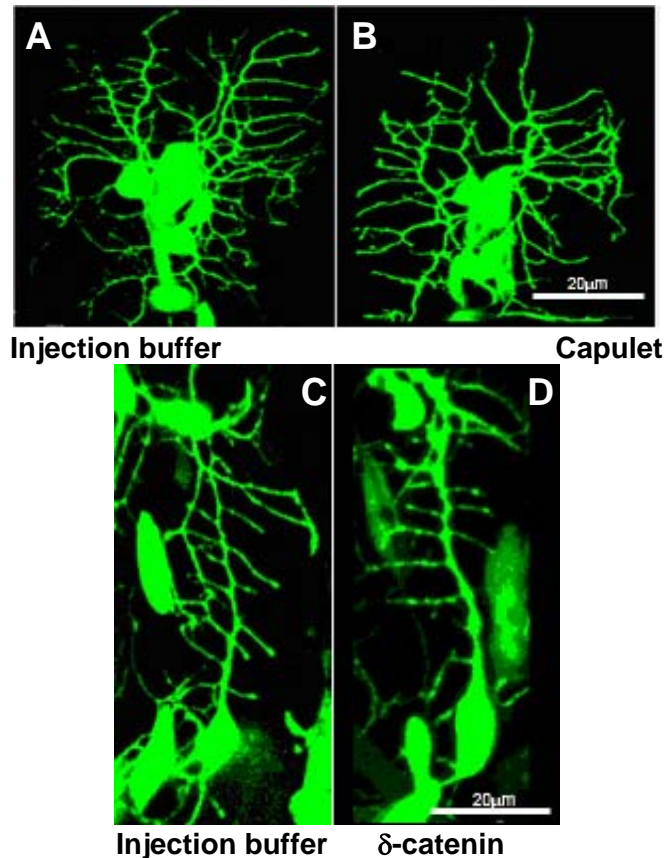


Figure 16: Lack of Detectable Phenotype (A,B) Dorsal cluster neurons from stage 17 embryos injected with capulet-dsRNA (B) exhibiting overall normal dendritic morphology with no significant deformity compared to that of the ones injected with injection buffer (A). (C,D) vpda neuron from stage 17 embryos injected with δ -catenin-dsRNA (D) showed normal dendritic morphology compared with that of the ones injected with injection buffer (C). Scale bar 20 μ m

3.1.5 Interesting candidates with interesting phenotype

From the list of 14 molecules screened, 5 molecules showed defective dendritic morphogenesis and they were: *kelch*, *quail*, *chickadee*/ Profilin and *diaphanous*.

In case of *diaphanous* (*dia*) and *chickadee* (*chic*), the knock-down of either gene produced a clear overbranching phenotype of Class I neurons (Figure 17). In the screening conditions the other neuronal classes did not seem affected. Injection of either dsRNA reduced the viability compared to injection of buffer only, but both dsRNAs produced a consistent phenotype with a convincing penetrance. 779 embryos were injected with dsRNA specific for the *chic* transcript, 47 survived without injection defects to stage 17 (6%) and out of those 32 showed a dendritic overbranching phenotype, whereas out of 675 embryos injected with dsRNA specific for the *dia* transcript 74 survived to stage 17 (11%), of which 23 showed an overbranching phenotype.

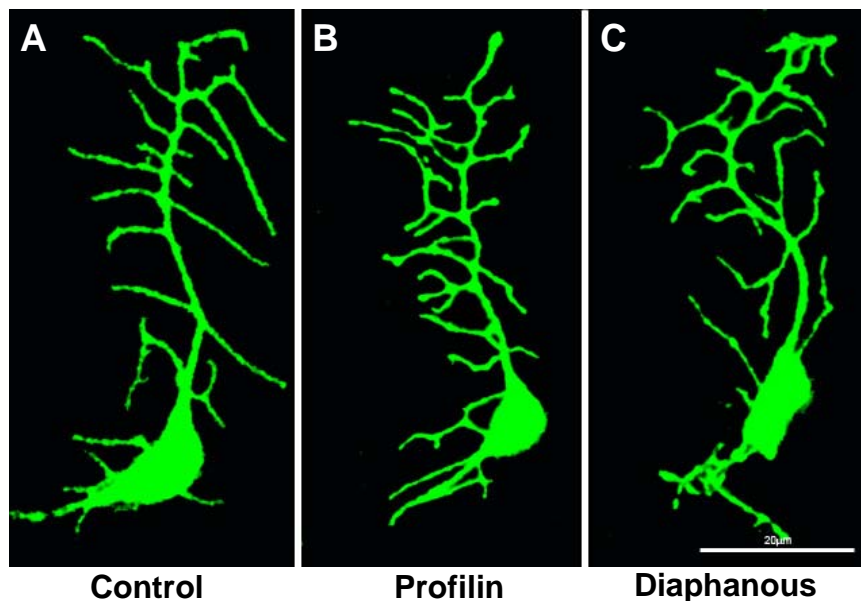


Figure 17: Dendritic phenotype of Diaphanous and Profilin upon RNAi Class I -vpda neurons from stage 17 embryos injected with (B) Diaphanous dsRNA and (C) Profilin dsRNA show dendritic over branching phenotype compared with that of those injected with injection buffer (A).

The knock down of the third candidate- *kelch* -produced a dendritic phenotype in the dorsal cluster neurons. 374 embryos were injected with dsRNA specific for *kelch* transcript. 45 embryos survived without any injection defects and 18 of those showed a dendritic phenotype. Kelch expression was reported mainly in gonads and imaginal discs including brain tissue in developing *Drosophila* larvae (Robinson and Cooley, 1997). However, no clear expression pattern is known in the nervous system and also the penetrance of the RNAi phenotype seemed

weaker than other candidates. Thus, Kelch was excluded from the short list of positive candidates.

The other 2 positive candidates, Cappuccino and Quail, looked very weak. In case of cappuccino, only 5 embryos showed a phenotype out of 81 embryos and in case of quail, out of 42 surviving embryos, only 5 showed a dendritic phenotype. Since the penetrance was very low compared to other positive candidates, cappuccino and quail were the second choices and Profilin and Diaphanous were selected for further analysis.

Diaphanous and Profilin are known to be binding partners from biochemical studies in yeast and in HT1080 human fibrosarcoma or Swiss 3T3 cell cultures (Chang et al., 1997; Watanabe et al., 1997). Profilin and Diaphanous are also hypothesized to interact with each other in *Drosophila* (Afshar et al., 2000; Verheyen and Cooley, 1994). Their similar dendritic phenotypes upon RNAi hinted at their cooperative function in dendritic morphogenesis. Their role in dendritic morphogenesis was further analyzed using genetic tools.

CHAPTER 4- RESULTS (II)

GENETIC ANALYSIS

To confirm the dendritic phenotype of *diaphanous* and *chickadee* and study their role in detail in dendritic morphogenesis *in vivo*, further genetic studies were carried out. The genetic analysis was done using gain of function and loss of function analyses with null and hypomorphic alleles of both *dia* (Castrillon and Wasserman, 1994; Spradling et al., 1999) and *chic* (Verheyen and Cooley, 1994).

4.1 Diaphanous

Diaphanous is a Formin Homology domain protein (Figure 18) and is the founding member of the Diaphanous Related Formins (DRF) subfamily, with actin nucleating activity as well as anti-capping activity for fast growing ends of actin filaments (Kovar and Pollard, 2004) (see introduction 1.5.1).



Figure 18: Domain structure of Diaphanous protein Diaphanous protein binds to actin and other actin binding molecules through its FH2 domain. It binds to Profilin through its poly proline rich FH1 domain. It binds to Rho GTPase through its N-terminal GTPase Binding Domain (GBD). The FH3 domain lies between GBD and FH1 domain and its exact function is not clear yet. Its auto-regulatory domain lies at its C-terminal.

There is only one known *diaphanous* gene in *Drosophila* and it is located at 38E7-38E8 on the left arm of the second chromosome. The phenotypic analysis of *diaphanous* was done using both gain of function as well as loss of function analysis. All the analyses were carried out in late 3rd instar larvae unless mentioned otherwise. The gain of function analysis will be presented first followed by loss of function analysis.

4.1.1 Gain of function analysis

For gain of function analysis, we obtained or made different constructs of *diaphanous* so that we could identify its role in dendritic morphogenesis. We first obtained a fly stock containing a genomic rescue construct of *dia*, $P[w^+ pDC4]$ [referred to as $P(dia^+)$] ubiquitously expressed in the endogenous *dia* expression pattern (Castrillon and Wasserman, 1994). It contains the entire 11 kb genomic fragment containing the full *dia* gene cloned into a germline transformation vector. This stock was homozygous lethal and the lethality could be due to insertion of the construct in some vital gene or actually due to ubiquitous 'over-expression' of *diaphanous*. Since this construct was ubiquitously expressed, it did not allow us to analyze cell autonomous role of *diaphanous*.

We generated fly lines carrying full-length un-tagged and *RFP*-tagged *dia* constructs under the control of *UAS* sequences (see Materials and Methods). These constructs could be expressed cell specifically under the control of any *Gal4* driver. We used 2 fly lines with full length untagged *dia* constructs on the X chromosome and on the 3rd chromosome respectively. Besides these, we also used a *RFP*-tagged fly line on the 3rd chromosome for our analysis. In addition, we obtained a fly stock with constitutively active (CA) *dia* gene under *UAS* promoter, (*UAS-dia-CA*), which allowed tissue specific overexpression of the CA Diaphanous (Somogyi and Rorth, 2004). In this construct the sequence encoding the *dia* N-terminal 449 amino acids (predicted Rho binding domain) is replaced by a short sequence encoding three HA tags, and the C-terminal amino acids 1029 to 1091 (predicted autoinhibitory domain, DAD) are removed. Since it lacks its N terminal Rho GTPase binding domain along with its DAD domain, it results in an open and active conformation of the Diaphanous molecule. This construct could help us understand regulation of *diaphanous* by its upstream activator RhoA.

4.1.1.1 Overexpression of *dia* in class I neurons:

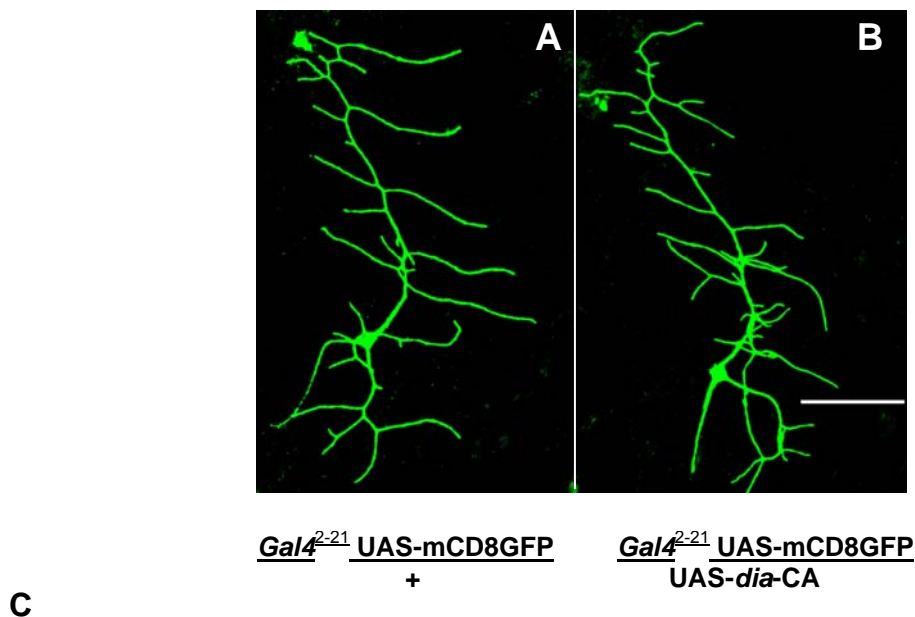
Since class I neurons showed the most dramatic phenotype in RNAi assay and we had tools to observe class I neurons specifically, they were the focus for gain of function analysis. For this purpose, all the *dia* constructs were used and analyzed using the *Gal4²⁻²¹ UASmCD8GFP* driver-reporter combination to allow class I neuron visualization (Grueber et al., 2003a). Most of the constructs were located on the 3rd chromosome and so were the marker line constructs and all the analysis was done only in heterozygous marker line background. All the gain of function experiments were carried out in a wild type *dia* background.

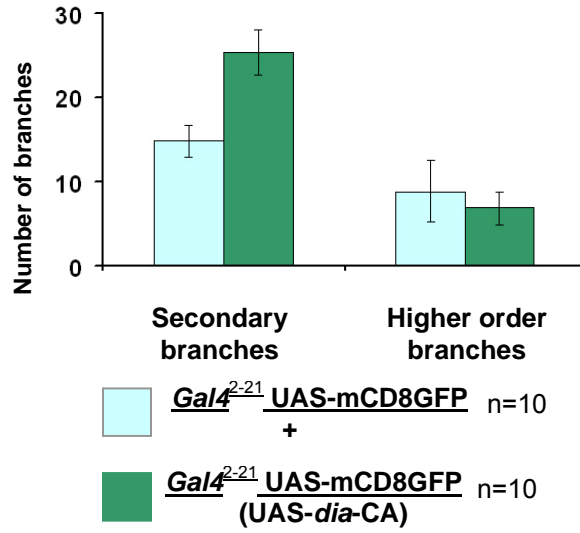
By adding one copy of the P(*dia*+) construct, the total number of dendritic branches of class I vpda neuron were 28.5 ± 4.9 , n=10 [*Gal4²⁻²¹ UASmCD8GFP*/P(*dia*)] (Figure 19D). These were significantly more compared to the control (*Gal4²⁻²¹ UASmCD8GFP*/+) 22.75 ± 3.2 , n=20, p<0.05. Since this specific construct was expressing Diaphanous ubiquitously, increasing the normal level of the protein all over the animal, the effect could also be a non-cell autonomous effect.

The *UAS-dia-FL* and *UAS-dia-mRed* constructs could be selectively overexpressed in class I neurons using the *Gal4²⁻²¹* driver, thus allowing for cell autonomous overexpression. Interestingly, the total number of branches of vpda neuron upon overexpression of mRed-*UAS-dia* construct (*mRed-UAS-dia*)^{E3-1}/*Gal4²⁻²¹ UASmCD8GFP*, was 29.6 ± 6.4 , n=20, p<0.05 similar to the genomic transgene overexpression. However, the overexpression of a full length *dia* construct resulted in almost twice the total number of dendritic branches of vpda neuron in case of both the fly line insertions- on X-chromosome, (*UAS-dia*)^{A3-1}/Y; *Gal4²⁻²¹ UASmCD8GFP*+, (40.85 ± 7.46 , n=20, p<0.05) and 3rd chromosome, (*UAS-dia*)^{G3-1}/*Gal4²⁻²¹ UASmCD8GFP*, (38.8 ± 5 , n=20, p<0.05) . This result indicated that independent of the insertion site, this was an authentic phenotype owing to overexpression of *dia* by those individual constructs (Figure 19D). It might also suggest that tagged *dia* is not fully functional.

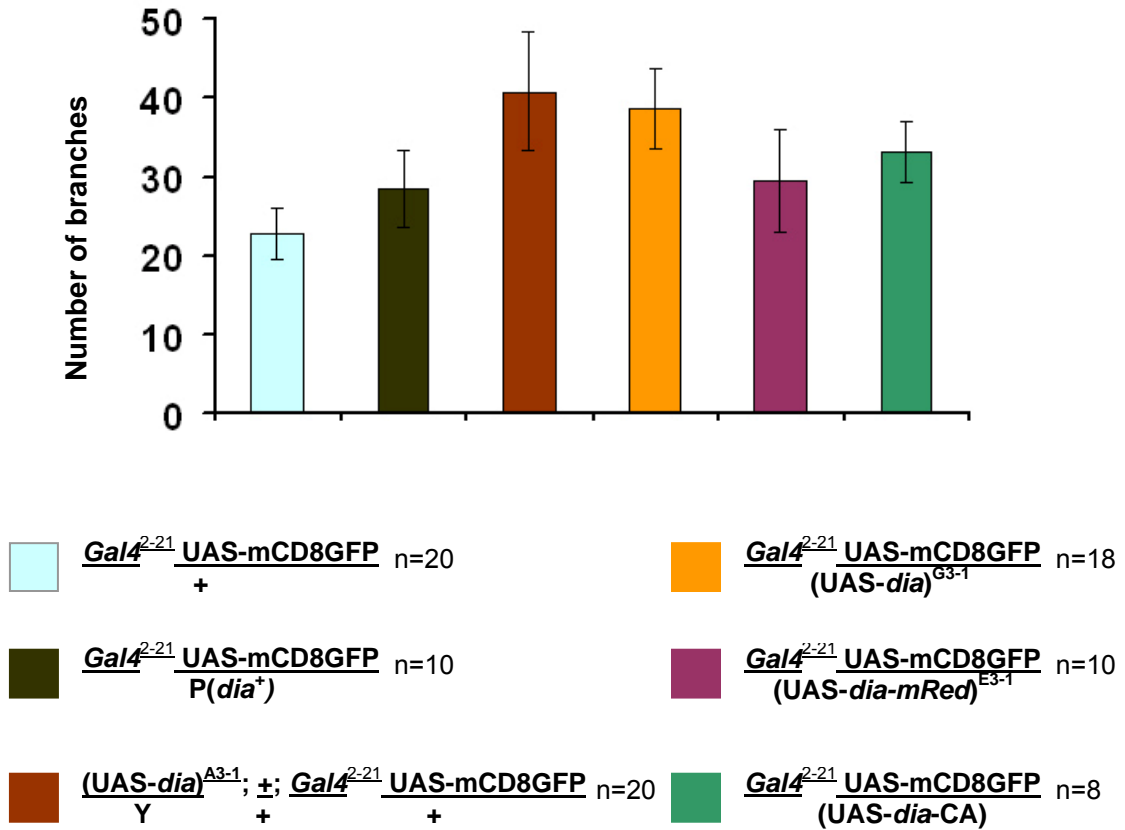
We then overexpressed the constitutively active form of Diaphanous (*UAS-dia-CA*) using the same *Gal4*²⁻²¹ driver. In this case, the total number of branches was increased to 33.25±3.9, n=8 compared to the control *Gal4*²⁻²¹ *UASmCD8GFP* + (Figure 19A,B). To add to this, the overexpression of this construct showed many filopodia like branches emerging from the primary branches of *vpda* neurons, which was not observed with overexpression of other constructs of *dia* used till now. Thus, the number of secondary branches was increased to 25.38±3.6, n=8, p<0.05 compared to control (14.9±1.9) whereas the number of higher order branches was decreased a bit to 6.9±2, n=8, p=0.04 compared to control (8.9±2.6) (Figure 19C).

Figure 19: Overexpression of *dia* results in dendritic over branching phenotype of class I –*vpda* neuron (A-C) *vpda* neuron from late 3rd instar larvae with overexpression of constitutively active *dia* constructs (B) shows easily visible dendritic over branching compared to that of the control (A). The number of secondary branches is significantly increased with overexpression of *dia-CA*, at the same time, the number of higher order branches is decreased compared to that of the control (C). The overexpression of all the tested *dia* constructs show a significant increase in total number of branches of class I *vpda* neuron in late 3rd instar larva (D).





D



Thus, all the constructs used for *diaphanous* overexpression exhibited an increase in total number of dendritic branches of class I – vpda neuron suggesting a role of Diaphanous in dendritic morphogenesis.

4.1.1.2 Overexpression of *diaphanous* in class IV neurons

Since overexpression of *diaphanous* showed dendritic over branching phenotype in class I neuron, it was interesting to see if the overexpression of *diaphanous* would affect the dendritic morphology of most complex branching pattern class IV neurons. For this purpose, 3 constructs- genomic transgene P(*dia*+), constitutively active construct (*dia*-CA) and full length *UAS-dia* construct- were used. We concentrated on class IV ddaC neuron from the dorsal cluster of 3rd instar larvae since the dendritic structure of class IV neurons is completely developed at this stage.

Given that the overexpression was ubiquitous in the case of genomic transgene, P(*dia*+), only a class IV highlighting strain –*ppk-eGFP*- was needed to visualize the morphology of class IV neurons. The *ppk-GFP* strain expresses *eGFP* under the promoter of *pickpocket* gene specifically in class IV neurons (Grueber et al., 2003b). The class IV ddaC neuron from P(*dia*+)*/ppk-eGFP* larvae showed 264.4±31.3 (n=5) of total dendritic branches which were not significantly different (p=0.09) compared with that of the control, *ppk-eGFP/+*, with 288±18.1 (n=5) number of branches (data not shown).

A strain called *Gal4^{A77} UASmCD8GFP* was used for overexpression of *UAS-dia* constructs (Grueber et al., 2003a). This strain expressed *GFP* under the control of *Gal4^{A77}* driver primarily in Class IV neurons with a very light expression in class I neurons. We first overexpressed the 3rd chromosome full length untagged construct of *dia* using this marker line. No significant difference in the total number of dendritic branches was observed upon overexpression. The overexpression of *UAS-dia* [(*UAS-dia*)^{G3-1}/*Gal4^{A77} UASmCD8GFP*] produced 508.75±42.2 (n=4, p=0.4) dendritic branches of class IV ddaC neuron,

comparably to the control $Gal4^{477} UASmCD8GFP/+$ showing 500 ± 61.6 (n=4) dendritic branches (data not shown).

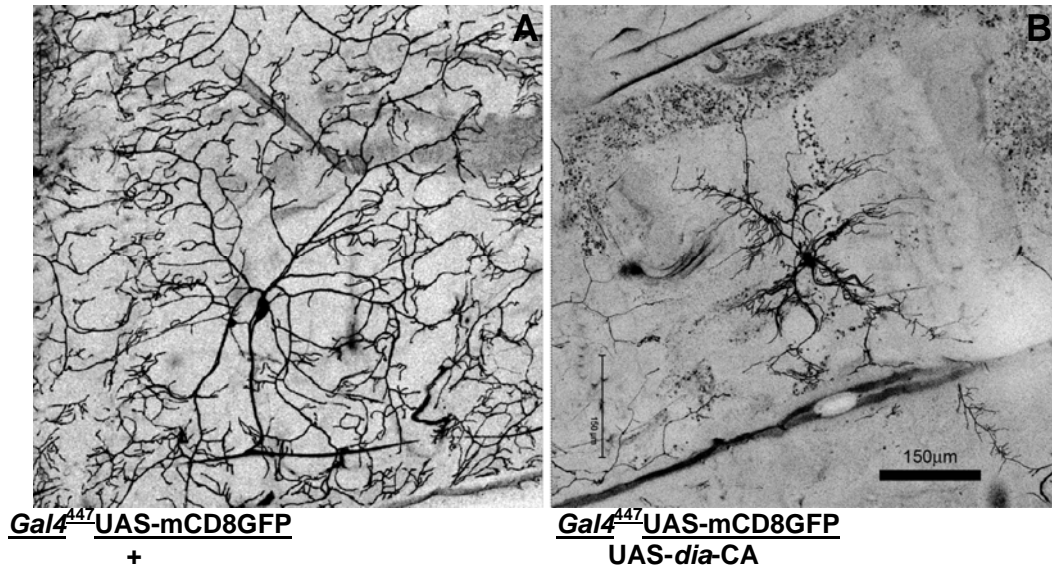


Figure 20: Overexpression of (*UAS-dia-CA*) in class IV neurons
Overexpression of constitutively active form of *diaphanous* in class IV neurons (B) affected the dendritic arborization pattern severely with much reduced dendritic field and many small filopodia like branches compared to its control (A). Scale bar $150\mu m$.

The same $Gal4^{477}$ line was used for the overexpression of constitutively active form of *diaphanous*, *UAS-dia-CA*, in class IV neurons (Figure 20). The result of this overexpression was remarkable! The class IV – ddaC neuron showed a dramatic bushy phenotype upon *UAS-dia-CA* overexpression with many long filopodia like branches emerging from the primary branches. The number of dendritic branches were so high in numbers and dense that it was not possible to quantify them. However, the primary branches did not seem affected and most of the additional branches were either secondary or higher order branches. This result may suggest that *dia* activity is very tightly regulated through Rho GTPases and *dia* is very important for the biological role of Diaphanous in dendritic morphogenesis of both, class I and class IV, neurons.

4.1.2 Loss of function

Since the RNAi and the gain of function data indicated plausible function for *diaphanous* in dendritic morphogenesis, it was important to see if we could support these data with loss of function analysis. For this purpose we took advantage of available genetic mutant alleles of *diaphanous*. In *Drosophila*, null mutants of *dia* are lethal only at the pupal stage. The survival of *dia* null animals through embryonic and larval stage is most likely due to maternal contribution of *dia* mRNA and/or protein. The lethality at pupal stage occurs due to dilution of the maternal *dia* gene protein below threshold over time during development (Castrillon and Wasserman, 1994). Since the lethal phase was at pupal stages and the embryos and larvae looked completely healthy till that stage, we studied the dendritic phenotype of the PNS neurons in stage-17 embryos as well as late third instar larvae. For observing the dendrites of PNS and to analyze any dendritic phenotype at different developmental stages, *dia* null mutants were generated with the required reporter combinations. In particular, the null allele *dia*^{K07135} (Butler et al., 2001; Chen et al., 2004; Spradling et al., 1999), the null allele *dia*⁵ and a hypomorph allele *dia*⁹ (Afshar et al., 2000; Castrillon and Wasserman, 1994) were used for mutant analysis.

4.1.2.1 Dendritic phenotype of null mutant *dia*^{K07135}

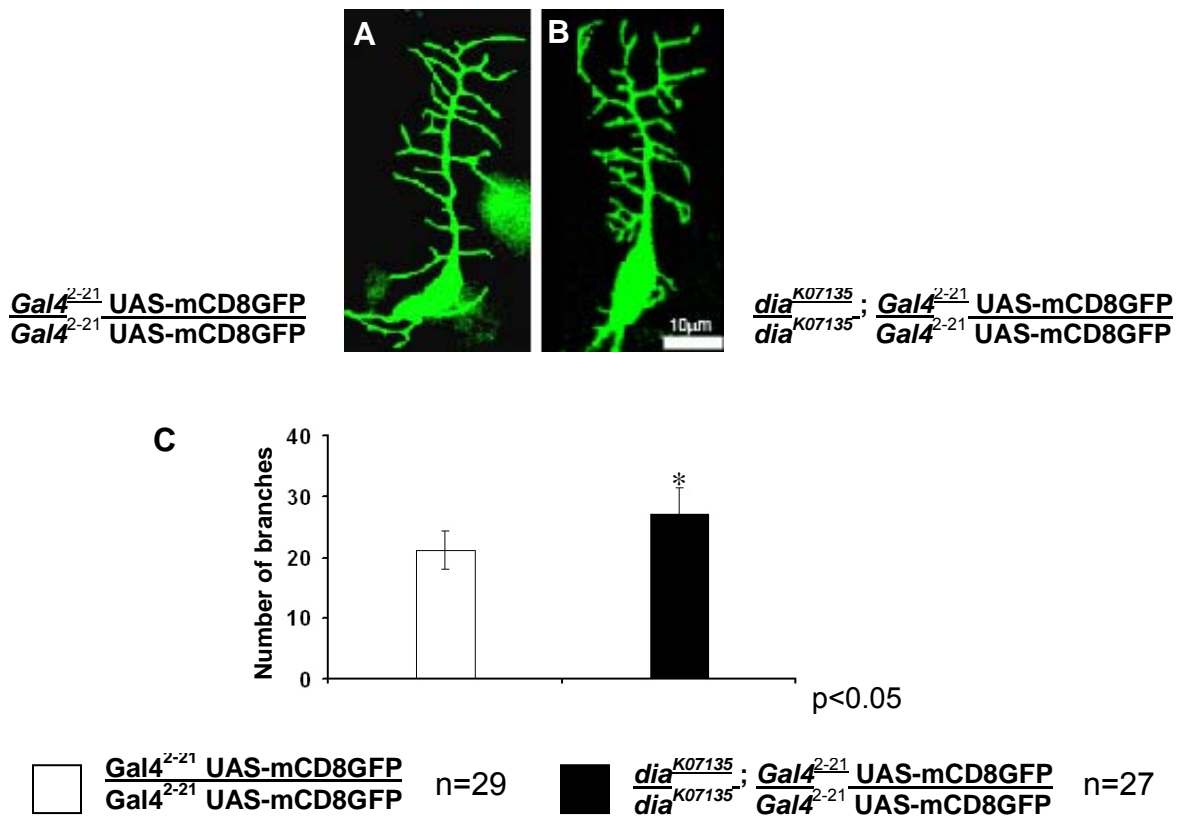
The *dia*^{K07135} allele is a null allele due to a 10.691Kb P-element P (Butler et al., 2001) insertion at position 2L:20746014-20746015 in the first coding exon (2L:20745740-20746256) of *dia*, 174bp downstream of the ATG. No detectable protein product of *diaphanous* gene is produced resulting in a null mutant.

4.1.2.1.1 *dia*^{K07135} – dendritic over branching phenotype in class I neurons

Since a clear phenotype was observed in Class I neurons upon RNAi, the initial phenotypic analysis of *dia*^{K07135} was carried out in Class I neurons using the Gal4²⁻²¹UAS-mCD8-GFP driver-reporter combination. Consistent with the dendritic phenotype observed upon RNAi assay, *dia*^{K07135} mutants showed significant

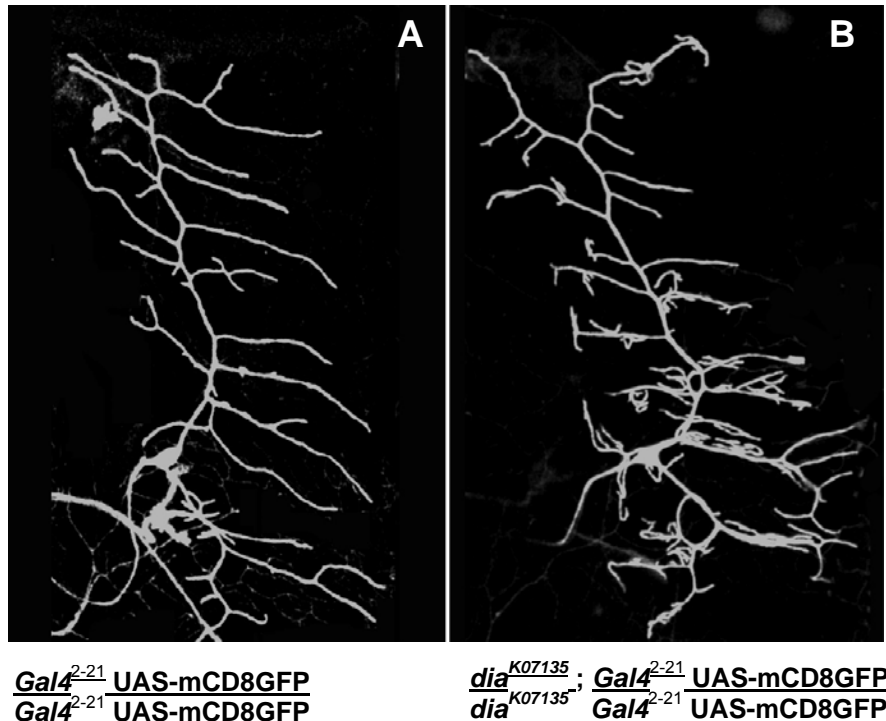
overbranching of class I neurons in the dorsal (data not shown) as well as in the ventral cluster. Interestingly, the onset of the dendritic overbranching phenotype was evident at late embryonic stage 17, when the maternal supplement of Diaphanous protein is sufficient for survival of animals. At this stage the total number of branch termini of the ventral cluster Class I vpda neuron in *dia*^{K07135} homozygous embryos was slightly, but significantly increased (26.96 ± 4.4 ; n=27) compared to control (21.24 ± 3.1 ; n=29; p<0.05) (Figure 21A-C). However, the severity of the over-branching phenotype increased when the Diaphanous protein levels dropped in the mutants at late 3rd instar larval stage (Figure 22A,B).

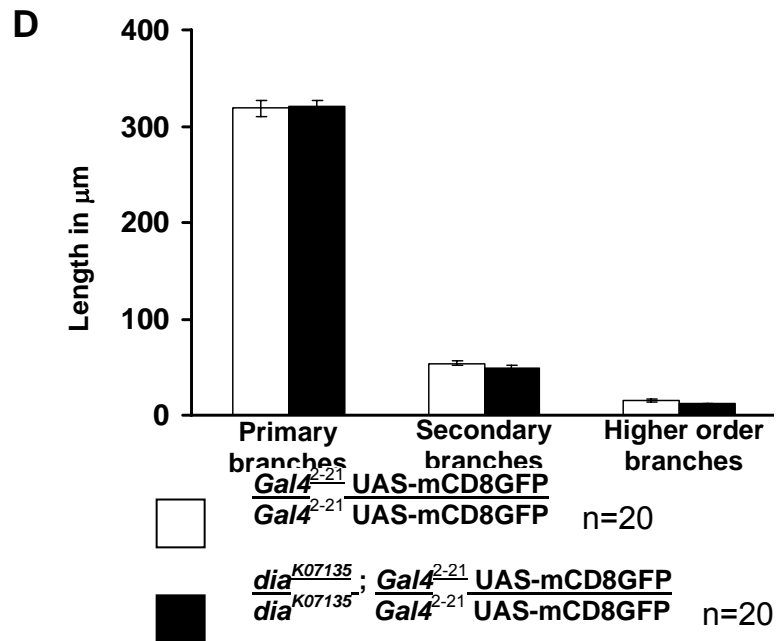
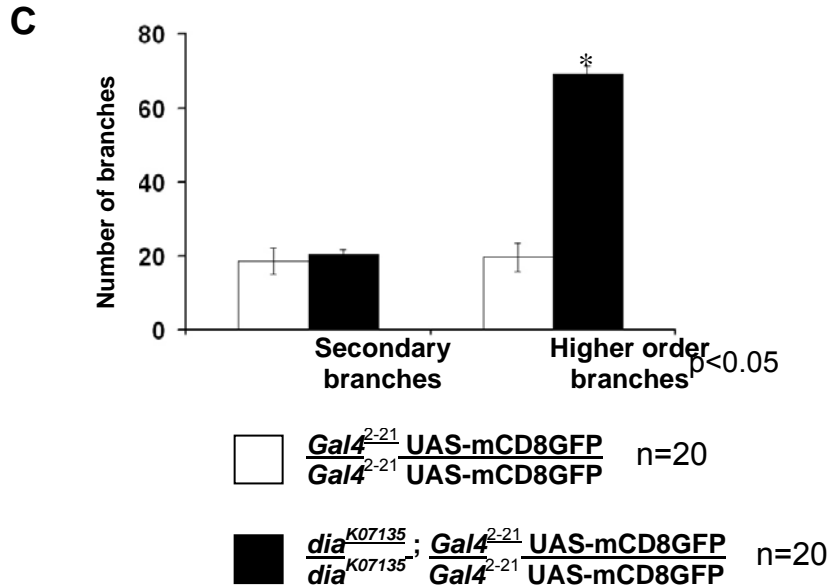
Figure 21: Dendritic phenotype of class I vpda neuron of *dia*^{K07135} embryos (A,B) Class I vpda neuron of *dia*^{K07135} (B) from embryonic stage 17 shows significant increase in dendritic branches compared to that of control (A). C) Quantitative analysis showing a significant increase in total number of branches of vpda neuron in *dia*^{K07135} compared to the control.



In the 3rd instar larvae, the total number of dendritic branch termini of vpda was more than two fold increased in mutant larvae (90.9 ± 12.1 ; $n=20$, $p < 0.05$) compared to the control (39.65 ± 8.5 ; $n=20$). The overbranching did not regard all orders of dendrites. The number of primary (one; $n=20$) and secondary order branches were unaffected in *dia*^{K07135} mutant vpda neurons (19.8 ± 3.9 , $n=20$) compared with control (18.6 ± 3.6 , $n=20$; $p=0.16$). However, the total number of higher order branches was increased more than three fold in mutant vpda neurons (69.1 ± 10.8 , $n=20$) compared with control (20.2 ± 7.2 , $n=20$; $p < 0.05$) (Figure 22C).

Figure 22 Dendritic phenotype of class I vpda neuron of *dia*^{K07135} at late 3rd instar larval stage (A,B) Class I vpda neuron of *dia*^{K07135} (B) from late 3rd instar larvae shows significant increase in dendritic branches compared to that of control (A). C) Quantitative analysis showing a significant increase in the number of higher order branches but not in the number of primary and secondary branches in *dia*^{K07135}. D) Quantitative analysis showing the average length of primary, secondary and higher order branches being unaffected in *dia*^{K07135} compared to the control.





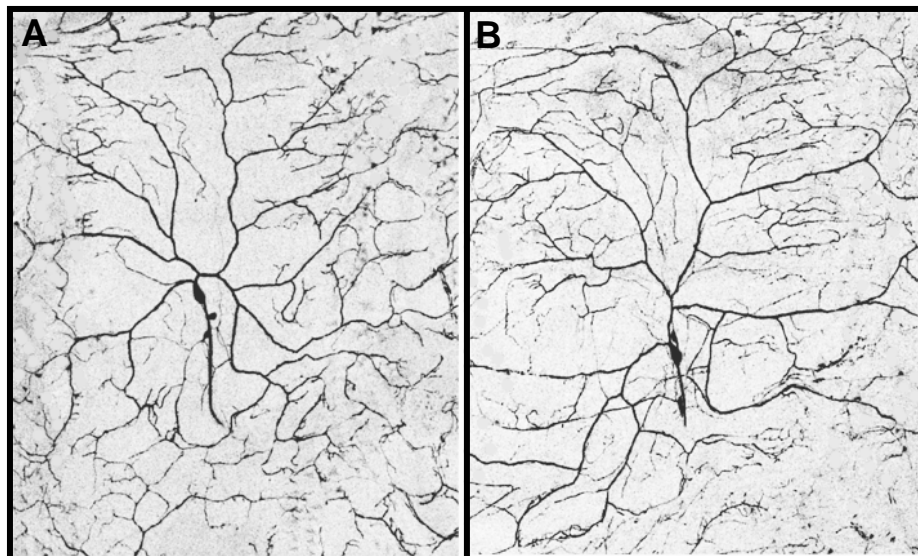
Interestingly, in contrast to the effect on branching, the average dendritic length was not affected in the dia^{K07135} mutants (Figure 22D). Although a significant increase in total dendritic length in dia^{K07135} vpda neuron ($2093.98 \pm 384.7 \mu\text{m}$, n=20) was observed compared to that of the control ($1577.43 \pm 208.3 \mu\text{m}$, n=20), the mean average length of the primary ($318.4 \pm 40.4 \mu\text{m}$ in control, $320.4 \pm 29 \mu\text{m}$ in dia^{K07135} ; n=20; $p=0.43$), secondary (53.83 ± 7.8 in control, 48.55 ± 10.9 in dia^{K07135} ; n=10; $p=0.11$) and tertiary branches (14.87 ± 4.4 in control, 11.6 ± 3.7 in

dia^{K07135}; n=10; p=0.044) was not significantly affected (Figure 22D). These results thus indicated that *dia* primarily may regulate branching but not growth of dendrites.

4.1.2.1.2 *dia*^{K07135} – no dendritic phenotype in class IV neurons

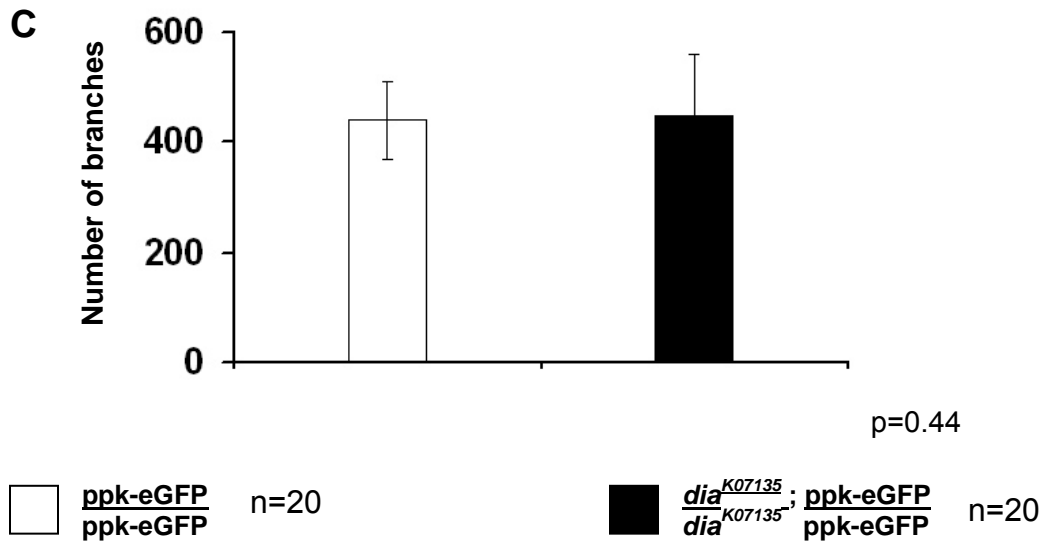
In the gain of function analysis only the constitutively active form of *dia* affected the dendritic morphology of class IV neuron unlike what was seen in class I neurons. To test whether only class I neurons are affected by mutations in *dia* we furthermore analyzed the morphology of the highly complex Class IV neurons that we visualized by adding *ppk-eGFP* in the *dia* mutant background. There was no significant effect in the total number of dendritic branches between *dia*^{K07135} and control (Figure 23A,B). The total number of dendrite termini was 448±111.6 (n=8) in mutant *dia*^{K07135} ddaC neurons compared to control ddaC (440.37±70, n=8, p=0.44) (Figure 23C).

Figure 23 Absence of dendritic phenotype of class IV ddaC neuron of *dia*^{K07135} at late 3rd instar larval stage (A,B) Class IV ddaC neuron of *dia*^{K07135} (B) from late 3rd instar larval stage shows no significant alteration in dendritic morphology compared to that of control (A). C) Quantitative analysis of total number of branches of class IV ddaC neuron showing no significant difference between *dia*^{K07135} and the control.



ppk-eGFP
ppk-eGFP

dia^{K07135}; ppk-eGFP
dia^{K07135} ppk-eGFP



Thus, complex neurons are not affected by mutations in the *dia* gene, indicating that *dia* may not exert an important influence in regulating branching in class IV neurons under normal physiological conditions and may do so only when its regulation by RhoA or any other unknown upstream regulator is perturbed.

4.1.2.2 Dendritic phenotype of null mutant *dia*⁵

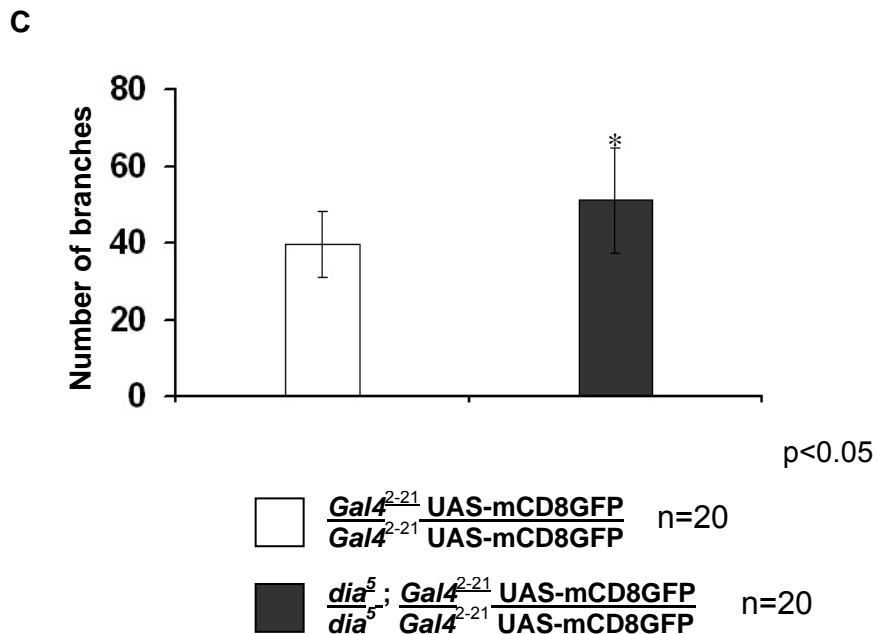
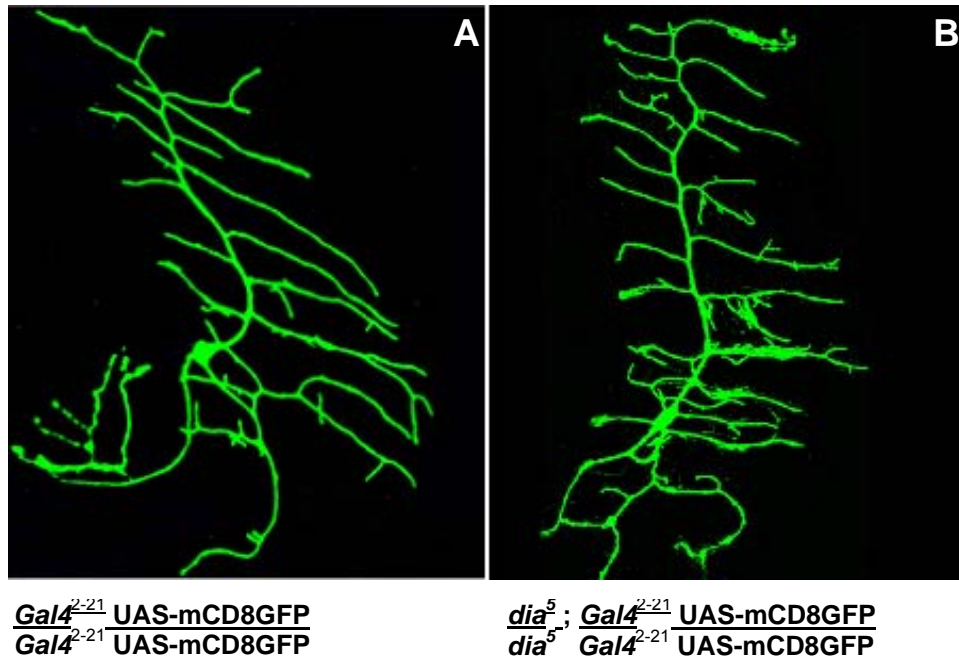
An additional independently generated null allele of *dia*, *dia*⁵ was also analyzed. This allele was generated when an original P-element inserted in the first exon of *dia* gene got imprecisely excised leaving a 3KB region inserted in the *diaphanous* gene causing a null mutation (Castrillon and Wasserman, 1994; Grosshans et al., 2005).

4.1.2.2.1 *dia*⁵ – dendritic over branching phenotype in class I neurons

Since *dia*^{K07135} allele showed a phenotype in class I but not in class IV neurons, the focus of analysis were class I neurons in case of *dia*⁵ allele. An appropriate stock of *dia*⁵ allele with the marker line was generated and tested for dendritic phenotype. The *dia*⁵ allele also showed a very similar dendritic over branching phenotype (number of branches 51.1 ± 13.6 , n=20, p<0.05), although it was much less severe compared to the other null allele, *dia*^{K07135} (Figure 24 A,B). The

penetrance of the dendritic phenotype in *dia*⁵ larvae was reduced to 50% compared with the ~100% penetrance observed with *dia*^{K07135} allele.

Figure 24 Dendritic phenotype of class I vpda neuron of *dia*⁵ at late 3rd instar larval stage (A,B) Class I vpda neuron of *dia*⁵ (B) from late 3rd instar larvae shows significant increase in dendritic branches compared to that of control (A). C) Quantitative analysis showing a significant increase in total number of branches of vpda neuron in *dia*⁵ compared to the control.

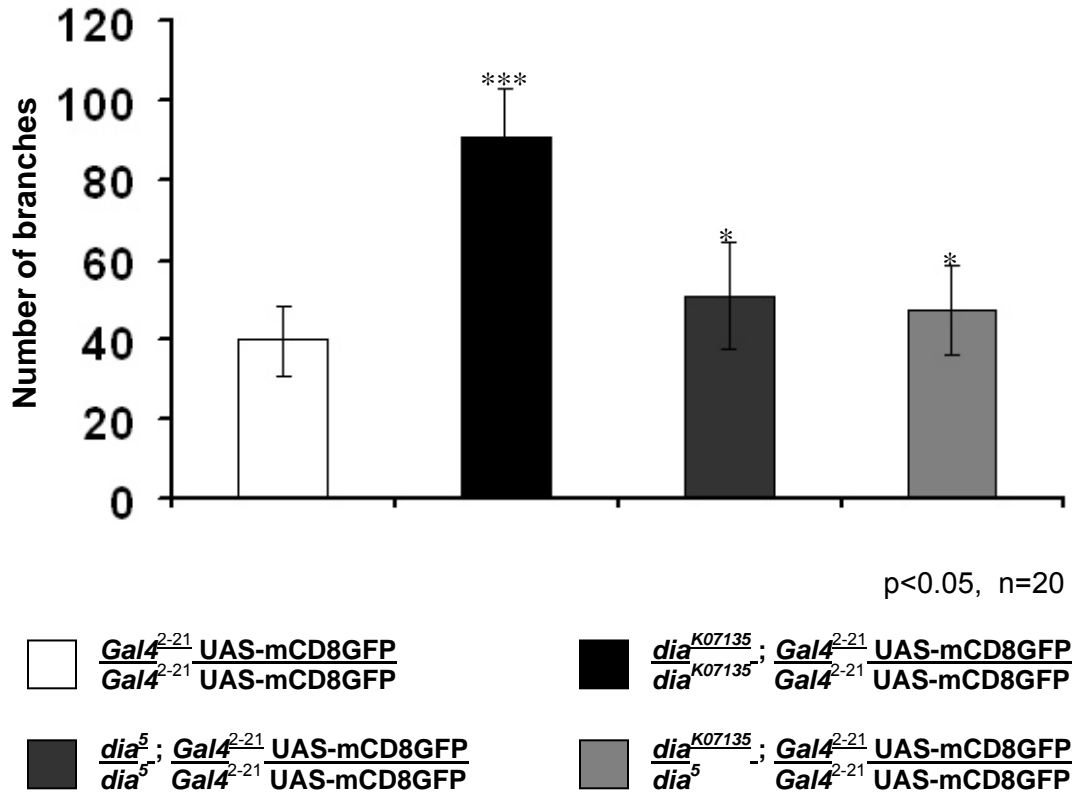


A viable hypomorphic allele *dia*⁹ (Castrillon and Wasserman, 1994), showed no dendrite phenotype at late 3rd instar larval stage (data not shown).

4.1.2.3 Dendritic phenotype in trans-allelic combination of null mutants-*dia*⁵ and *dia*^{K07135}

It was surprising that one of the null alleles, *dia*^{K07135}, showed a much more severe phenotype compared to the other null allele *dia*⁵. Therefore, the trans-allelic combination of these two alleles was generated and analyzed for dendritic phenotype. Surprisingly, in trans-allelic condition, the total number of dendritic branches were 47.4 ± 11.18 , $n=20$, $p=0.0092$ which was significantly more than the control but was less severe than the dendritic phenotype of each of the null alleles respectively (Figure 25). Thus the phenotype of the trans-allelic null mutant combination was milder than both the null mutants respectively. This was a puzzling observation and led to some more genetic experiments which are described and discussed further on.

Figure 25: Dendritic phenotype of class I vpda neuron in transallelic combination Quantitative analysis of total number of branches of transallelic combination of *dia*^{K07135}/*dia*⁵ showing a milder but significant dendritic over branching of class I vpda neuron compared to both the null alleles respectively.

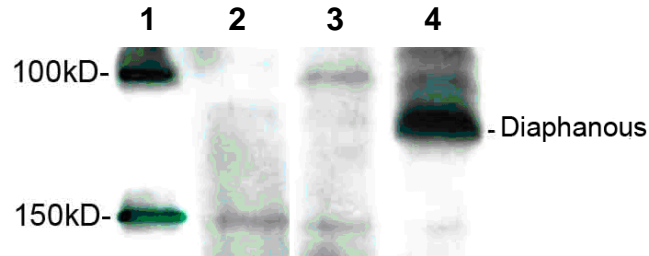


4.1.4 Western blot analysis: no Diaphanous protein in null mutants

To gauge the authenticity of the null alleles, homozygous 3rd instar larvae were tested for Diaphanous protein using western blot analysis. The protein contents were quantified and equal concentrations of all the samples were loaded on the gel. Rabbit antibodies raised against C-terminal (including intact FH1 and FH2 domain) of Diaphanous were used at 1:5000 dilution to assess the presence of Diaphanous protein by western blot analysis (Grosshans et al., 2005). The control lane, Gal-4²⁻²¹UAS-mCD8-GFP, showed a distinct band for Diaphanous protein at ~123kD. No Diaphanous protein was seen at the appropriate molecular weight in both the null alleles of *diaphanous*, *dia*^{K07135} and *dia*⁵,

compared to the control (Figure 26). Neither of the mutant alleles should produce a protein of reduced molecular weight. Thus, both the null mutant alleles of *diaphanous* used for the studies did not retain detectable amount of maternally contributed Diaphanous protein at late 3rd instar larval stages.

Figure 26: Detecting Diaphanous protein on Western blot A western blot showing the absence of Diaphanous protein in third instar larvae of both the *dia* null alleles- *dia*^{K07135} and *dia*⁵.



Lane 1: Protein marker

Lane 2: *dia*⁵

Lane 3: *dia*^{K07135}

Lane 4: *Gal4*²⁻²¹ *UASmCD8GFP*- control

4.1.5 Expression pattern

Diaphanous is expressed in many tissues. Since the dendritic phenotype was evident only in a specific class of md-da neurons, it was interesting to find out whether Diaphanous is particularly located in some and not all PNS md-da neurons. The antibodies used for western blot analysis were used for the antibody staining also. Different concentrations of the Ab were tested and a concentration of 1:5000 was used for most of the preparations. The staining was performed in embryos and dissected 3rd instar larval fillets. Unfortunately, conclusive staining could not be obtained after much of experimentation with conditions. In most of the cases, the staining was seen mostly in muscles and trachea and some cells in CNS which resembled glia from their localization (covering the ventral nerve cord). However, staining pattern could not be often reproduced.

4.1.6 MARCM- generating homozygous mutant clones in heterozygous animals

The dendritic phenotype observed in *diaphanous* null mutants could be a secondary phenotype and not a cell autonomous phenotype due to some other primary phenotype, for example, misformation of surrounding tissues resulting in over branching of the dendrites of md-da neurons. To probe into this possibility, MARCM (Mosaic Analysis with a Repressible Cell Marker) analysis was done. In this technique, homozygous mutant mosaic clones can be induced using a heat shock promoter in specific tissues in a heterozygous animal. This helps in analyzing the cell autonomy of the mutant phenotype in otherwise normal heterozygous animals (Lee and Luo, 2001).

For producing MARCM clones, appropriate stocks of *dia* mutants carrying an FRT (Flippase recognition targets) sequence at the base of 2L chromosome were obtained by recombining the chromosome of *dia* mutant with the chromosome of correct FRT insertion. FRT sequences present the target sites for the Flippase recombinase enabling mitotic recombination between homologous arms of a chromosome in presence of this enzyme (Harrison and Perrimon, 1993). Such a stock was available for *dia*⁵ (Grosshans et al., 2005) and it was generated by recombination techniques for *dia*^{K07135}. Appropriate lines were crossed and progeny was heat shocked as described in methods to get MARCM clones of mutant md-da neurons.

Unfortunately, many rounds of MARCM experiments gave no clones in the nervous system although clones were produced for different tissues. Therefore, no conclusion about the role of *dia* could be drawn from these experiments.

4.1.7 Analysis with deficiency:

In *Drosophila* genetics, the authenticity of any mutant phenotype is often tested using an appropriate deficiency line. A deficiency is a deletion uncovering a genomic region of variable lengths. There are many such deficiency stocks for

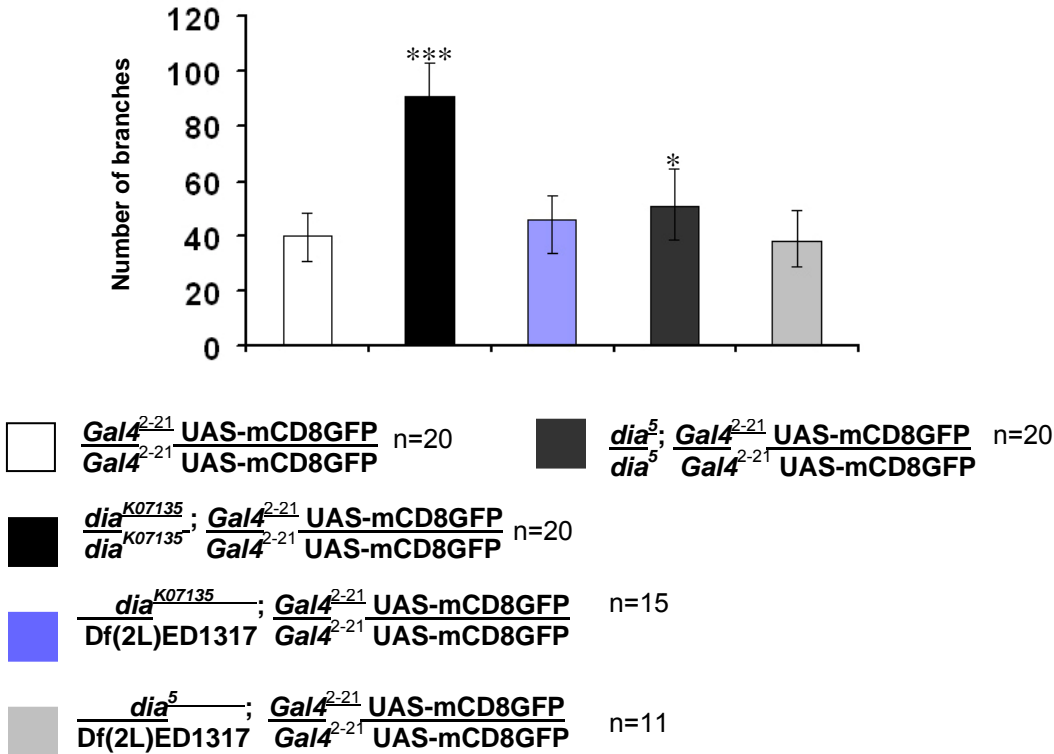
different regions of different chromosomes sometimes with definite break points. One such deficiency, Df(2L)ED1317, uncovering the *dia* gene and many others with definite boundary 38D1-38F5, was tested in trans for both the null mutants of *dia*.

A deficiency should behave as a null mutant for each of the genes it uncovers. As expected, the null mutant of *dia*, *dia*^{K07135} over deficiency Df(2L)ED1317 did not give any survivors indicating that the *diaphanous* gene was indeed deleted in the Df(2L)ED1317. However, the 3rd instar larvae of *dia*^{K07135}/Df(2L)ED1317; *Gal4*²⁻² *UASmCD8GFP*/ *Gal4*²⁻²¹ *UASmCD8GFP* showed a very mildly significant dendritic over branching phenotype with 45.73±9.3, n=20, p=0.026 branches per vpda neuron compared to the control (Figure 27). This phenotype was considerably milder than homozygous *dia*^{K07135}.

The other null allele, *dia*⁵, showed no dendritic over branching phenotype with 38±11, n=20 branches per vpda neuron when tested in trans with the deficiency (Figure 27). This result indicated that the dendritic over branching phenotype may not be a direct phenotype of mutated *diaphanous* gene.

This data suggested that there is at least one more mutation in the stocks generated for analysis which is contributing to the phenotype. Since we were using a marker line stock which had at least 2 insertions of P-elements on the 3rd chromosome, we decided to check where these insertions were located and whether they were contributing to the dendritic phenotype seen in *dia* null mutants.

Figure 27: Deficiency analysis of *diaphanous* null mutants Quantitative analysis of total number of branches of both the null alleles of *dia* with deficiency showing a lack of dendritic over branching phenotype seen in both the alleles in homozygous conditions respectively.



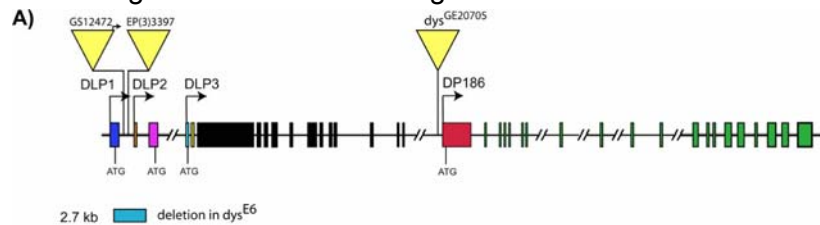
4.1.8 Dystrophin: insertion of *Gal4*²⁻²¹ causes a dendritic phenotype!

The marker line *Gal4*²⁻²¹ *UASmCD8GFP* has at least 2 known constructs. The first is *Gal4*²⁻²¹ and the other is *UASmCDGFP*.

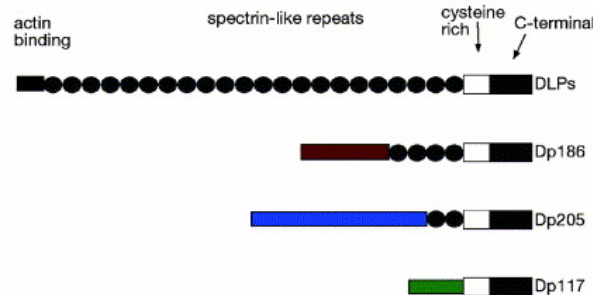
The *Gal4*²⁻²¹ construct insertion was mapped to the *dystrophin* gene which encodes for Dystrophin protein (unpublished data- Andre' Reissaus). Dystrophin is a scaffolding protein and members of the dystrophin family of proteins perform a critical but incompletely characterized role in the maintenance of membrane-associated complexes at points of intercellular contact in many vertebrate cell types. They interact with, amongst others, the transmembrane laminin receptor dystroglycan and cytoskeletal actin (Roberts and Bobrow, 1998).

Drosophila melanogaster genome contains only one *dystrophin* gene which encodes for seven protein isoforms bearing a number of highly conserved domains. The three large isoforms DLP1, DLP2, and DLP3 have an N-terminal actin-binding domain of spectrin repeats, and a C-terminal cysteine-rich domain speculated to interact with other dystrophin-glycoprotein complex proteins (Figure 28). One of the four shorter isoforms, Dp186, has a unique N-terminal domain appended to the pan-Dystrophin C-terminal domain. The lack of the large dystrophin isoforms in the postsynaptic muscle cell leads to elevated evoked neurotransmitter release from the presynaptic apparatus. However, absence of the large dystrophin isoforms does not lead to changes in muscle cell morphology or alterations in the postsynaptic electrical response to spontaneously released neurotransmitter (Neuman et al., 2005; van der Plas et al., 2006).

Figure 28: Dystrophin gene and transcripts in *Drosophila* (A) There are seven known dystrophin isoforms, the large isoforms DLP1, DLP2, and DLP3 and the short Dp186 isoform have been worked upon. The position of the *dys*^{EP3397} is indicated. Exons are indicated as bars and introns as horizontal lines. B) The domain structure of the various transcripts products, and the product-specific N-termini. The truncated products are named according to their molecular weights.



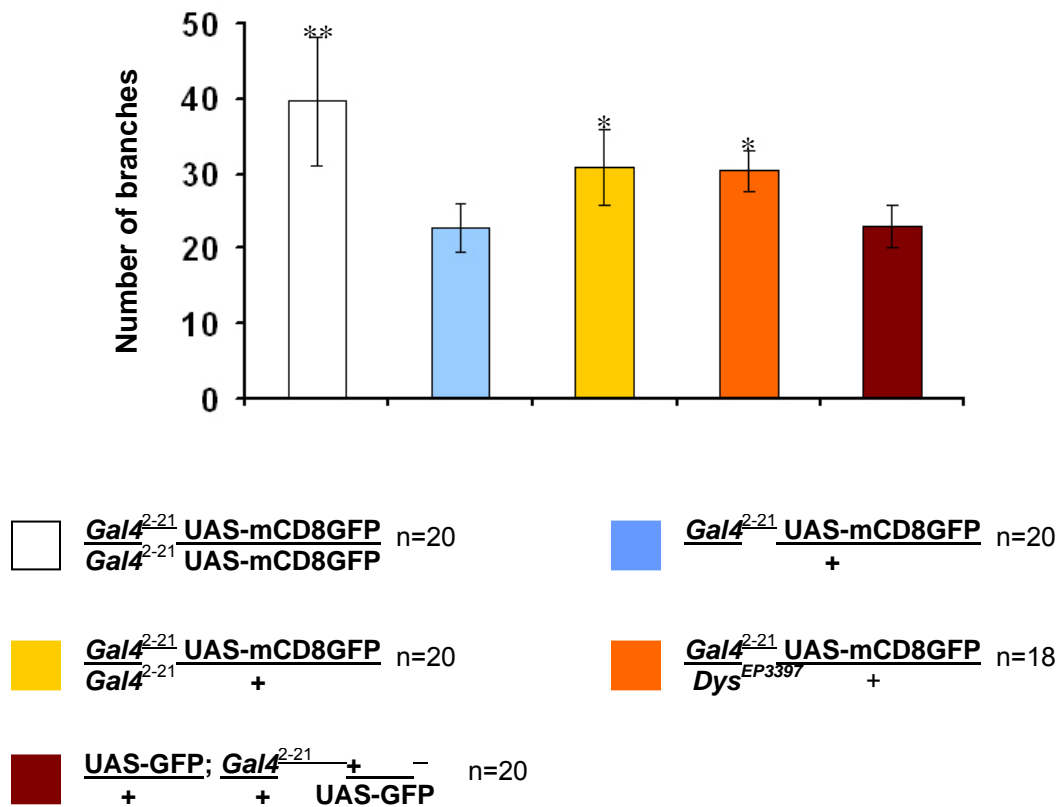
B)



[Adapted from J Neurosci. 4;26(1):333-44 (2006) and FEBS Lett. 10;579(24):5365-71 (2005)]

We first analyzed the phenotype of heterozygous, $Gal4^{2-21}UASmCD8GFP/+$ larvae which came as a surprise, showing 22.75 ± 3.2 ($n=20$, $p<0.05$) dendritic branches of the class I vpda neuron compared to homozygous $Gal4^{2-21}UASmCD8GFP/Gal4^{2-21}UASmCD8GFP$, with 39.65 ± 8.5 ($n=20$) dendritic branches (Figure 29). It became clear that the control line had a phenotype on its own, and that in homozygous condition the control line had twice as many dendritic branches as the heterozygous condition.

Figure 29: Dendritic over branching phenotype of Dystrophin Dystrophin is not the only molecule responsible for the dendritic phenotype of the marker line. Quantitative analysis of total number of branches showing a significant increase in the homozygous marker line compared to heterozygous condition or with heterozygous $Gal4^{2-21}$ insertion and another reporter. Similar over branching phenotype was observed when the heterozygous marker line is checked with only $Gal4^{2-21}$ insertion or a *dystrophin* allele, Dys^{EP3397} ; however, the same severity (like that of the homozygous marker line) is not observed indicating partial contribution of *dystrophin* in the dendritic phenotype.



To investigate separately the contribution of *Gal4*²⁻²¹ insertion in the dendritic phenotype, *Gal4*²⁻²¹ was analyzed in homozygous condition with heterozygous *UASmCD8GFP* insertion to visualize dendrites (Figure 29). The 3rd instar larvae of *Gal4*²⁻²¹ *UASmCD8GFP*/*Gal4*²⁻²¹ + genotype exhibited 30.9±5, n=20 dendritic branches which was significantly more (p<0.05) than heterozygous *Gal4*²⁻²¹ *UASmCD8GFP*/+ but still significantly less (p<0.05) than homozygous *Gal4*²⁻²¹ *UASmCD8GFP*. This result confirmed that *Gal4*²⁻²¹ is contributing to the dendritic phenotype of the control line. However, it is only partially responsible for the expressivity of the phenotype. There is some other mutation which is also responsible for the dendritic phenotype of the control line.

To confirm that the dendritic phenotype was due to the insertion in *dys* gene, a *dystrophin* mutant allele, *dys*^{EP3397}, was checked for phenotypic non-complementation with *Gal4*²⁻²¹. This *dys* allele is a P-allele with a P element inserted 750 bp upstream of the DLP2 initiator codon (van der Plas et al., 2006). This allele was crossed with *Gal4*²⁻²¹ *UASmCD8GFP* and the 3rd instar larvae of genotype *dys*^{EP3397}/*Gal4*²⁻²¹ *UASmCD8GFP* were tested for dendritic phenotype (Figure 29). These larvae showed 30.38±2.71, n=20, p<0.05 branches per vpda neuron. This result confirmed that the insertion in *Gal4*²⁻²¹ was in the *dystrophin* gene because of the non-complementation of the phenotype of the *dystrophin* mutant and *Gal4*²⁻²¹ insertion. Further, these results indicated that *dystrophin* is not the only gene contributing the phenotype of marker line, *Gal4*²⁻²¹ *UASmCD8GFP*/*Gal4*²⁻²¹ *UASmCD8GFP*.

In this case, the insertion site of the other construct *UASmCD8GFP* could also be responsible for the phenotype. To confirm this hypothesis, the *Gal4* 2-21 driver was crossed with *UAS-GFP* construct line. In the progeny, the dendrites of class I neurons could be visualized due to expression of *GFP* in class I neurons. The total number of branches of vpda neuron were 23±2.9, n=20 indicating that the insertion site of *UASmCD8GFP* was perhaps contributing to the phenotype of the marker line *Gal4*²⁻²¹ *UASmCD8GFP*/*Gal4*²⁻²¹ *UASmCD8GFP*. This insertion site was roughly mapped to one of the introns of *fruitless* gene on the 3rd

chromosome (Unpublished data- Andre' Reissaus). If the construct is inserted in the intron then it is difficult to judge its impact on mutating the gene. However, all the results obtained till now have indicated that the dendritic overbranching phenotype observed is not solely due to mutation in *dystrophin* gene.

4.1.9 Dendritic over branching phenotype of *dia* null mutants is lost in heterozygous marker condition

Although both the null mutants of *dia* showed a significant dendritic over branching phenotype, many of these results were confusing as noted below:

- The two null alleles of *diaphanous* exhibited different levels of severity of the dendritic over branching phenotype,
- The transallelic combination of these two alleles showed a much milder dendritic phenotype and
- Both null mutants lost their dendritic phenotype over the deficiency chromosome

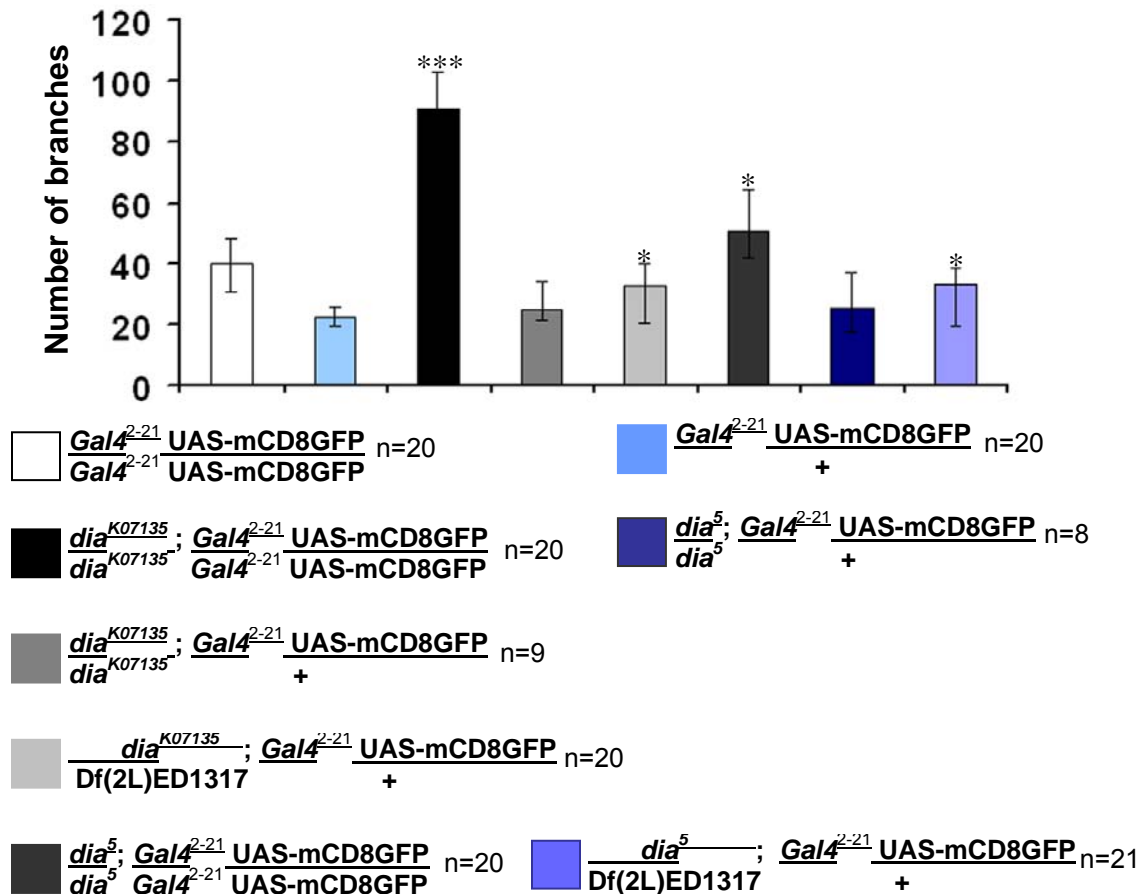
It was clear from the above experiments that, the marker line was interfering with the dendritic phenotype seen in *dia* null alleles. We then set out to check the dendritic phenotype of *dia*^{K07135} and *dia*⁵ in the heterozygous background of the marker line *Gal4*²⁻²¹ *UASmCD8GFP* + and the result came as a surprise (Figure 30). The total number of dendritic branches of the class I vpda neuron of *dia*^{K07135} / *dia*^{K07135}; *Gal4*²⁻²¹ *UASmCD8GFP* + were 25±9.1, n=9 and it was 25.3±5.7, n=8 for *dia*⁵, which were similar to the control, *Gal4*²⁻²¹ *UASmCD8GFP* +, with 22.75±3.2, n=20 and much lesser than the homozygous marker line, *Gal4*²⁻²¹ *UASmCD8GFP* / *Gal4*²⁻²¹ *UASmCD8GFP*, 39.65±8.5, n=20 itself.

When checked over the deficiency Df(2L)ED1317, both the null alleles, *dia*^{K07135} and *dia*⁵, in heterozygous marker background showed significantly more dendritic branches in class I neurons (Figure 30). *dia*^{K07135} / Df(2L)ED1317; *Gal4*²⁻²

UASmCD8GFP + exhibited 32.6 ± 7.4 , $n=20$, $p < 0.05$ dendritic branches of vpda neuron while *dia*⁵/Df(2L)ED1317; *Gal4*²⁻²¹ *UASmCD8GFP* exhibited 32.9 ± 11.64 , $n=21$, $p < 0.05$ dendritic branches of vpda neuron compared to its control – heterozygous marker line, *Gal4*²⁻²¹ *UASmCD8GFP* +, 22.75 ± 3.2 , $n=20$.

However, this observation was different compared to the results obtained with homozygous marker background for deficiency analysis. Since the deficiency deletes some more genes including *diaphanous*, the differences in the observations can be due to some unknown interactions between different mutations due to variability of genomic background.

Figure 30: Dendritic phenotype of *dia* null mutants is lost in heterozygous marker line condition Quantitative analysis of total number of branches in late 3rd instar larvae. Both the null mutants of *dia*, *dia*^{K07135} and *dia*⁵, lost their over branching phenotype when tested in heterozygous marker line background. Interestingly, both these allele showed a mildly significant dendritic over branching phenotype when tested in trans with the deficiency, Df(2L)ED1317.



Nevertheless, based on above experiments, it became evident that the dendritic phenotype of *dia* null mutants was a result of complicated interactions between at least 2 genes on the 3rd chromosome and 2 from the 2nd chromosome. Diaphanous seems not have a dendritic phenotype by itself but may contribute to the dendritic phenotype along with other genes.

4.2 Profilin (*chickadee*)

Profilin is a very well known actin binding molecule. Profilin sequesters monomeric actin when barbed ends are capped. However in case of uncapped actin filaments, low Profilin concentrations increase elongation rates by adding actin (in complex with Profilin) to the fast growing filament ends, although high Profilin concentrations increase depolymerization at these ends. Profilin also binds to poly-proline sequences and these interactions with proline-rich ligands can further modulate actin polymerization (Polet et al., 2007) (see introduction 1.5.2).

In *Drosophila*, there is only a single gene for Profilin located on the 2nd chromosome at 26A5- 26B2 and it is called *chickadee* (*chic*). The *chic* gene codes 2 mRNAs of 1.0 and 1.2 kb with identical open reading frames, which code for a small protein of 126 amino acids that is 40% identical to Profilins from *Saccharomyces cerevisiae*. When conservative amino acid substitutions are considered, the homology increases to greater than 60% similarity (Cooley et al., 1992).

Interestingly, *chickadee* showed a dendritic over branching phenotype in RNAi assay and genetic analysis was carried out to probe into its possible role in dendritic morphogenesis. We did both gain of function and loss of function analysis for *chickadee* also similar to *diaphanous*.

4.2.1 Gain of function analysis

We used an existing *UAS-chic* construct for the gain of function analysis. Since this construct was placed on the 3rd chromosome, it was expressed only in heterozygous conditions using class I or class IV neuron specific *Gal4* lines which were also located on the 3rd chromosome.

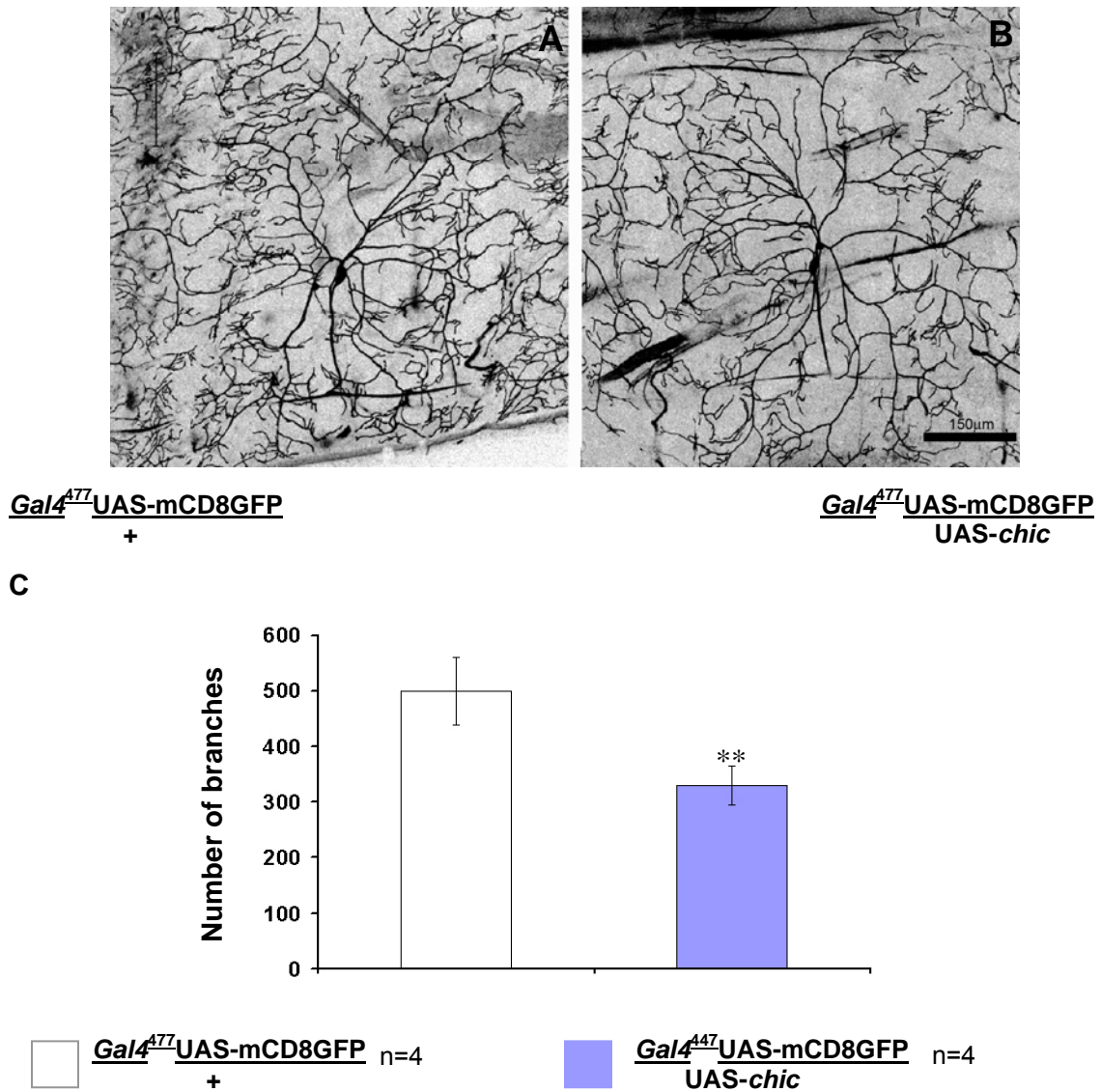
4.2.1.1 Overexpression of *chic* in class I and class IV neurons

Overexpression of Profilin selectively in class I neurons using *Gal4*²⁻²¹ *UASmCDGFP* line did not show any significant difference in the total number of dendritic branches (23.85 ± 3.2 , $n=20$) compared to control. This indicated that Profilin may not have a significant role in class I neurons.

To test whether Profilin plays a role in regulating dendritic branching of high complexity Class IV neurons, we overexpressed *UAS-chic* using *Gal4*⁴⁷⁷ in those neurons. Indeed, overexpression of *chic* reduced dendritic branching of class IV ddaC neuron (330.25 ± 36.2 , $n=4$, $p < 0.05$) (Figure 31) compared to that of the control.

Thus overexpression of Profilin affects the dendritic morphology of class IV but not class I neurons. These data suggest that Profilin may have an effect on dendritic branching in a neuronal class specific manner in class IV neurons and perhaps not in class I neurons.

Figure 31: Dendritic phenotype of class IV ddaC neuron upon Profilin overexpression (A,B) Cell specific overexpression of *UAS-chic* (B) significantly reduces the total number of dendritic branches of class IV ddaC neuron compared to that of the control (A). C) Quantitative analysis of total number of dendritic branches showing a significant reduction upon Profilin overexpression.



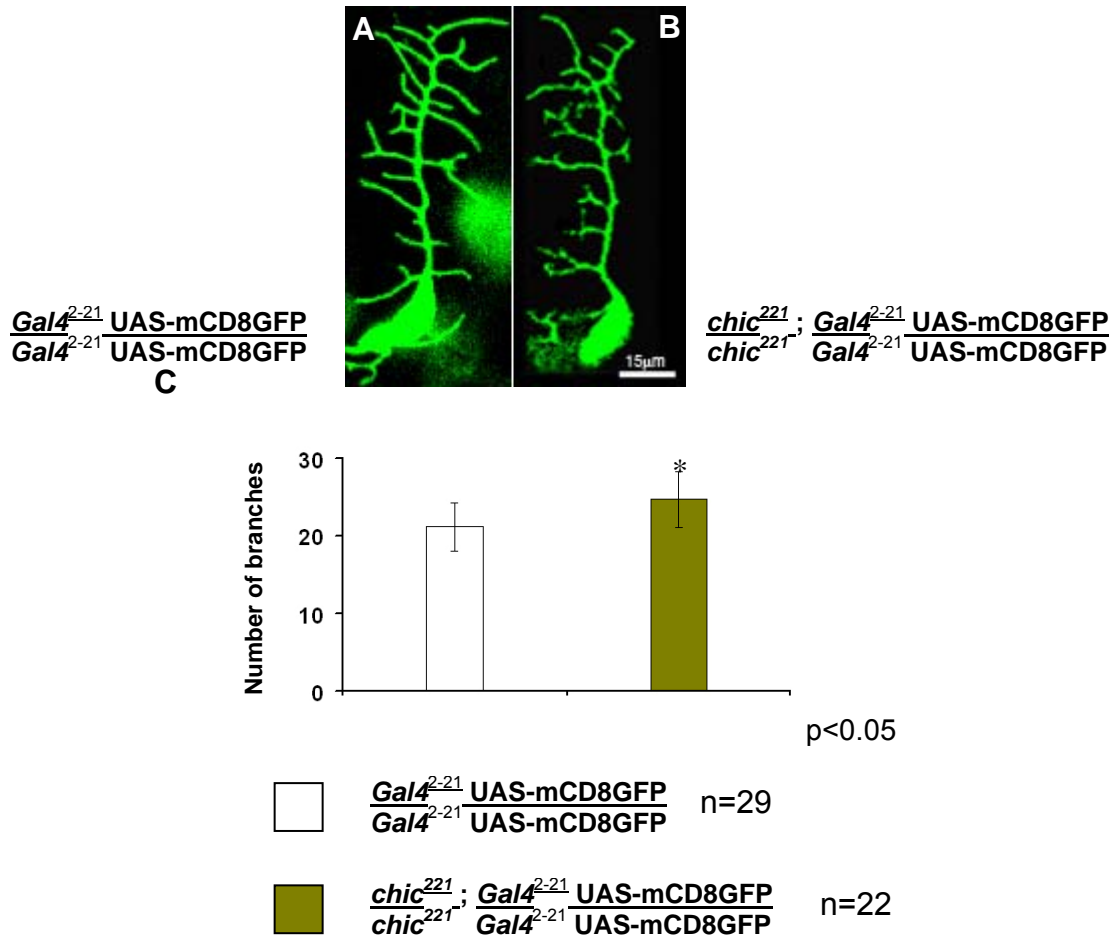
4.2.2 Loss of function analysis

Since overexpression of Profilin showed a neuron specific effect, it was then interesting to analyze loss of function effects on dendritic morphology. For this purpose, we obtained different alleles of *chickadee*. Hypomorphic alleles of *chic* are viable and are female sterile. However, the null alleles are late embryonic or early larval lethal. Null alleles of *chickadee* exhibit an axon growth cone arrest phenotype in inter-segmental nerve in late embryos. It also plays an important role in axon outgrowth (Wills et al., 1999).

4.2.2.1 Dendritic phenotype of null *chic*²²¹ and hypomorphic *chic*¹¹ and *chic*³⁷ alleles

Three different alleles of *chic* were chosen for analysis. The hypomorph alleles *chic*¹¹ and *chic*³⁷ are viable with female sterility whereas *chic*²²¹ is a null allele. The null allele, *chic*²²¹, did show a mild but significant increase in dendritic branches at stage 17, in agreement to what was observed upon RNAi. The total number of dendritic branches was 24.72 ± 3.6 (n=22, p<0.05) in *chic*²²¹; *Gal4*²⁻²¹UASmCD8GFP/ *Gal4*²⁻²¹UASmCD8GFP embryos compared to dendritic branches of control vpda from *Gal4*²⁻²¹UASmCD8GFP/ *Gal4*²⁻²¹UASmCD8GFP (21.24±3.1, n=29) (Figure 32a,b). The phenotype was minor but significant. However, *chic* null mutants are lethal at late embryonic / early first instar larval stages (Cooley et al., 1992), conclusive judgment could not be drawn from the phenotypic analysis carried out in *chic*²²¹ homozygous mutant embryos. The dendritic phenotype could have been a secondary effect due to defects in the surrounding tissues or the neuron itself of the embryos. In the light of the experiments described in previous sections, the *chic* dendritic phenotype in embryos will need to be re-evaluated in the *Gal4*²⁻²¹UASmCD8GFP/ + background.

Figure 32 Dendritic phenotype of class I vpda neuron of *chic*²²¹ at embryonic stage (A,B) Class I vpda neuron of *chic*²²¹ (B) from embryonic stage 17 shows significant increase in dendritic branches compared to that of control (A). C) Quantitative analysis showing a significant increase in total number of branches of vpda neuron in *chic*²²¹ compared to the control.



Since hypomorphic alleles of *chic*, *chic*¹¹ and *chic*³⁷, were viable, it was possible to assess their phenotype at 3rd instar larval stages. The phenotypic analysis of *chic*¹¹ and *chic*³⁷ did not show any significant difference in dendritic morphology in these 2 hypomorphic alleles (data not shown) (Castrillon and Wasserman, 1994; Verheyen and Cooley, 1994).

It was conceivable to think that the transallelic combination of *chic* null with *chic* hypomorph could be viable till later stages of development and it could be possible to analyze the effect on dendritic morphology in such a combination.

Therefore a transallelic combination of *chic*²²¹ with *chic*¹¹ was made which was viable and when assayed at 3rd instar larval stages did not show any significant dendritic phenotype. The total number of branches of vpda neuron in *chic*²²¹/*chic*¹¹ were 36.3±6.7, n=10, p>0.05.

The class IV neuronal marker lines show *GFP* expression only at late embryonic stages resulting in very weak *GFP* signal in all the fine dendritic branches of class IV neurons and making it difficult to analyze their dendritic morphology. Since the null allele of chickadee was late embryonic lethal, it was not feasible to analyze the dendritic morphology of class IV neurons in this allele.

4.2.3 Expression pattern using antibody staining

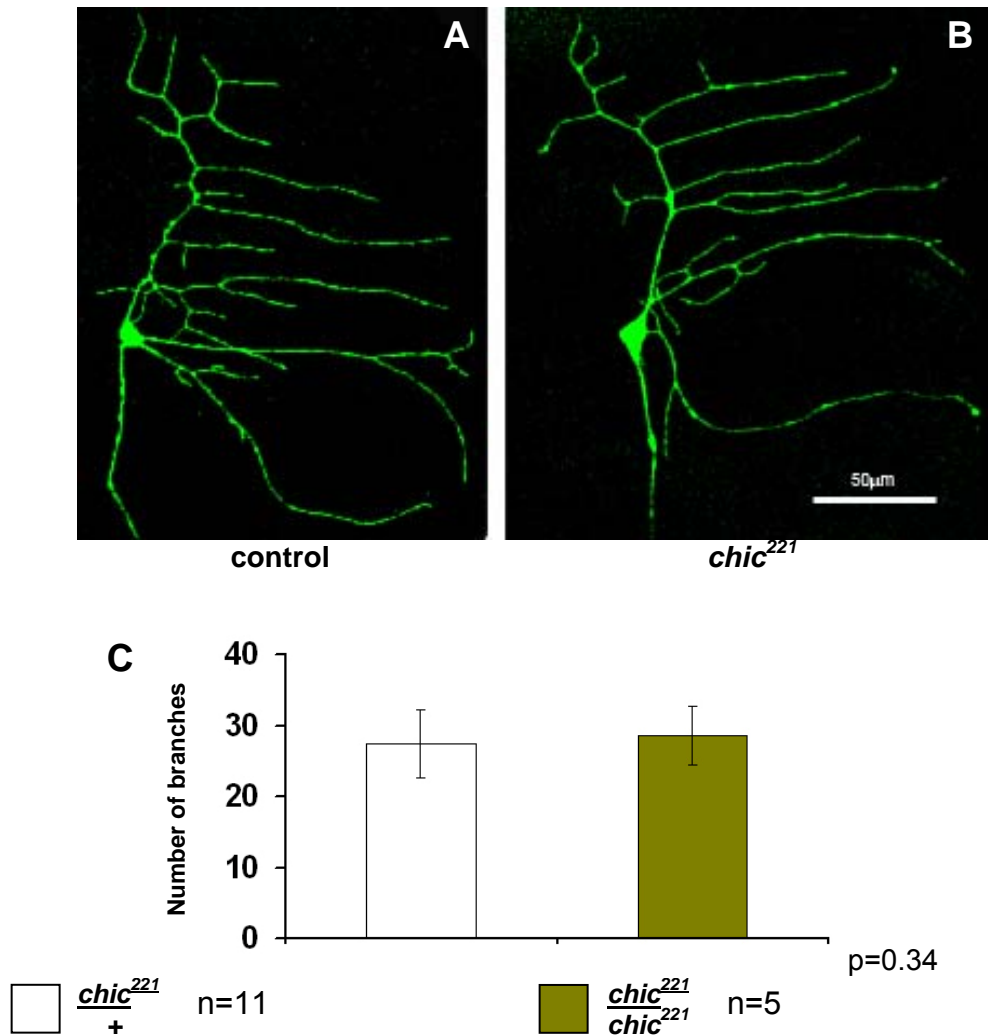
Profilin is a ubiquitously expressed molecule. However, its expression pattern in the PNS is not known. Given that *chic* RNAi showed a dendritic phenotype in PNS neurons and *chic* null mutant did show an inconclusive dendritic over branching phenotype, checking its expression pattern in the PNS became an obvious step. Monoclonal antibodies raised against Profilin protein were used for staining the embryos. Every time, the staining was very prominent in muscles and because the PNS neurons lie just above the muscles, it was really difficult to visualize any staining in the PNS. Thus, the expression pattern analysis using antibody staining was not successful.

4.2.4 MARCM- generating homozygous mutant clones in heterozygous *chic*²²¹ animals

Because the null *chic* alleles are late embryonic lethal, I used MARCM analysis to address the cell autonomous role of Profilin in dendritic arborization. The null allele, *chic*²²¹, was recombined with appropriate FRT site construct and used for inducing homozygous mutant MARCM clones in heterozygous animals. The MARCM mutant clones were not obviously different than the control clones for all different classes of neurons (Figure 33a). The quantification of total number of dendritic branches of class I neuron ddaE from the dorsal cluster in both control

(27.5 ± 4.8 , $n=11$) and *chic*²²¹ mutant clones (28.6 ± 4.12 , $n=5$, $p < 0.05$) showed no significant difference (Figure 33b).

Figure 33: MARCM Analysis Clones of *chic*²²¹ (A) do not show any significant difference in dendritic morphology compared to that of control (B). Quantitative analysis of total number of dendritic branches in class I neuron ddaE from dorsal cluster showing no significant difference in dendritic branching in *chic*²²¹



The absence of any obvious dendritic phenotype in the mutant clones could be explained by the fact that *chic* is not required in these neurons. Alternatively, it may reveal that the phenotype observed upon RNAi is non-cell autonomous, or, finally, there might be sufficient levels of Profilin protein in the clones to allow for normal dendrite differentiation. This latter possibility is difficult to test because of

the high level of the protein present in the tissues in which these neurons are embedded that makes conclusive immuno-staining in single cell mutant clones very difficult.

4.3 *chickadee* and *diaphanous*: analyzing the interaction

Diaphanous-related-formins from yeast to mouse are known to directly bind *in vitro* to Profilin, an important regulator of actin dynamics, via their poly-proline-rich FH1 domain and the cdc12p formin interacts genetically with Profilin in yeast (Chang et al., 1997; Kovar and Pollard, 2004). The single *Drosophila* Profilin gene, *chickadee* is proposed to interact with *dia*, however no interaction has been shown *in vivo* to date (Castrillon and Wasserman, 1994; Verheyen and Cooley, 1994).

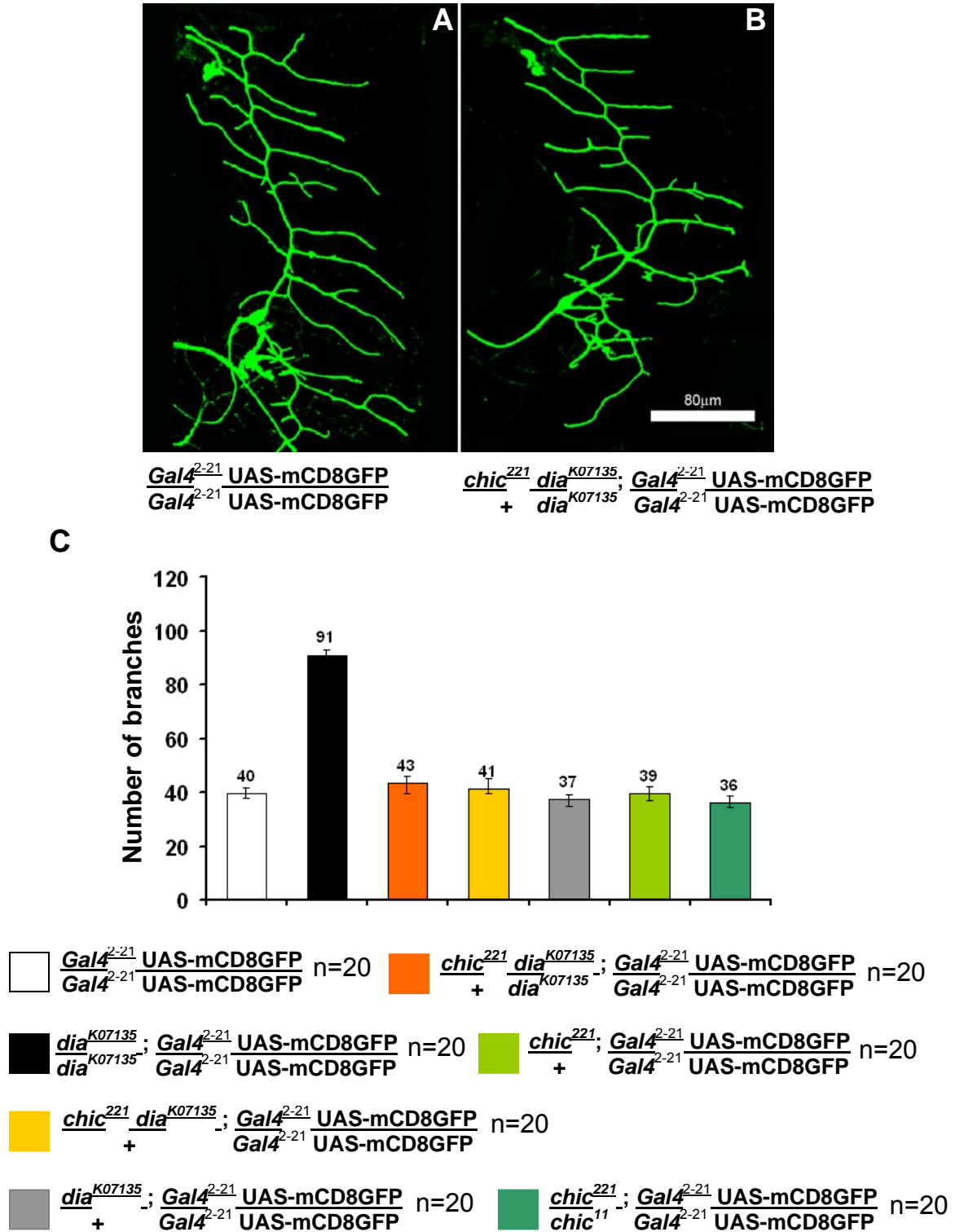
Both these molecules showed a similar dendritic over branching phenotype in RNAi assay. However, the overexpression of *diaphanous* showed an increase in the total number of branches whereas the overexpression of Profilin had no effect on class I neurons. The Profilin loss of function data could not clearly give an idea about the role of these two molecules. Since both these molecules are shown to interact *in vitro* and *in vivo* as well as they are hypothesized to do so *in vivo* in *Drosophila*, we decided to look at the double mutants of both *chickadee* and *diaphanous*.

Animals heterozygous for either *chic* or *dia* null mutations or transheterozygous for the two mutations (*dia*^{K07135} / *chic*²²¹) showed normal dendritic morphology with no significant changes in the total number of branches or total dendrite length of vpda neurons. To study the interaction further we recombined a *chic* null mutant, *chic*²²¹ (Verheyen and Cooley, 1994) with *dia*^{K07135}. While heterozygous recombinant animals showed no phenotype (41.4±6.7, n=15) (Figure 34b), homozygous recombinant animals were lethal. Using these flies we could eliminate one copy of *chic* in the *dia* mutant background (*chic*²²¹ *dia*^{K07135}/ + *dia*^{K07135}). In this condition, the dendritic overbranching

phenotype of *dia*^{K07135} mutant larvae was completely suppressed (Figure 34a). vpda neurons of *chic*²²¹*dia*^{K07135}/*dia*^{K07135} third instar larvae showed normal number of dendritic branch termini (43.39±15.9, n=18) compared to *dia*^{K07135} homozygous (Figure 34b). Correspondingly, the total dendritic length was also restored to normal (1421.87±240, n=18) in *chic*²²¹*dia*^{K07135}/*dia*^{K07135} animals.

Considering previous results, the phenotype exhibited by *diaphanous* null mutant results from complex interactions and one of the responsible interactor may be placed on the second chromosome as *chic* and *dia* genes. Hence it is possible that while recombining *chickadee* allele with *dia*, this particular interactor which was contributing to the dendritic over branching phenotype, was lost and thus the double mutant does not show the same dendritic phenotype anymore. Thus, the suppression of dendritic phenotype may not be actually due to *chickadee* but it may be due to loss of this unknown interactor. The possibility of the *diaphanous* chromosome harboring an interactor can be tested by crossing the *dia* allele out for many generations to lose this possible interactor and then testing the *dia* allele for dendritic phenotype. Taken together, this data shows that the two genes in combination do not show a dendritic phenotype suggesting that they may not have a significant role in dendritic morphogenesis in this system.

Figure 34: *chic*²²¹ genetically interacts with *dia*^{K07135} (A,B) One copy of *chic*²²¹ suppresses the dendritic phenotype of class I vpda neuron of *dia*^{K07135} in the marker line background. C. Quantitative analysis of total number of branches of vpda neuron showing the suppression of phenotype of *dia*^{K07135} phenotype by *chic*²²¹ along with controls.



4.4 Time lapse analysis:

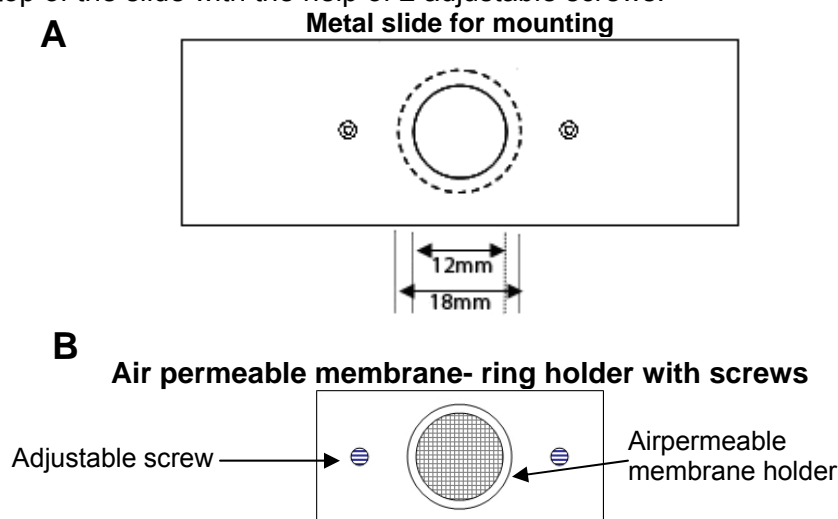
Dendritic branching is a very important step in dendritic morphogenesis, which defines the function, receptivity, connections and the coverage of the neuron. All the classes of neurons which are a part of this study differ in their repertoire of primary, secondary and higher order branches. How are these branches formed? Does a branch form once and then it is stabilized or there is a process of formation and retraction going on? Are the branches formed at some particular time of development and do they grow as they are formed? To answer several of these questions, a time lapse approach was undertaken. A single vpda neuron was observed over time during larval morphogenesis. From preliminary analysis, it was clear that the dendritic branches are still formed at the late third instar larval stages. The total number of branches keeps increasing. Since most of our analyses were carried out at 3rd instar larval stages, the same stage was chosen for time lapse analysis.

4.4.1 Standardizing time lapse assay

The time lapse assay offers a very interesting possibility to look inside a live animal and assess the changes. In our case, we wanted to see changing shapes and numbers of dendrites. However, this assay had to be set up to working conditions. *Drosophila* late 3rd instar larvae are called wandering larvae and as the name suggests, the larvae at this stage are very motile. It is very difficult to keep them motionless. Use of any anesthetic might affect the development and/or morphology of dendrites and that is why it was avoided. Another possibility was to pin down the larvae but they would still show peristaltic movement. The next options was to press them in a way that they don't get squashed and die but still are not able to move. Since the time lapse procedure would have taken at least few minutes, it was important to keep the larvae alive and breathing. For this purpose, a metal slide was designed with a hole with certain depth (1mm) and diameter. A cover-slip was fixed with Vaseline at the base of the hole which worked as a window for imaging (Figure 35a). The

larvae, placed on the cover-slip in halocarbon oil, were covered with a ring of porous membrane which could be tightened on the larvae with adjustable screws (Figure 35b). Different depths and diameters for the hole, different porous membranes and rings were tried out and finally a time lapse slide set up was standardized.

Figure 35: Live imaging slide outlay (A) A metal slide with a 12mm wide hole at the center was used as the mounting surface. This hole was surrounded by an equicentral wider circle of 18mm with a depression of 1mm in a way to fit a cover-slip in it. (B) A plastic rectangle fitted with a permeable ring holder of 18mm diameter was used to fix on top of the slide with the help of 2 adjustable screws.



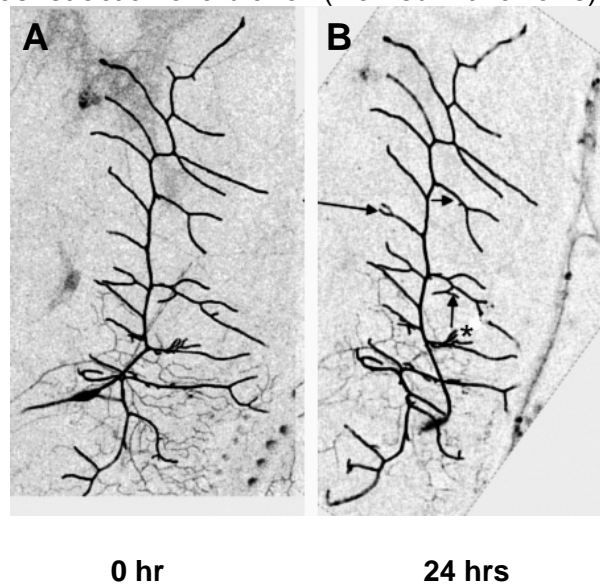
4.4.2 Imaging dendrites *in vivo* over time

After the basic requirement of the time lapse set up was achieved, the next step was to actually image the larvae. For this purpose, late 3rd instar larvae were selected and imaged to observe dendritic morphology of class I vpda neuron (Figure 36). Previously it has been described that class I neurons from dorsal cluster, ddaD and ddaE, almost fixed the shape of overall dendritic arbors at early larval stages (Sugimura et al., 2003). Only two to three lateral/second- or higher-order branches are generated per cell during the initial 13-15 hr of larval development and new branches are hardly seen for the next 13-15 hr. Particularly, ddaE achieves its final complexity possibly by 50 hr after egg laying.

However, class I vpda neuron shows a very dynamic branching process in case of higher order branches (Grueber et al., 2003a). The 3rd instar larval vpda neuron exhibits shortening of branches, complete retraction of branches and *de novo* formation of branches.

After imaging the 3rd instar larvae the first time, they were let develop further for additional 20-24 hours at 18^oC, then they were imaged again and then the number of new branches formed and the number of retractions were counted. On average, 7 novel branch formation (depicted by arrows) and 1 retraction events (depicted by *) were observed in vpda neurons of control *Gal4²⁻²¹UASmCD8GFP* larvae (n=5). New branches are formed and some of them are retracted while some of them are stabilized. At the same time previously stabilized branches keep growing in length.

Figure 36: Time lapse analysis of 3rd instar larvae- visualizing dendritic morphogenesis in live vpda neuron from the marker line *Gal4²⁻²¹UASmCD8GFP* visualized over time for 24 hrs – showing formation of new branches(marked with asterisk) as well as retraction of a branch (marked with arrows)



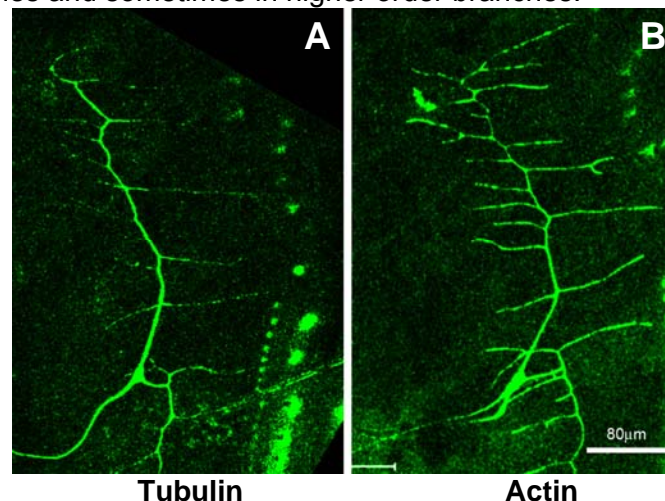
This analysis confirms previous observations that formation and retraction of branches is a constantly happening process for class I vpda neuron during late larval development unlike its counterpart class I neurons from dorsal cluster

(Sugimura et al., 2003). Thus, time lapse imaging was successfully set up for further studies to understand dendritic morphogenesis.

4.5 How do actin and microtubule contribute to dendrite formation?

Cortical actin limits and defines processes whereas microtubules fill them up. How do actin and microtubule filaments act during formation of a new branch? In case of axons, cortical actin destabilization is necessary for microtubules to extend to form a new branch (Dent and Kalil, 2001). However, axons are enriched in microtubules so it is conceivable that microtubules play a major role in axonal branch formation and extension. Does the same principle hold for dendrites? To probe into this possibility, localization of tubulin and actin were studied in the dendritic branches of class I vpda neuron. *UAS*-controlled and *GFP*-tagged constructs were handy for visualization of both actin and tubulin. For tubulin, a *UAS-tub-GFP* construct (Grieder et al., 2000) was used whereas for actin, a *UAS-GMA* construct (Dutta et al., 2002) was used. *UAS-GMA* is a chimeric construct that fuses the actin binding region of *Drosophila* moesin to the C-terminal of *GFP*. Both the constructs were expressed using *Gal4²⁻²¹* driver.

Figure 37: Localization of tubulin and actin Expression of *GFP* tagged Tubulin and actin showed distinctly different localization than one another A. Tubulin is more enriched in the primary branches and it becomes sparser in secondary branches and not seen much in higher order branches. B, Actin is enriched not only in primary but also in secondary branches and sometimes in higher order branches.



Tubulin was mainly spotted in primary branches with a lower intensity in secondary branches. The intensity dropped below detection level in higher order branches. Although, actin was enriched at the base of secondary and higher order branches and its intensity also dropped below detection level like that of tubulin. Nevertheless, the localization of actin and tubulin was distinctly different than one another. The predominance of tubulin in lower order branches and actin in higher order branches could be established. This localization can be further studied using time lapse analysis to see how the distribution of tubulin and actin changes during branch formation, retraction and growth.

CHAPTER 5- DISCUSSION

Structural, functional and developmental aspects of dendritic architecture have been the focus of research in the field of developmental neuroscience in the last few years. Dendritic morphologies form the key to neuronal connectivity and function. From the developmental point of view, the dendritic branching pattern is a hallmark of a neuronal type. Even neighboring neurons may exhibit strikingly different dendritic branching patterns. To appreciate the genesis of neuronal diversity, one has to understand how the dendritic branching pattern of individual neurons is controlled. Since dendritic arborizations form an identity of every neuron, the topic of study of this thesis has been to understand the morphogenesis of dendrites. Both extrinsic and intrinsic factors contribute to the sculpturing of neuronal dendritic arbors. It is postulated that they act on cytoskeletal molecules and their regulators to shape dendrites (Jan and Jan 2001). However, the number of such cytoskeletal players known to affect dendritic morphogenesis is not very big considering the plethora of cytoskeletal molecules. Thus, dendritic morphogenesis and cytoskeletal molecules involved in shaping it have been the major aim of study in this thesis. We have used the well characterized embryonic and larval PNS of *Drosophila* as a model system for our studies (Gao, Brenman et al. 1999). We have also tried to follow the development of dendrites *in vivo* over time and to examine actin and microtubules localization in dendritic structures.

5.1 RNA interference screen

Traditional loss of function genetic screenings in *Drosophila* using chemical mutagens or P-element have been rewarding. Although these screenings are sometimes complicated due to several reasons like presence of cold spots in DNA that are somewhat refractory to P-element insertion and loci that are less

susceptible to chemically induced mutations or maternal rescue of mutant phenotype or redundant gene functions (Koizumi, Higashida et al. 2007) and also the time required for achieving saturated mutagenesis. Therefore, RNA interference (RNAi) can be a useful tool to overcome hurdles of conventional genetic screens (Koizumi, Higashida et al. 2007; Parrish, Emoto et al. 2007).

We took a candidate based reverse genetics approach using RNAi as an assay system to isolate prospective cytoskeletal molecules involved in dendritic morphogenesis. Such approaches have been successfully used in *C. elegans* and have proven invaluable in the analysis of basic aspects of cell and developmental biology (Lee, Nam et al. 2004). In past years, several such screens have been carried out successfully in *Drosophila* also to fish out regulating molecules for different developmental processes (Zhang, Yeromin et al. 2006; Koizumi, Higashida et al. 2007; Parrish, Emoto et al. 2007). A very recent *in vivo* RNAi screening for the genes required for the development of embryonic nervous system has resulted in isolation of many known and novel genes. This screen encompassed around 7,312 genes corresponding to approximately 50% of the *Drosophila* genes and led to isolation of around 65 positive candidate genes. The positive candidates include transcription factors, chromatin-remodeling proteins, membrane receptors, signaling molecules, and proteins involved in cell adhesion, RNA binding, and ion transport. Thus, it is possible to cover high number of genes and screen them for mutant phenotypes successfully. To add to this advantage, comparison of the phenotypes identified from this RNAi screen with the corresponding mutant phenotypes obtained in genetic screens showed that RNAi-induced mutant phenotypes resemble genetic mutant phenotypes, indicating that RNAi can be used efficiently to identify genes that are involved in the development of the embryonic nervous system of *Drosophila* (Koizumi, Higashida et al. 2007).

A latest RNAi screen to isolate transcriptional regulators of dendrite development has yielded many interesting candidates which control and co-ordinate various aspects of dendrite arborizations. These candidates could be sorted in 3

different groups depending on their differential effects on dendritic branching and outgrowth- one group promoting or inhibiting dendritic arborization, a second group with opposing effects on branching and outgrowth and a third group affecting dendrite routing (Parrish, Emoto et al. 2007). Thus, RNAi assay presented a very apt screening assay to screen for potential cytoskeletal molecules effectively in relatively short period.

We took advantage of the successfully completed *Drosophila* genome project along with recently developed RNAi technique as a genetic tool to quickly assign a function to the selected few genes. Such an approach on bigger scale will help delineate the complex web of interactions or networks linking them at the systemic level (Ma, Creanga et al. 2006). The RNAi assay was successfully set up to give reasonable survival rate of injected embryos (Table 1). We checked the reliability of the assay system by injecting GFP-siRNA in GFP expressing fly embryos and were able to successfully knock down the GFP expression (Figure 12). Though the assay was successfully set up and used, it should be noted that it did take much longer than one would expect -a few months- for the entire procedure including the standardization and the screen. Considering the various limitations of RNAi as a genetic tool, it would have been advantageous to directly analyze genetic mutants of prospective candidates for dendritic phenotype.

Nonetheless, a preliminary screen with 14 cytoskeletal molecules likely to have a role in neuronal development resulted in 5 positive candidates- Diaphanous, Profilin, Cappuccino, Kelch and Quail (Table 2). Thus, the efficiency of isolating positive candidates was about 33% which was really impressive compared to other RNAi screens described above. Although, it should be mentioned that we had selected prospective positive candidates for screening and considering this fact, it is not very surprising that the efficiency of isolating positive candidates from the screen was as anticipated. Many of the screened candidates showed no dendritic phenotype which was surprising considering their important role in cytoskeletal dynamics. However, the negative results could be due to following reasons. First the *Drosophila* eggs contain many transcripts and protein

products produced by the mother during oogenesis, which may result in nullifying RNAi effect. Second, dsRNA has been proven not to be completely successful and shows false negative results at times (Dykxhoorn, Novina et al. 2003). The other possibility is that some genes may not show specific dendritic phenotype because of their ubiquitous expression and pleiotropic phenotype which may lead to lethality resulting in low survival rates. Thus the survivors are only the unaffected ones.

All the positive candidate molecules were important regulators of the actin cytoskeleton. However, further analysis was focused on Diaphanous and Profilin because they showed more penetrance of the dendritic phenotype. Additionally, both -Diaphanous and Profilin- are known to be binding partners from *in vitro* studies and *in vivo* studies in yeast (Chang, Drubin et al. 1997). We, then, analyzed the functional role of both these molecules in dendritic morphogenesis with extensive genetic analysis.

5.2 Diaphanous: Role in dendritic morphogenesis

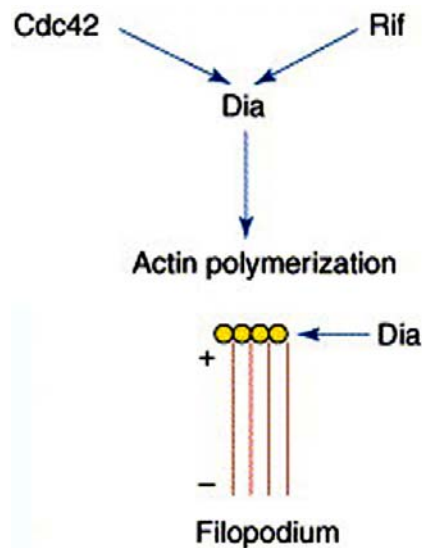
Diaphanous was an attractive candidate since it affects axonal initiation and elongation *in vitro* in cell cultures but its neuronal role *in vivo* is not explored yet. Similarly, its role in dendritic morphogenesis *in vitro* and *in vivo* is also unknown. Diaphanous nucleates actin and can affect actin turnover differentially in different model systems depending on its binding partners (Goode and Eck 2007). Thus its role in actin dynamics appears to vary depending on different factors including its binding partners, upstream regulators, type of tissue and developmental stage and species.

We tested the role of *diaphanous* in dendritic morphogenesis with profound genetic analysis. Gain of function analysis using different independently generated constructs increased the total number of dendritic branches indicating that *diaphanous* may have a role in the formation of dendritic branches (Figure 18D). It should be noted that overexpression of constitutively active *diaphanous*

(*dia-CA*) resulted in increased number of secondary branches which resembled long filopodia like structures (Figure 18B). This phenotype was not exhibited by other full length constructs of *diaphanous*. Interestingly, overexpression of only the same *dia-CA* and not of the full length form of *diaphanous* affected the dendritic morphology of class IV neurons (Figure 19). In this case also it exhibited formation of numerous filopodia like branches emerging from primary or secondary branches suggesting that activated *diaphanous* is causing formation of these filopodia structures. This was a particularly interesting observation since Diaphanous is regulated by members of the RhoGTPase family, especially RhoA, and withdrawing this regulation demonstrates a remarkable effect on a particular class of neurons, namely class IV neurons. I discuss it in detail below after providing some insight into filopodial structures in neuronal growth.

Filopodia are finger-like membrane protrusions that contain parallel bundles of actin filaments. They are believed to be important for sensing the extracellular environment, either for soluble signals or for other cells (Kater and Rehder 1995). Cdc42 is activated at the filopodia of migrating fibroblasts and plays a crucial role in actin reorganisation. Cdc42 has always been thought to be the main mediator of filopodium extension, however, Cdc42-null fibroblastoid cells can still form filopodia (Czuchra, Wu et al. 2005). Interestingly, some other Rho GTPases like Rif/RhoF, RhoD and Wrch1 can all induce filopodium extension and might therefore substitute for Cdc42 in Cdc42-null cells (Ellis and Mellor 2000; Aspenstrom, Fransson et al. 2004; Pellegrin and Mellor 2005). Recent evidence indicates that DRFs are the major controllers of actin polymerization in filopodia, both in mammalian cells and Dictyostelium (Schirenbeck, Arasada et al. 2005), and Cdc42 and Rif induce filopodia through Diaphanous (Peng, Wallar et al. 2003; Pellegrin and Mellor 2005) (Figure 38).

Figure 38: Rho family proteins, actin filaments and membrane dynamics At the plasma membrane Rho GTPases stimulate membrane protrusions through actin polymerization. Rac activates the WAVE protein complex, leading to Arp2/3 complex-mediated actin polymerization to form a branching actin filament network in lamellipodia, where the Arp2/3 complex induces a new filament to polymerize from the side of an existing filament. Cdc42 might also contribute to lamellipodial extension through WASP proteins, which activate the Arp2/3 complex. Cdc42 and Rif activate the DRFs Dia1 and/or Dia2, which bind to the barbed (+) ends of filaments and induce actin polymerization in parallel bundles at the plasma membrane, forming filopodia. + indicates barbed ends, - indicates pointed ends of filaments.



(Adapted from Ridley AJ, Trends Cell Biol. 2006 Oct;16(10):522-9.)

Filopodia are thought to be important for steering events during neuronal growth cone navigation and pathfinding (Aspenstrom, Fransson et al. 2004). It is proposed that filopodia are the precursors of dendritic branches which are stabilized during development. The early phase of branch growth happens before the formation of synaptic contact and is initiated by the appearance of a filopodium. The filopodium protrudes to form a new branch segment, the stabilization of which probably involves the invasion of microtubules. As the neuron matures, branch growth enters the late phase. Synapses start to form along the dendrite and provide a new mechanism for stabilization of the dynamic branches. This synaptic-contact-dependent stabilization mechanism is functionally selective because only dendritic branches that are contacted by the appropriate inputs are stabilized and, therefore, maintained (Ye and Jan 2005).

Indeed, *in vivo* imaging of synapse formation on a growing dendritic arbor in Zebrafish indicates that almost all synapses form initially on newly extended dendritic filopodia. A fraction of these nascent synapses are maintained, which in turn stabilizes the subset of filopodia on which they form. Stabilized filopodia mature into dendritic branches, and successive iterations of this process result in growth and branching of the arbor (Niell, Meyer et al. 2004). For dendrites of sensory neurons, which do not receive synaptic input, little is known about how the dynamics are stabilized in the late stage, although it is conceivable that the target tissues of these neurons, in addition to the homotypic dendritic exclusion that exists in some types of sensory neuron might provide a stabilization signal (Ye and Jan 2005). In this scenario, under normal conditions, upstream RhoGTPase/s are down regulated to facilitate formation of filopodia turning into dendritic branches in class IV neurons.

When full length *diaphanous* is overexpressed in class IV neuron, there is not enough of RhoGTPase/s to activate it. Thus, overexpressed full length *dia* still undergoes repression or it is kept under control by rationing its upstream regulatory RhoGTPase/s. In this case, it may be possible to evoke the same filopodia like over branching phenotype with full length *dia* construct by over expressing an appropriate RhoGTPase along with it.

Alternatively, it is possible that Diaphanous has different binding partners in different classes of neurons and therefore it behaves differently depending on the concentration, types or number of binding partners present in a particular class of neuron. Another possibility is that, the *dia*-CA construct acts as a dominant negative form giving a loss-of-function-like phenotype. Considering RhoA as an upstream positive regulator, the phenotype can be compared with that of RhoA loss of function in mushroom body neurons. It is interesting to note that in *Drosophila* mushroom body neurons, *RhoA* clones exhibit drastically increased length, frequency, and number of overextended dendrites compared with wild type (Lee, Winter et al. 2000). RhoA being an upstream positive regulator of Diaphanous, it is very much likely that *diaphanous* also would mutate to show a

similar dendritic phenotype. However, diaphanous has a branching phenotype whereas Rho has a growth and extension phenotype. The model system which was used for the analysis of RhoA clones doesn't offer an easy differentiation between branching and extension phenotypes. Finally, it is possible that the *dia*-CA construct is inserted in a gene which may mutate to give this dendritic filopodia like phenotype. Taken together, these results suggested that *diaphanous* is delicately regulated to sculpture dendritic arborizations both in class I as well as class IV neurons. Our analysis did not cover other classes of neurons because of lack of specific markers and it will be interesting to see whether the Rho GTPases and Diaphanous pathway affect any of other classes of neurons.

However, the loss of function analysis suggests that *dia* does not have a primary role in dendrite differentiation in class I and class IV neurons. Both tested null alleles, *dia*^{K07135} and *dia*⁵, showed a dendritic over branching phenotype specifically of higher order branches and not the primary and secondary branches of class I vpda neuron (Figure 21). Although, the transallelic combination of the two null alleles showed a milder dendritic over branching phenotype of class I- vpda neuron compared to each of them respectively (Figure 24). Similarly, when checked in trans-heterozygous condition with the deficiency chromosome, both the alleles showed either no phenotype or very mildly significant phenotype (Figure 29). Western blot analysis of homozygous 3rd instar larvae from both the alleles did not show any Diaphanous protein indicating that the mutations were not lost and they indeed knocked out Diaphanous protein (Figure 25). All these experiments were done in homozygous marker line background. However, when checked in heterozygous marker line background both the *dia* null alleles failed to show any dendritic phenotype. These results suggest the possibility that the dendritic phenotype is not caused by *diaphanous* alone or not at all by *diaphanous* and perhaps due to some other background mutations either on the marker line or on the *dia* chromosomes of both the null alleles. Although, it is difficult to imagine that both the independently generated

dia alleles harbor the same mutation on their chromosome, which gives a similar dendritic over branching phenotype. On the contrary, it is likely that some other mutations on other chromosomes (eg. the marker line chromosome) are contributing/ interfering with the dendritic phenotype seen in *dia* null alleles.

5.3 Dystrophin

Detailed analysis of the marker line with *Gal4* and *UAS-GFP* insertions on the 3rd chromosome, *Gal4²⁻²¹UASmCD8GFP*, which was used to analyze the dendritic arborizations of class I neurons in *dia* null alleles, showed a dendritic phenotype on its own (Figure 28). The *Gal4* insertion of the marker line was found to be in the *dystrophin* gene which is conserved and is found to be mutated in muscular dystrophy patients (Zhou, Xie et al. 2006). The *Drosophila dystrophin* gene encodes for 7 different isoforms and they are mostly expressed throughout development in different tissues including muscles, gut, mesoderm, etc. Interestingly one of the short isoforms, Dp186, is highly expressed in embryonic CNS but absent from the musculature (van der Plas, Pilgram et al. 2006). Our analysis using homozygous *Gal4* insertion or heterozygous *Gal4* insertion in transheterozygous condition with a *dystrophin* allele, *dys^{EP3397}*, showed the same result with over branching of dendrites. This result confirmed that the *Gal4* insertion was indeed in the *dystrophin* gene indicating that the phenotype observed was due to a mutation in *dys* (Figure 28). However in both these cases, the over branching was not as severe as it was seen in the homozygous marker line and in fact it was around 50% more compared to the heterozygous marker line. This result indicates that the *Gal4* insertion in the *dystrophin* gene is certainly contributing to the dendritic over branching phenotype of the marker line but it is not solely responsible for it. The role of *dystrophin* in dendritic morphogenesis has never been studied before and this is the first evidence indicating its function in dendritic branching. However, due to complications with genetic backgrounds, we did not investigate this possibility further in depth. The above results suggest that the other insertion of *UAS-mCD8GFP* construct or some other mutation on the particular chromosome may also contribute to the

marker line phenotype. The insertion of the *UAS-mCD8GFP* construct is roughly mapped to an intron in the *fruitless* gene and it is not possible to estimate its contribution to affect the gene to much extent. We haven't probed much into the contribution of this *UAS-mCD8GFP* construct in the marker line phenotype.

5.4 Diaphanous: Ambiguous results from loss of function analysis

To rule out possible genetic interaction, we also tested for a dendritic phenotype in the heterozygous marker line condition. Both the *dia* null alleles lost their phenotype in heterozygous marker condition again suggesting that *diaphanous* by itself doesn't have a dendritic phenotype and it is contributing to or enhancing the dendritic over branching phenotype of the marker line. Although, since the marker line phenotype is not due to a single mutation, it is difficult to comprehend the interaction of *dia* with the marker line mutation/s. To add to this, both the null alleles of *dia* showed a mild but significant dendritic over branching phenotype in transheterozygous condition with the deficiency suggesting that perhaps, *dia* has a role in dendritic morphogenesis. On the other hand, the deficiency used for the analysis covers ~ 400kb region with 52 known and predicted genes (Flybase). Since the deficiency covers many genes other than *diaphanous*, it is possible that this effect is due to the deletion of some other gene and not due to *diaphanous* itself. It will be a very tedious task to test each of these genes for their role in dendritic morphogenesis considering the fact that many of them are just predicted genes and most of them do not have any mutants available. We can test this again with a smaller deficiency which would delete fewer genes and a deficiency deleting only the *diaphanous* gene would be the best option. However, we do not have these resources available at this point of time and can test these possibilities in future if they become available. Other possibilities include, testing *dia* null mutants for dendritic phenotype using another marker line for class I neurons such as IG1-1 (Sugimura, Yamamoto et al. 2003). This, the only other available marker line for class I neurons, also consists of 2 insertions- one of *Gal4* and another of *UAS* on the same chromosome where *dia* gene resides, making it difficult to recombine all these three loci on the same

chromosome. Another possibility is to standardize the genetic background of both the null mutants to get rid of possible interactors by crossing them out for several generations and then to test these 'purified' stocks for a dendritic phenotype. This process is surely time demanding and the outcome can not be predicted.

Taken together, the loss of function results till now suggest that *diaphanous* may not have a dendritic phenotype on its own and perhaps acts as a homozygous enhancer of the dendritic over branching phenotype of the marker line. The dendritic phenotype seen in null alleles of *diaphanous* is a result of complex interactions between more than two genes placed on 2nd and 3rd chromosome including *dystrophin*. However, the gain of function analysis surely suggests that *diaphanous* may have an important function in dendritic filopodia formation. The gain of function analysis also suggests a neuronal class specific role as well as a possible regulatory mechanisms for *diaphanous*. This is a very interesting possibility and a systematic loss of function analysis with domain deletions will help to comprehend the role of *diaphanous* in dendritic morphogenesis.

5.5 Profilin

Profilin was another appealing candidate because it is a well known important regulator of actin dynamics playing a role in actin polymerization as well as actin depolymerization (Yarmola and Bubb 2006). As mentioned above, it is also known to be a binding partner of Diaphanous from *in vitro* studies and in yeast. Like its binding partner Diaphanous, Profilin also can affect actin dynamics differently depending upon its binding partners, concentration of actin monomers and its own concentration. Its *in vivo* role has been characterized to some extent - it is known to function in many actin dependent developmental processes including oogenesis, spermatogenesis and cell division (Witke 2004). It also has a role in the nervous system, since it is supposed to affect axonal growth in *Drosophila* (Wills, Marr et al. 1999) and it is known to get localized in dendritic spines upon neuronal activity in mammals (Ackermann and Matus 2003).

However, its role in dendritic morphogenesis is not yet known. Another point why it was appealing is because both Profilin and its binding partner Diaphanous showed a similar dendritic over branching phenotype upon RNAi. Thus, a thorough genetic analysis was carried out to unravel its role in dendritic morphogenesis.

Gain of function analysis of Profilin using a full length construct showed no effect on the dendritic morphology of class I vpda neurons. However, it did reduce total number of branches of class IV –ddaC neuron in late 3rd instar larvae (Figure 31). This result indicates that Profilin may have a neuronal class specific effect on dendritic morphology. It is also possible that it has different binding partners in different classes of neurons and thus its overexpression shows different results accordingly.

In loss of function analysis, the null allele of *chickadee* showed a mild but significant dendritic over branching phenotype of class I neurons (Figure 32) but since the analysis could only be done close to the lethal phase of the animals, we couldn't conclude anything from this experiment. *chic* null alleles completely block oogenesis, preventing the use of germline mosaics for the study of zygotic phenotypes in the absence of maternal expression. Further experiments using MARCM analysis to study cell autonomous function of Profilin resulted in null mutant MARCM clones with no significant alterations in dendritic phenotype of class I neurons (Figure 33). Dendritic morphology of other classes of neurons also seemed very much unaffected in these clones. It would have been interesting to see whether dendritic morphology of class IV neuron MARCM clones gets affected since overexpression of *chic* affects these neurons. The negative results of MARCM experiments suggest that Profilin may not function in dendritic morphogenesis in md-da neurons. Although, the negative results may also be due to maintenance of maternal supplement of the protein in the clones, leading to normal development of dendrites. Thus, we did not have a definite conclusion from this experiment either. We also tried studying the expression pattern of Profilin in embryonic stages and since the expression was really high

in muscles, it was almost impossible to see its expression in the PNS neurons which lay right over the muscles. We were not able to impart any neuronal expression pattern for Profilin. Taken together, we could not confirm the RNAi results for Profilin using genetic and immunochemical analysis.

5.6 Higher order branches of vpda neuron are dynamic at late larval stages

The *in vivo* time lapse analysis presents a great tool to actually observe the way processes are generated in live. This technique has been used before to study dendritic branching and growth of PNS md-da neurons *in vivo* (Sugimura, Yamamoto et al. 2003). However, it is very difficult to image the active processes in live samples due to movements of the animal. I have successfully standardized this technique and was able to use it to examine dendrite development *in vivo*. Previous studies have demonstrated that the two class I neurons from the dorsal cluster stabilize their basic dendritic architecture at late embryonic stage and there are very few higher order branches formed afterwards till late larval stages (Sugimura, Yamamoto et al. 2003). The preformed branches just grow in length to cover more surface area. We followed the development of dendrites of class I vpda neuron in third instar larvae (Figure 36). In agreement with previous results we found that no primary or secondary branches are formed *de novo* at the late larval stages. However, the higher order branches are dynamic with some new branches forming over a period of 24hrs at 18⁰C and we also saw retraction of branches. Thus, the primary and secondary branches are not changed but only the higher order branches are formed *de novo* or retracted. These observations may also explain why the dendritic phenotype seen in class I vpda neuron affected only higher order branches. Since primary and secondary branches are already formed and stabilized by the time the effect of mutation sets in during development, only higher order branches are affected since they are dynamic at relatively later stages also.

At the end, it should be noted that the strain used for time lapse analysis of class I vpda neuron was the same marker line $Gal4^{2-21}UASmCD8GFP$, which shows a

dendritic overbranching phenotype of these neurons. Thus, the observations of our time lapse analysis could be actually due to the mutant phenotype of this marker line. Therefore, it is important to find an appropriate control line for this analysis.

5.5 Localization of actin and tubulin varies in class I vpda neuron

Although much progress has been made in characterizing molecular players affecting dendritic morphogenesis, it is not clear how exactly the new branches are formed during dendritogenesis *in vivo*. How much do actin cytoskeleton and microtubules contribute to this branch formation event? How are actin and tubulin localized and distributed in preformed branches- primary, secondary and higher order branches and during branch formation? Are the *de novo* branches formed of actin exclusively at the beginning and then are inhabited by microtubules or microtubules are needed to form the *de novo* branches at the beginning? Studies till date show that class III md-da neurons show actin rich spike like structures which are very dynamic. The same studies also demonstrate enrichment of Nod, a minus-end reporter for microtubules, using Nod-GFP at the tips of some of the da neuron dendrites (Andersen, Li et al. 2005). However, not much is known about actin and tubulin localization in class I neurons and their contribution to *de novo* branch formation. We looked at the localization of actin and tubulin in class I- vpda neurons in late 3rd instar larvae using GFP labeled constructs to visualize both these molecules (Figure 37). In preliminary experiments, we found that tubulin is mainly localized in primary branches and its concentration becomes faded in secondary and higher order branches. This was very different than actin which was localized not only in primary branches but also in secondary and to some extent in higher order branches. These preliminary results indicate that primary branches are richer in microtubules and as the order of branches keeps on increasing the concentration of tubulin decreases. On the other hand, actin is more or less equally concentrated in first couple of orders of branches and then its concentration seems to drop down in higher order braches. It will be interesting to follow the

distribution of tubulin and actin at higher resolution during branch formation *in vivo* using time lapse with signal to volume quantifications.

Concluding remarks:

This thesis describes an attempt to investigate role of two important cytoskeletal regulators- Diaphanous and Profilin- in dendritic morphogenesis. Overall genetic analysis along with histo-chemical analysis failed to confirm a definite function for both these molecules in dendritic development. Both these molecules are important regulators of actin and it will be very surprising if they do not affect dendritic morphogenesis. At this point, we lack appropriate genetic tools to study their role especially of Profilin. However, with technological advances, it may be possible in the coming future to manipulate protein levels at particular time during development and examine the effects *in vivo*. In case of Diaphanous, our results suggest no significant role for it in dendritic differentiation.

Our preliminary efforts to study dendrite development *in vivo* over time were successful and this system now can be used to observe different dendritic mutants to see how exactly they play a role in dendritic morphogenesis. Further we tried to analyze localization of Actin and Tubulin in dendritic branches of class I neurons. This aspect can be studied ahead with appropriate quantifications to understand how the dendritic branching actually takes place with respect to microtubule and actin cytoskeleton interplay.

REFERENCES

- Ackermann, M. and A. Matus (2003). "Activity-induced targeting of profilin and stabilization of dendritic spine morphology." *Nat Neurosci* 6(11): 1194-200.
- Adams, C. M., M. G. Anderson, et al. (1998). "Ripped pocket and pickpocket, novel *Drosophila* DEG/ENaC subunits expressed in early development and in mechanosensory neurons." *J Cell Biol* 140(1): 143-52.
- Adams, J., R. Kelso, et al. (2000). "The kelch repeat superfamily of proteins: propellers of cell function." *Trends Cell Biol* 10(1): 17-24.
- Afshar, K., B. Stuart, et al. (2000). "Functional analysis of the *Drosophila* diaphanous FH protein in early embryonic development." *Development* 127(9): 1887-97.
- Ainsley, J. A., J. M. Pettus, et al. (2003). "Enhanced locomotion caused by loss of the *Drosophila* DEG/ENaC protein Pickpocket1." *Curr Biol* 13(17): 1557-63.
- Andersen, R., Y. Li, et al. (2005). "Calcium/calmodulin-dependent protein kinase II alters structural plasticity and cytoskeletal dynamics in *Drosophila*." *J Neurosci* 25(39): 8878-88.
- Arakawa, Y., H. Bito, et al. (2003). "Control of axon elongation via an SDF-1alpha/Rho/mDia pathway in cultured cerebellar granule neurons." *J Cell Biol* 161(2): 381-91.
- Asikainen, S., S. Vartiainen, et al. (2005). "Selective sensitivity of *Caenorhabditis elegans* neurons to RNA interference." *Neuroreport* 16(18): 1995-9.
- Aspenstrom, P., A. Fransson, et al. (2004). "Rho GTPases have diverse effects on the organization of the actin filament system." *Biochem J* 377(Pt 2): 327-37.
- Beck, H. N., K. Drahushuk, et al. (2001). "Bone morphogenetic protein-5 (BMP-5) promotes dendritic growth in cultured sympathetic neurons." *BMC Neurosci* 2: 12.
- Benlali, A., I. Draskovic, et al. (2000). "act up controls actin polymerization to alter cell shape and restrict Hedgehog signaling in the *Drosophila* eye disc." *Cell* 101(3): 271-81.
- Bodmer, R., S. Barbel, et al. (1987). "Transformation of sensory organs by mutations of the cut locus of *D. melanogaster*." *Cell* 51(2): 293-307.

Bogdan, S., O. Grewe, et al. (2004). "Sra-1 interacts with Kette and Wasp and is required for neuronal and bristle development in *Drosophila*." *Development* 131(16): 3981-9.

Borst, A. and M. Egelhaaf (1994). "Dendritic processing of synaptic information by sensory interneurons." *Trends Neurosci* 17(6): 257-63.

Brenman, J. E., F. B. Gao, et al. (2001). "Sequoia, a tramtrack-related zinc finger protein, functions as a pan-neural regulator for dendrite and axon morphogenesis in *Drosophila*." *Dev Cell* 1(5): 667-77.

Butler, H., S. Levine, et al. (2001). "Map position and expression of the genes in the 38 region of *Drosophila*." *Genetics* 158(4): 1597-614.

Campbell, R. E., O. Tour, et al. (2002). "A monomeric red fluorescent protein." *Proc Natl Acad Sci U S A* 99(12): 7877-82.

Castrillon, D. H. and S. A. Wasserman (1994). "Diaphanous is required for cytokinesis in *Drosophila* and shares domains of similarity with the products of the limb deformity gene." *Development* 120(12): 3367-77.

Chang, F., D. Drubin, et al. (1997). "cdc12p, a protein required for cytokinesis in fission yeast, is a component of the cell division ring and interacts with profilin." *J Cell Biol* 137(1): 169-82.

Chen, G. C., P. Gajowniczek, et al. (2004). "Rho-LIM kinase signaling regulates ecdysone-induced gene expression and morphogenesis during *Drosophila* metamorphosis." *Curr Biol* 14(4): 309-13.

Cline, H. T. (2001). "Dendritic arbor development and synaptogenesis." *Curr Opin Neurobiol* 11(1): 118-26.

Cooley, L., E. Verheyen, et al. (1992). "chickadee encodes a profilin required for intercellular cytoplasm transport during *Drosophila* oogenesis." *Cell* 69(1): 173-84.

Crosby, M. A., Goodman, J. L., Strelets, V. B., Zhang, P., and Gelbart, W. M. (2007). FlyBase: genomes by the dozen. *Nucleic Acids Res* 35, D486-491.

Czuchra, A., X. Wu, et al. (2005). "Cdc42 is not essential for filopodium formation, directed migration, cell polarization, and mitosis in fibroblastoid cells." *Mol Biol Cell* 16(10): 4473-84.

Da Silva, J. S., M. Medina, et al. (2003). "RhoA/ROCK regulation of neuritogenesis via profilin IIa-mediated control of actin stability." *J Cell Biol* 162(7): 1267-79.

Dent, E. W. and K. Kalil (2001). "Axon branching requires interactions between dynamic microtubules and actin filaments." *J Neurosci* 21(24): 9757-69.

Dutta, D., J. W. Bloor, et al. (2002). "Real-time imaging of morphogenetic movements in *Drosophila* using Gal4-UAS-driven expression of GFP fused to the actin-binding domain of moesin." *Genesis* 34(1-2): 146-51.

Dykxhoorn, D. M., C. D. Novina, et al. (2003). "Killing the messenger: short RNAs that silence gene expression." *Nat Rev Mol Cell Biol* 4(6): 457-67.

Ellis, S. and H. Mellor (2000). "The novel Rho-family GTPase *rif* regulates coordinated actin-based membrane rearrangements." *Curr Biol* 10(21): 1387-90.

Emoto, K., Y. He, et al. (2004). "Control of dendritic branching and tiling by the Tricornered-kinase/Furry signaling pathway in *Drosophila* sensory neurons." *Cell* 119(2): 245-56.

Endo, M., K. Ohashi, et al. (2003). "Control of growth cone motility and morphology by LIM kinase and Slingshot via phosphorylation and dephosphorylation of cofilin." *J Neurosci* 23(7): 2527-37.

Euler, T. and W. Denk (2001). "Dendritic processing." *Curr Opin Neurobiol* 11(4): 415-22.

Faix, J. and R. Grosse (2006). "Staying in shape with formins." *Dev Cell* 10(6): 693-706.

Fink, C. C., K. U. Bayer, et al. (2003). "Selective regulation of neurite extension and synapse formation by the beta but not the alpha isoform of CaMKII." *Neuron* 39(2): 283-97.

Friederich, E., K. Vancompernelle, et al. (1999). "Villin function in the organization of the actin cytoskeleton. Correlation of in vivo effects to its biochemical activities in vitro." *J Biol Chem* 274(38): 26751-60.

Gao, F. B. and B. A. Bogert (2003). "Genetic control of dendritic morphogenesis in *Drosophila*." *Trends Neurosci* 26(5): 262-8.

Gao, F. B., J. E. Brenman, et al. (1999). "Genes regulating dendritic outgrowth, branching, and routing in *Drosophila*." *Genes Dev* 13(19): 2549-61.

Goode, B. L. and M. J. Eck (2007). "Mechanism and Function of Formins in Control of Actin Assembly." *Annu Rev Biochem*.

Grieder, N. C., M. de Cuevas, et al. (2000). "The fusome organizes the microtubule network during oocyte differentiation in *Drosophila*." *Development* 127(19): 4253-64.

Grosshans, J., C. Wenzl, et al. (2005). "RhoGEF2 and the formin *Dia* control the formation of the furrow canal by directed actin assembly during *Drosophila* cellularisation." *Development* 132(5): 1009-20.

Grueber, W. B., L. Y. Jan, et al. (2002). "Tiling of the *Drosophila* epidermis by multidendritic sensory neurons." *Development* 129(12): 2867-78.

Grueber, W. B., L. Y. Jan, et al. (2003). "Different levels of the homeodomain protein cut regulate distinct dendrite branching patterns of *Drosophila* multidendritic neurons." *Cell* 112(6): 805-18.

Grueber, W. B. and Y. N. Jan (2004). "Dendritic development: lessons from *Drosophila* and related branches." *Curr Opin Neurobiol* 14(1): 74-82.

Grueber, W. B., B. Ye, et al. (2003). "Dendrites of distinct classes of *Drosophila* sensory neurons show different capacities for homotypic repulsion." *Curr Biol* 13(8): 618-26.

Grueber, W. B., B. Ye, et al. (2007). "Projections of *Drosophila* multidendritic neurons in the central nervous system: links with peripheral dendrite morphology." *Development* 134(1): 55-64.

Gunsalus, K. C., S. Bonaccorsi, et al. (1995). "Mutations in *twinstar*, a *Drosophila* gene encoding a cofilin/ADF homologue, result in defects in centrosome migration and cytokinesis." *J Cell Biol* 131(5): 1243-59.

Harada, A., J. Teng, et al. (2002). "MAP2 is required for dendrite elongation, PKA anchoring in dendrites, and proper PKA signal transduction." *J Cell Biol* 158(3): 541-9.

Harrison, D. A. and N. Perrimon (1993). "Simple and efficient generation of marked clones in *Drosophila*." *Curr Biol* 3(7): 424-33.

Hausser, M., N. Spruston, et al. (2000). "Diversity and dynamics of dendritic signaling." *Science* 290(5492): 739-44.

Helfer, E., E. M. Nevalainen, et al. (2006). "Mammalian twinfilin sequesters ADP-G-actin and caps filament barbed ends: implications in motility." *Embo J* 25(6): 1184-95.

Henkemeyer, M., O. S. Itkis, et al. (2003). "Multiple EphB receptor tyrosine kinases shape dendritic spines in the hippocampus." *J Cell Biol* 163(6): 1313-26.

Hernandez, M. C., P. J. Andres-Barquin, et al. (1997). "ENC-1: a novel mammalian kelch-related gene specifically expressed in the nervous system encodes an actin-binding protein." *J Neurosci* 17(9): 3038-51.

Higgs, H. N. (2005). "Formin proteins: a domain-based approach." *Trends Biochem Sci* 30(6): 342-53.

Hopmann, R. and K. G. Miller (2003). "A balance of capping protein and profilin functions is required to regulate actin polymerization in *Drosophila* bristle." *Mol Biol Cell* 14(1): 118-28.

- Hughes, M. E., R. Bortnick, et al. (2007). "Homophilic Dscam interactions control complex dendrite morphogenesis." *Neuron* 54(3): 417-27.
- Ibarra, N., A. Pollitt, et al. (2005). "Regulation of actin assembly by SCAR/WAVE proteins." *Biochem Soc Trans* 33(Pt 6): 1243-6.
- Jan, Y. N. and L. Y. Jan (2001). "Dendrites." *Genes Dev* 15(20): 2627-41.
- Jones, S. B., H. Y. Lu, et al. (2004). "Abl tyrosine kinase promotes dendrogenesis by inducing actin cytoskeletal rearrangements in cooperation with Rho family small GTPases in hippocampal neurons." *J Neurosci* 24(39): 8510-21.
- Kater, S. B. and V. Rehder (1995). "The sensory-motor role of growth cone filopodia." *Curr Opin Neurobiol* 5(1): 68-74.
- Kennerdell, J. R. and R. W. Carthew (1998). "Use of dsRNA-mediated genetic interference to demonstrate that frizzled and frizzled 2 act in the wingless pathway." *Cell* 95(7): 1017-26.
- Koizumi, K., H. Higashida, et al. (2007). "RNA interference screen to identify genes required for Drosophila embryonic nervous system development." *Proc Natl Acad Sci U S A* 104(13): 5626-31.
- Komiyama, T., L. B. Sweeney, et al. (2007). "Graded expression of semaphorin-1a cell-autonomously directs dendritic targeting of olfactory projection neurons." *Cell* 128(2): 399-410.
- Kosik, K. S., C. P. Donahue, et al. (2005). "Delta-catenin at the synaptic-adherens junction." *Trends Cell Biol* 15(3): 172-8.
- Kovar, D. R. (2006). "Molecular details of formin-mediated actin assembly." *Curr Opin Cell Biol* 18(1): 11-7.
- Kovar, D. R., J. R. Kuhn, et al. (2003). "The fission yeast cytokinesis formin Cdc12p is a barbed end actin filament capping protein gated by profilin." *J Cell Biol* 161(5): 875-87.
- Kovar, D. R. and T. D. Pollard (2004). "Progressing actin: Formin as a processive elongation machine." *Nat Cell Biol* 6(12): 1158-9.
- Landgraf, M. and J. F. Evers (2005). "Control of dendritic diversity." *Curr Opin Cell Biol* 17(6): 690-6.
- Lee, J., S. Nam, et al. (2004). "Functional genomic approaches using the nematode *Caenorhabditis elegans* as a model system." *J Biochem Mol Biol* 37(1): 107-13.
- Lee, T. and L. Luo (2001). "Mosaic analysis with a repressible cell marker (MARCM) for Drosophila neural development." *Trends Neurosci* 24(5): 251-4.

Lee, T., C. Winter, et al. (2000). "Essential roles of *Drosophila* RhoA in the regulation of neuroblast proliferation and dendritic but not axonal morphogenesis." *Neuron* 25(2): 307-16.

Li, W., Y. Li, et al. (2005). "Abelson, enabled, and p120 catenin exert distinct effects on dendritic morphogenesis in *Drosophila*." *Dev Dyn* 234(3): 512-22.

Liu, Z., R. Steward, et al. (2000). "*Drosophila* Lis1 is required for neuroblast proliferation, dendritic elaboration and axonal transport." *Nat Cell Biol* 2(11): 776-83.

Lolle, S. J., J. L. Victor, et al. (2005). "Genome-wide non-mendelian inheritance of extra-genomic information in *Arabidopsis*." *Nature* 434(7032): 505-9.

Ma, Y., A. Creanga, et al. (2006). "Prevalence of off-target effects in *Drosophila* RNA interference screens." *Nature* 443(7109): 359-63.

Matova, N., S. Mahajan-Miklos, et al. (1999). "*Drosophila* quail, a villin-related protein, bundles actin filaments in apoptotic nurse cells." *Development* 126(24): 5645-57.

Matthews, B. J., M. E. Kim, et al. (2007). "Dendrite self-avoidance is controlled by Dscam." *Cell* 129(3): 593-604.

McAllister, A. K. (2000). "Cellular and molecular mechanisms of dendrite growth." *Cereb Cortex* 10(10): 963-73.

McAllister, A. K., L. C. Katz, et al. (1997). "Opposing roles for endogenous BDNF and NT-3 in regulating cortical dendritic growth." *Neuron* 18(5): 767-78.

Millard, T. H., S. J. Sharp, et al. (2004). "Signalling to actin assembly via the WASP (Wiskott-Aldrich syndrome protein)-family proteins and the Arp2/3 complex." *Biochem J* 380(Pt 1): 1-17.

Miller, F. D. and D. R. Kaplan (2003). "Signaling mechanisms underlying dendrite formation." *Curr Opin Neurobiol* 13(3): 391-8.

Misquitta, L. and B. M. Paterson (1999). "Targeted disruption of gene function in *Drosophila* by RNA interference (RNA-i): a role for nautilus in embryonic somatic muscle formation." *Proc Natl Acad Sci U S A* 96(4): 1451-6.

Moore, A. W., L. Y. Jan, et al. (2002). "hamlet, a binary genetic switch between single- and multiple- dendrite neuron morphology." *Science* 297(5585): 1355-8.

Moseley, J. B., K. Okada, et al. (2006). "Twincillin is an actin-filament-severing protein and promotes rapid turnover of actin structures in vivo." *J Cell Sci* 119(Pt 8): 1547-57.

Neely, M. D. and J. G. Nicholls (1995). "Electrical activity, growth cone motility and the cytoskeleton." *J Exp Biol* 198(Pt 7): 1433-46.

Neuhoff, H., M. Sassoe-Pognetto, et al. (2005). "The actin-binding protein profilin I is localized at synaptic sites in an activity-regulated manner." *Eur J Neurosci* 21(1): 15-25.

Neuman, S., M. Kovalio, et al. (2005). "The Drosophila homologue of the dystrophin gene - introns containing promoters are the major contributors to the large size of the gene." *FEBS Lett* 579(24): 5365-71.

Niell, C. M., M. P. Meyer, et al. (2004). "In vivo imaging of synapse formation on a growing dendritic arbor." *Nat Neurosci* 7(3): 254-60.

Niessen, C. M. and A. S. Yap (2006). "Another job for the talented p120-catenin." *Cell* 127(5): 875-7.

Niwa, R., K. Nagata-Ohashi, et al. (2002). "Control of actin reorganization by Slingshot, a family of phosphatases that dephosphorylate ADF/cofilin." *Cell* 108(2): 233-46.

Novina, C. D. and P. A. Sharp (2004). "The RNAi revolution." *Nature* 430(6996): 161-4.

Okada, K., H. Ravi, et al. (2006). "Aip1 and cofilin promote rapid turnover of yeast actin patches and cables: a coordinated mechanism for severing and capping filaments." *Mol Biol Cell* 17(7): 2855-68.

Ono, S. (2003). "Regulation of actin filament dynamics by actin depolymerizing factor/cofilin and actin-interacting protein 1: new blades for twisted filaments." *Biochemistry* 42(46): 13363-70.

Palmgren, S., M. Vartiainen, et al. (2002). "Twinfilin, a molecular mailman for actin monomers." *J Cell Sci* 115(Pt 5): 881-6.

Parrish, J. Z., K. Emoto, et al. (2007). "Mechanisms That Regulate Establishment, Maintenance, and Remodeling of Dendritic Fields." *Annu Rev Neurosci*.

Pearson, H. (2006). "Genetics: what is a gene?" *Nature* 441(7092): 398-401.

Pellegrin, S. and H. Mellor (2005). "The Rho family GTPase Rif induces filopodia through mDia2." *Curr Biol* 15(2): 129-33.

Peng, J., B. J. Wallar, et al. (2003). "Disruption of the Diaphanous-related formin Drf1 gene encoding mDia1 reveals a role for Drf3 as an effector for Cdc42." *Curr Biol* 13(7): 534-45.

Polet, D., A. Lambrechts, et al. (2007). "On the origin and evolution of vertebrate and viral profilins." *FEBS Lett* 581(2): 211-7.

- Prokop, A., J. Uhler, et al. (1998). "The kakapo mutation affects terminal arborization and central dendritic sprouting of *Drosophila* motorneurons." *J Cell Biol* 143(5): 1283-94.
- Rassoulzadegan, M., V. Grandjean, et al. (2006). "RNA-mediated non-mendelian inheritance of an epigenetic change in the mouse." *Nature* 441(7092): 469-74.
- Reaume, C. J. and M. B. Sokolowski (2006). "The nature of *Drosophila melanogaster*." *Curr Biol* 16(16): R623-8.
- Redmond, L. and A. Ghosh (2001). "The role of Notch and Rho GTPase signaling in the control of dendritic development." *Curr Opin Neurobiol* 11(1): 111-7.
- Ridley, A. J. (2006). "Rho GTPases and actin dynamics in membrane protrusions and vesicle trafficking." *Trends Cell Biol* 16(10): 522-9.
- Roberts, R. G. and M. Bobrow (1998). "Dystrophins in vertebrates and invertebrates." *Hum Mol Genet* 7(4): 589-95.
- Robinson, D. N. and L. Cooley (1997). "Examination of the function of two kelch proteins generated by stop codon suppression." *Development* 124(7): 1405-17.
- Rodal, A. A., J. W. Tetreault, et al. (1999). "Aip1p interacts with cofilin to disassemble actin filaments." *J Cell Biol* 145(6): 1251-64.
- Rogers, S. L., U. Wiedemann, et al. (2003). "Molecular requirements for actin-based lamella formation in *Drosophila* S2 cells." *J Cell Biol* 162(6): 1079-88.
- Sagot, I., A. A. Rodal, et al. (2002). "An actin nucleation mechanism mediated by Bni1 and profilin." *Nat Cell Biol* 4(8): 626-31.
- Sarmiere, P. D. and J. R. Bamberg (2004). "Regulation of the neuronal actin cytoskeleton by ADF/cofilin." *J Neurobiol* 58(1): 103-17.
- Sasaki, Y., C. Cheng, et al. (2002). "Fyn and Cdk5 mediate semaphorin-3A signaling, which is involved in regulation of dendrite orientation in cerebral cortex." *Neuron* 35(5): 907-20.
- Schirenbeck, A., R. Arasada, et al. (2005). "Formins and VASPs may cooperate in the formation of filopodia." *Biochem Soc Trans* 33(Pt 6): 1256-9.
- Scott, E. K. and L. Luo (2001). "How do dendrites take their shape?" *Nat Neurosci* 4(4): 359-65.
- Sholl, D. A. (1956). "The measurable parameters of the cerebral cortex and their significance in its organization." *Prog Neurobiol*(2): 324-33.

- Silacci, P., L. Mazzolai, et al. (2004). "Gelsolin superfamily proteins: key regulators of cellular functions." *Cell Mol Life Sci* 61(19-20): 2614-23.
- Soba, P., S. Zhu, et al. (2007). "Drosophila sensory neurons require Dscam for dendritic self-avoidance and proper dendritic field organization." *Neuron* 54(3): 403-16.
- Somogyi, K. and P. Rorth (2004). "Evidence for tension-based regulation of Drosophila MAL and SRF during invasive cell migration." *Dev Cell* 7(1): 85-93.
- Song, W., M. Onishi, et al. (2007). "Peripheral multidendritic sensory neurons are necessary for rhythmic locomotion behavior in Drosophila larvae." *Proc Natl Acad Sci U S A* 104(12): 5199-204.
- Spradling, A. C., D. Stern, et al. (1999). "The Berkeley Drosophila Genome Project gene disruption project: Single P-element insertions mutating 25% of vital Drosophila genes." *Genetics* 153(1): 135-77.
- Stradal, T. E., K. Rottner, et al. (2004). "Regulation of actin dynamics by WASP and WAVE family proteins." *Trends Cell Biol* 14(6): 303-11.
- Sugimura, K., M. Yamamoto, et al. (2003). "Distinct developmental modes and lesion-induced reactions of dendrites of two classes of Drosophila sensory neurons." *J Neurosci* 23(9): 3752-60.
- Szebenyi, G., F. Bollati, et al. (2005). "Activity-driven dendritic remodeling requires microtubule-associated protein 1A." *Curr Biol* 15(20): 1820-6.
- Togashi, H., K. Abe, et al. (2002). "Cadherin regulates dendritic spine morphogenesis." *Neuron* 35(1): 77-89.
- Vaillant, A. R., P. Zanassi, et al. (2002). "Signaling mechanisms underlying reversible, activity-dependent dendrite formation." *Neuron* 34(6): 985-98.
- Van Aelst, L. and H. T. Cline (2004). "Rho GTPases and activity-dependent dendrite development." *Curr Opin Neurobiol* 14(3): 297-304.
- van der Plas, M. C., G. S. Pilgram, et al. (2006). "Dystrophin is required for appropriate retrograde control of neurotransmitter release at the Drosophila neuromuscular junction." *J Neurosci* 26(1): 333-44.
- Vartiainen, M. K. and L. M. Machesky (2004). "The WASP-Arp2/3 pathway: genetic insights." *Curr Opin Cell Biol* 16(2): 174-81.
- Verheyen, E. M. and L. Cooley (1994). "Profilin mutations disrupt multiple actin-dependent processes during Drosophila development." *Development* 120(4): 717-28.

- Wahlstrom, G., M. Vartiainen, et al. (2001). "Twinstillin is required for actin-dependent developmental processes in *Drosophila*." *J Cell Biol* 155(5): 787-96.
- Waller, B. J. and A. S. Alberts (2003). "The formins: active scaffolds that remodel the cytoskeleton." *Trends Cell Biol* 13(8): 435-46.
- Wasserman, S. (1998). "FH proteins as cytoskeletal organizers." *Trends Cell Biol* 8(3): 111-5.
- Watanabe, N., P. Madaule, et al. (1997). "p140mDia, a mammalian homolog of *Drosophila* diaphanous, is a target protein for Rho small GTPase and is a ligand for profilin." *Embo J* 16(11): 3044-56.
- Wills, Z., M. Emerson, et al. (2002). "A *Drosophila* homolog of cyclase-associated proteins collaborates with the Abl tyrosine kinase to control midline axon pathfinding." *Neuron* 36(4): 611-22.
- Wills, Z., L. Marr, et al. (1999). "Profilin and the Abl tyrosine kinase are required for motor axon outgrowth in the *Drosophila* embryo." *Neuron* 22(2): 291-9.
- Witke, W. (2004). "The role of profilin complexes in cell motility and other cellular processes." *Trends Cell Biol* 14(8): 461-9.
- Yarmola, E. G. and M. R. Bubb (2006). "Profilin: emerging concepts and lingering misconceptions." *Trends Biochem Sci* 31(4): 197-205.
- Ye, B. and Y. N. Jan (2005). "The cadherin superfamily and dendrite development." *Trends Cell Biol* 15(2): 64-7.
- Zallen, J. A., Y. Cohen, et al. (2002). "SCAR is a primary regulator of Arp2/3-dependent morphological events in *Drosophila*." *J Cell Biol* 156(4): 689-701.
- Zhang, S. L., A. V. Yeromin, et al. (2006). "Genome-wide RNAi screen of Ca²⁺ influx identifies genes that regulate Ca²⁺ release-activated Ca²⁺ channel activity." *Proc Natl Acad Sci U S A* 103(24): 9357-62.
- Zhou, F., P. Leder, et al. (2006). "Formin-1 protein associates with microtubules through a peptide domain encoded by exon-2." *Exp Cell Res* 312(7): 1119-26.
- Zhou, G. Q., H. Q. Xie, et al. (2006). "Current understanding of dystrophin-related muscular dystrophy and therapeutic challenges ahead." *Chin Med J (Engl)* 119(16): 1381-91.
- Zhu, S., L. Liu, et al. (2006). "RhoA acts downstream of Wnt5 and Wnt11 to regulate convergence and extension movements by involving effectors Rho kinase and Diaphanous: use of zebrafish as an *in vivo* model for GTPase signaling." *Cell Signal* 18(3): 359-72.

Acknowledgements

I am grateful to everyone who contributed directly and indirectly to this thesis.

Curriculum vitae

Madhuri Shivalkar

E-mail: madhuri@neuro.mpg.de

Phone: (49) 8578 3203

Am Klopferspitz 18
82152 Martinsried, Germany

Academic Qualification:

- **M.A., Neuroscience** **May 2003**
Department of Neurobiology, Institute of Neuroscience,
The University of Texas at Austin, USA.
- **B.Sc., Microbiology** **June 1996**
The University of Mumbai, India.

Courses taken:

Principles of Neuroscience	Genetics
Developmental Neurobiology	Molecular Biology
Current concepts in Behavioral Neurobiology	Cell Biology
Basic Neurobiology	Vertebrate Physiology
Insect Immunology	Signal Transduction
Microbiology	Biochemistry
Zoology	Medical microbiology

Experience:

Research:

- **Max Planck Institute of Neurobiology, Munich, Germany.** **July 2003-current**
Final Year Graduate student, Developmental Neurobiology.

Characterizing the role of cytoskeletal molecules in Dendritic development in *Drosophila melanogaster*.

Carried out a RNA interference (RNAi) screen for known cytoskeletal molecules affecting dendritic development and morphogenesis. Analyzed two positive molecules from the screen, Diaphanous and Profilin, for dendritic phenotype using genetic analysis. The marker line used for analysis exhibited a dendritic overbranching phenotype by itself due to an insertion in the gene *dystrophin*. The dendritic phenotype of the genetic null mutants of *diaphanous* resulted from complicated genetic interactions with the marker line. No solid results could be obtained about the role of both *diaphanous* and *profilin* using gain of function and loss of function analysis.

- **The University of Texas at Austin, Texas, USA.** **Aug 2000-May 2003**
Master of Arts, Neuroscience.

Characterization of agrin-like molecules in *Drosophila melanogaster*.

Agrin-like genes from Flybase, were screened for functional homology to mammalian agrin using BLAST programs. An ORF of a homologous gene was identified, cloned and expressed in mammalian cell cultures. The ability to cluster acetylcholine receptors was used as a functional assay for the expressed protein. This was further analyzed using immunocytochemistry performed on C2 muscle cells. The techniques used were cloning, tissue culture methods, western blots, southern blots and fluorescent microscopy.

- **Tata Institute of Fundamental Research, Mumbai, India.** **March 1997- Aug 2000**
Scientific Assistant, Natural Sciences.

Study interaction between proteins involved in synaptic vesicle recycling.

Used *Drosophila melanogaster* as a model system for neuro-genetic studies of proteins involved in synaptic vesicle recycling. Temperature sensitive behavioral and developmental phenotypes of different genetic mutants were assayed for studying the interaction between *shibire* and *stoned*. One novel enhancer of *shibire*, *awd^{msm95}*, was studied and the gene involved was characterized using P-element hopping and screening methods. The responsibilities included maintenance of majority of fly stocks for the lab. Also, taught basic *Drosophila* genetics and Fly laboratory techniques to new personnel in the lab.

- **The University of Mumbai, India** **July 1996- March 1997**
Research Student, Life Sciences.

Analysis of cellular organization of pleuropedal ganglion of snail *Achatina Fulica*

Worked on the histochemical analyses, to study the cellular organization of pleuropedal ganglion in *A.fulica*. These snails were used due to their considerably large ganglia cells, which were amenable to study the synapse formation and learning and memory. The techniques involved dissections and histology.

- **The University of Mumbai, India.** **Aug 1993- Jun 1996**
Bachelor of Science, Microbiology.

Studied basic microbiology, genetics, genetic engineering and virology. Learnt basic laboratory techniques in microbiology, medical microbiology and immunology.

Teaching:

- **The University of Texas at Austin**
-Teaching Assistant for 'General Microbiology Laboratory' **Spring 2003**

I was a teaching assistant for a basic microbiology laboratory course. I had around 70 students who were learning different primary microbiology techniques including microscopy, culture techniques, staining techniques, etc. The position required careful instructing to new students and teaching them accurate aseptic techniques and rules.

- Teaching Assistant for 'Molecules to Organisms'** **Fall 2002**

I was also a teaching assistant for a non-major biology class of 160 students. It was a basic biology class, which explained fundamental terms and concepts to non-biology students. I conducted discussion sessions, grade quizzes and exams. I also managed online grade books, course documents, announcements and student communications. The position required extensive interaction with students to help and guide them to have better understanding of the subject.

- Teaching Assistant for 'Cell Biology'** **Fall 2001**

This class was an introduction to basic theories in cell and molecular biology. I led discussion sessions and graded exams and problem sets for a class of 60 students. The position required strong communication with students to understand their problems and resolving their difficulties. The position also involved maintenance of online students' grade book and contacts.

The class covered basic principles in neurophysiology including ion channel structure-function. The class also reviewed basic aspects of learning and memory and systems neurobiology. I organized discussion sessions and review sessions alongwith preparing quizzes, grading exams and home-works for a class of 120 students.

Activities:

- Gave a talk at the `**Axon Guidance, Synaptogenesis and Neural Plasticity`** meeting at **Cold Spring Harbor Laboratory** in New York, USA (September 2006)
- Gave a talk at the `**47th Annual Drosophila Research Conference`** in Houston, USA (March 2006)
- Was invited to give a talk at the `**Drosophila Neurobiology`** meeting at Cold Spring Harbor Laboratory in New York, USA (October 2005) (Could not attend the meeting because of Visa problems)
- Attended the **18th European Drosophila Research conference** in Goettingen, Germany (October 2003)
- Attended the **Annual Neuroscience Symposium** at UT Austin (February 2001 and 2002)
- Presented a poster on my research work- "*shibire-stoned* interaction in synaptic vesicle recycling" -at the **Annual seminars** at TIFR, India (August 1999)
- Presented research work at the **International Brain Research Organization (IBRO) conference** at Mahabaleshwar, India (December 1998)
- Attended the International **TIFR Golden Jubilee symposium** on "Present and Future of major aspects of Modern Biology" at the National Center for Biological Sciences (NCBS), Bangalore, India (October 1996)
- Active participant in **Neurobiology Journal Clubs** at TIFR and UT, Austin (1997-2002)

Publications:

K.S. Krishnan, Richa Rikhy, Sujata Rao, **Madhuri Shivalkar**, Michael Mosko, Radhakrishnan Narayanan, Paul Etter, Patricia S. Estes, and Mani Ramaswami. "*Nucleoside Diphosphate Kinase, a Source of GTP, Is Required for Dynamin-Dependent Synaptic Vesicle Recycling*". **Neuron**, 2001. 30 (1): 197-210.